BIOGEOCHEMICAL CYCLING OF METHANE AND NITROUS OXIDE IN THE NORTHERN INDIAN OCEAN

THESIS SUBMITTED TO
GOA UNIVERSITY
IN FULFILMENT OF THE REQUIREMENTS
FOR THE DEGREE OF
DOCTOR OF PHILOSOPHY
IN
MARINE SCIENCE

D. AMAL JAYAKUMAR, M.Sc.
CHEMICAL OCEANOGRAPHY DIVISION
NATIONAL INSTITUTE OF OCEANOGRAPHY
DONA PAULA, GOA 403 004
INDIA

JANUARY, 1999

CERTIFICATE

This is to certify that the thesis entitled **"BIOGEOCHEMICAL CYCLING OF METHANE AND NITROUS OXIDE IN THE NORTHERN INDIAN OCEAN"** submitted by **Mr. D. Amal Jayakumar** for the award of the degree of Doctor of Philosophy in Marine Science is based on his original studies carried out by him under my supervision. The thesis or any part thereof has not been previously submitted for any other degree or diploma in any universities or institutions.

Place: Dona Paula

Date: 14/10/99

Dr. R. SEN GUPTA

Research Guide
Emeritus Scientist
Chemical Oceanography Division
National Institute of Oceanography
Dona Paula - 403 004.

14/10/99

The corrections / suggestions made by the Examiner have been incorporated in the thesis

15/11/99

STATEMENT

As required under the University ordinance 0.19.8 (vi), I state that the present thesis entitled **"BIOGEOCHEMICAL CYCLING OF METHANE AND NITROUS OXIDE IN THE NORTHERN INDIAN OCEAN"** is my original contribution and the same has not been submitted on any previous occasion. To the best of my knowledge the present study is the first comprehensive work of its kind from the area mentioned.

The literature related to the problem investigated has been cited. Due acknowledgements have been made where ever facilities and suggestions have been availed of.

D. AMAL JAYAKUMAR

CONTENTS

4. Nitrate Deficit

5. Distribution of Nitrous oxide in the Northern Indian Ocean

6. Natural Abundance of Stable Isotopes in some Dissolved Nitrogen Species

7.Flux of Nitrous Oxide and Methane

Acknowledgements

I sincerely thank my research guide Dr.R.Sen Gupta, for his sustained interest in this work and valuable suggestions. I am grateful for his constant encouragement and patience.

I wish to thank Dr. Ehrlich Desa, Director National Institute of Oceanography, for the encouragement and the facilities made available for this work.

I am deeply indebted to Dr. S.W.A.Naqvi who has been instrumental in the conception and completion of this work and has been an understanding supervisor throughout. He has been a source of inspiration and has moulded me into what I am. My special thanks extend to Dr. Dileep Kumar for some very useful discussions on oceanographic processes and for the interest he has shown on my development.

I thank the Office of Naval Research (USA) for funding through the US-India Fund and in particular Dr. B.J. Zahuranec for his encouragement and support. I also thank the Department of Ocean Development (India) for making time on the research vessels available for this work. ONR funds were also made available to me for conducting isotopic analysis of nitrous oxide at Wadsworth Center, Albany, USA. I am grateful to Dr. Tadashi Yoshinari, New York State Department of Health, Albany, USA, and Prof. Bess Ward, Princeton University, New Jersey, USA for their keen interest in my work and progress. To Dr. Allan Devol University of Washington, Seattle, USA, Dr. Lou Codispoti, Old Dominion University, Norfolk, USA and Dr. Jay Brandes, Carnegie Institution of Washington, Washington, USA for their encouragement and support.

I record my thanks to my colleagues Dr. P.V.Narvekar, Dr. M.D. George, Dr. M.S. Shailaja, Mr. V.V.S.S. Sarma, Ms.S. Bagga, Ms. C. Nasnolkar, Ms. H. Naik, Mr. D. Shenoy, Ms. J. Kurien, H.S. Dalvi, Ms.L. Braganza and Ms.V. Kamat for their help in the collection of the physical, chemical and biological data during various cruises.

I gratefully acknowledge Dr. S. Shetye and Dr. S.S.C. Shenoy for their valued suggestions and information. I am grateful to Mr. G.S. Michael, Mr.G. Nampoothiri and Mr. D. Sundar for helping me in one way or the other during the course of this work. My thanks are also due to Mr. K.M. Sivakholundu, whom I could always depend upon to clear my doubts about graphics and computations.

Finally, I say thank you to my family for their extreme patience and unstinting support at all times.

1. Introduction

As a result of human activities the atmospheric concentrations of radiatively active gases have been increasing over the last century. These trace gases possess strong absorption bands in the infrared region of the spectrum, hence their increased concentrations in turn increase the heat trapping ability of the atmosphere. By virtue of their ability to trap the infrared radiation, these gases are known as 'Greenhouse gases'. Water vapour, carbon-dioxide, methane, nitrous oxide, ozone, hydroxyl radical and CFCs (chlorofluorocarbons) are the major greenhouse gases.

These gases are radiatively active at different wavelengths, have different heating contributions and have different growth rates in the atmosphere. When compared with carbon dioxide, methane is about 25 times more effective and nitrous oxide is about 200 times more effective in trapping IR radiation on a molar basis. The residence time in the atmosphere is also different for all these gases. Methane has a lifetime of 12 yrs, while carbon dioxide has 50-200 yrs and nitrous oxide has 120 yrs (Houghton et al., 1996). The greenhouse forcing due to the current levels of methane is about 10 to 15% (Lashof and Ahuja, 1990; Rodhe, 1990) and that of nitrous oxide is about 6% (Lashof and Ahuja, 1990). Apart from being radiatively active, biogenic trace gases such as methane and nitrous oxide play important roles in the atmospheric chemistry (Cicerone and Oremland, 1988).

The only significant sink for the atmospheric nitrous oxide is photo-dissociation and photo-oxidation in the stratosphere (Houghton et al., 1992; Houghton et al., 1995). In the troposphere some of the nitrous oxide is oxidised to NO, NO_2 and N_2O_5 by its reaction with OH and monoatomic oxygen, the rest ascends into the stratosphere. The NO so produced, in turn reacts with ozone in the stratosphere by a sequence of catalytic reactions leading to a reduction in

the ozone concentration (Bolle et al., 1986). Nitrous oxide has a long life time in the atmosphere and is broken down by photolysis in the stratosphere.

The principal pathway of the removal of methane in the atmosphere is its reaction with the hydroxyl radical. A major portion of methane ascending in the troposphere gets oxidised by the hydroxyl radical, thereby controlling the abundance of atmospheric water vapour, but still a large amount rises into the stratosphere. Carbon monoxide is a product of atmospheric methane oxidation. The major atmospheric sink for methane and CO is their reaction with OH radical, thus the increase in one will lead to an increase in the other because of the resuction of OH (Logan et al., 1981). Hence increase in methane and/or CO can in turn lead to the increase in other gases in the atmosphere as hydroxyl radical plays a key role in the removal of a wide range of radiatively active trace gases in the atmosphere.

Greenhouse gases are produced by anthropogenic as well as natural causes. But the extent of the contribution by various sources is unknown. Hence attempts are being made to study the various source strengths of greenhouse gases and their production mechanisms. More and more measurements of these gases are required to understand their natural cycling. Methane and nitrous oxide are two such greenhouse gases which are produced anthropogenically as well as naturally. Although we have a general understanding of their various sources, detailed measurements are required to understand and predict the changes in the global environment.

1.1. Nitrous Oxide Background:

The current level of nitrous oxide in the atmosphere is around 312ppb which is rising steadily by 0.25% every year (Prinn et al., 1990). The main anthropogenic sources of nitrous oxide to the atmosphere are the use of

nitrogenous fertilisers in agriculture, biomass burning and industrial processes. Natural sources are probably twice as large as anthropogenic ones. The contribution from the oceans is about 4 Tg N yr^{-1} (Nevison et al., 1995). The world ocean contributes about 50% of the total inputs of N_2O to the atmosphere from all the natural emissions.

Nitrous oxide in the sea water was first measured by Craig and Gordon (1963). Yoshinari (1976) developed a more sensitive method for the estimation of dissolved nitrous oxide in seawater and reported that nitrous oxide concentrations negatively correlated with oxygen. Studies by Law and Owens (1990) and Naqvi and Noronha (1991) revealed that nitrous oxide emission from the Arabian Sea made a substantial contribution to the global atmospheric budget. Bange et al. (1996), reported that the emissions from the Arabian Sea were considerably higher than previous estimates and suggested that Arabian Sea may be more important than previously believed in the global emissions of oceanic nitrous oxide.

In the marine environment nitrous oxide is produced biologically as an intermediate and as a by-product during the processes of denitrification and nitrification respectively (Fig.1.1). During denitrification N_2O can be further reduced to N_2. Although it is established now that the oceans are a net source of N_2O to the atmosphere, its magnitude is still uncertain. Moreover, it is still not clear as to which process is dominantly responsible for the accumulation of N_2O in the oceanic waters, as it could be produced by several processes (Rönner, 1983). Early workers suggested that in analogy to the production in the soil, denitrification could be the dominant mechanism of its production in the marine environment as well (Junge and Hahn, 1971; Hahn, 1974). But looking at the relationship of dissolved N_2O with dissolved O_2, it was widely accepted that nitrification was the dominant mechanism for the production of N_2O in the oceanic waters (Yoshinari 1976; Cohen and Gordon 1978,1979; Elkins et al.,

1978; Butler et al., 1989; Cline et al., 1987; Oudot et al., 1990). However the possibility that N_2O is also produced during

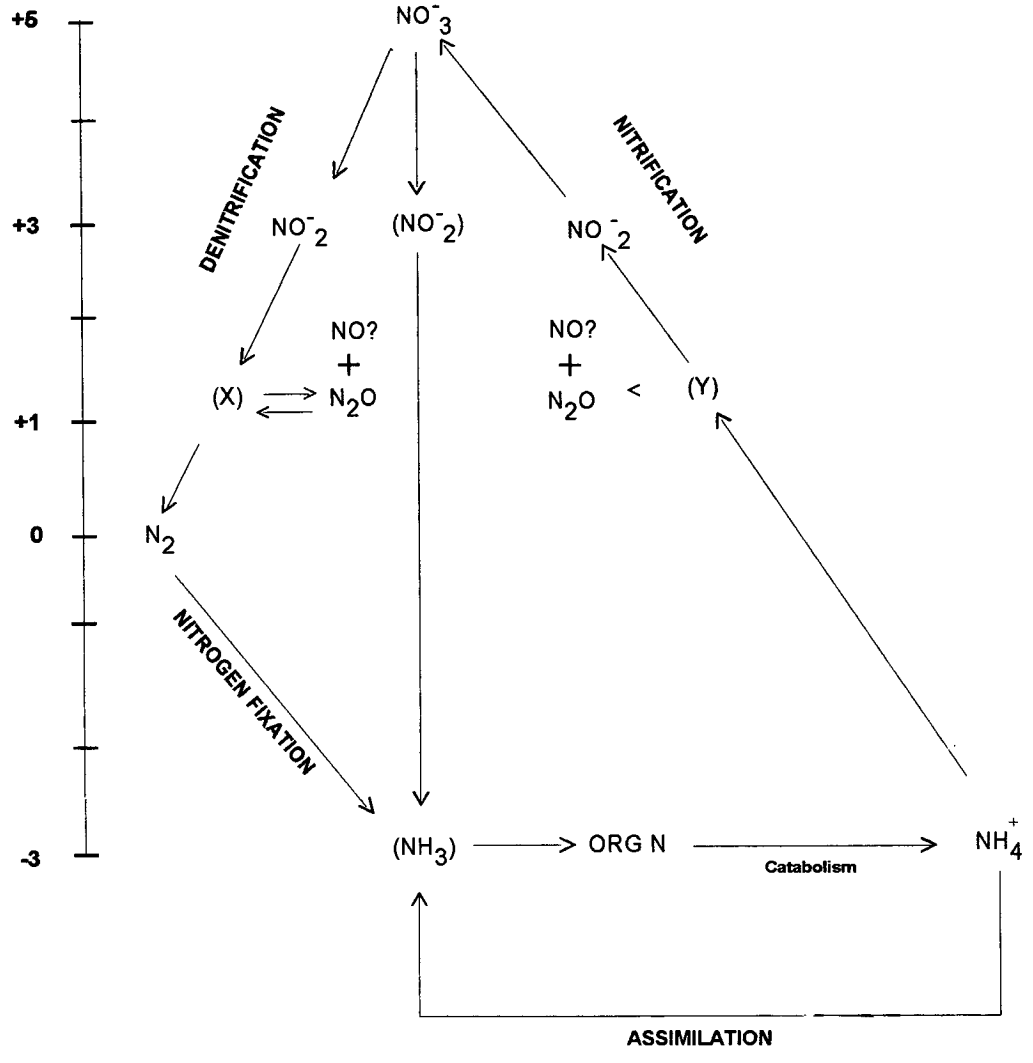

Fig.1.1. Diagram for marine nitrogen cycle (modified version of diagram presented by Codispoti and Christensen, 1985). (X) and (Y) represent intra-cellular intermediates that do not appear to accumulate in seawater. The diagram has been modified to suggest that N_2O is produced as well as consumed during denitrification in the sea.

denitrification cannot be ruled out (Pierotti and Rasmussen, 1980). As this problem could not be resolved by just measuring the concentration of N_2O, isotopic composition of N_2O was sought by several workers to resolve this

problem. Yoshida et al. (1989) made the first measurements on N isotopic composition of N_2O. They suggested that denitrification within micro-environments rather than nitrification may be responsible for the production of N_2O in the water column. Kim and Craig (1990) made the first measurements on the dual isotopic composition of dissolved N_2O and reported that their data supported production through nitrification.

1.2. Methane Background:

There has been a dramatic increase in the atmospheric methane content due to human activities over the past 200 years. The present concentration is ~1720 parts per billion by volume (ppbv), which is more than twice the pre-industrial value (~700 ppbv). The rate of increase of methane in the atmosphere is about 10ppbv/yr (Houghton et al., 1996) which is 1% of the atmospheric concentration (Rasmussen, and Khalil, 1981; Blake and Rowland, 1988). However some recent studies suggest that the atmospheric methane increased at a slower pace between 1983 and 1992, while other studies even found that methane concentration ceased to increase and might have even decreased a little after almost 200 years of continuous rise (Steele et al., 1992; Dlugokencky et al., 1994).

Large amount of methane is produced in the aquatic habitats by the activities of a group of archaebacteria known as the methanogens (Zeikus, 1977; Zehnder, 1978), which are strict anaerobes. There are other bacteria as well which are capable of producing methane, but the contributions from these are negligible compared to the methanogens. Although a large amount of methane is produced, only a fraction of this reaches the atmosphere as a major portion of this is oxidised by another group of bacteria known as the of methane oxidising bacteria.

In anaerobic habitats fermentative, acetogenic, and methanogenic bacteria convert organic matter to methane and carbon dioxide by an anaerobic microbial food chain. The metabolic activity of the methanogens, which are the terminal bacteria in this food chain, is coupled through a process termed 'interspecies hydrogen transfer'. Large organic molecules are converted to low molecular weight acids, CO_2 and molecular hydrogen by the fermentative bacteria. The activity of the fermentation process is enhanced by the methanogens by removing hydrogen and reducing the feedback inhibition. As a result of the interspecies hydrogen transfer, carbon turnover is enhanced and more oxidised end products are produced which in turn results in greater energy conservation for the fermentative organisms, increased growth of all organisms, and the displacement of unfavourable reaction equilibria. A consequence of this process is the nearly complete transformation of organic carbon in anaerobic environments to methane.

Although the anaerobic oxidation of methane has been well documented, little is known about the organisms that carry out this process. In contrast, plenty of information is available regarding the organisms that oxidize methane in aerobic environments. A major portion of methane that diffuses into the aerobic zone is metabolised by the methanotrophic bacteria, that are typically present in large numbers in or at the periphery of anaerobic zones. Methanotrophs (family Methylococcaceae) can obtain all of their carbon and energy from methane under aerobic conditions (Whittenbury and Kreig, 1984). A small perturbation to this group of bacteria can change the atmospheric methane budget to a large extent, hence it is important to know about the production and consumption of this gas in various ecosystems.

The main source of methane to the atmosphere is from paddy fields and other wetlands, animal husbandry, biomass burning and fossil fuel production and use. Data on the magnitudes of sinks and individual sources of methane are

still scarce and their quantification is necessary to predict further impacts on the world climate. Hence it is essential to budget the various natural and anthropogenic sources of methane to the atmosphere. The emission rate of methane from the oceans to the atmosphere is about 5-20 Tg per year (Cicerone and Oremland, 1988). The world oceans contribute about 2-4% of the natural emission of methane (Cicerone and Oremland, 1988; Bange et al., 1994). Thus the oceans play only a modest role in the global methane budget. About 60-80% of the methane contribution to the atmosphere are from anthropogenic activities.

Apart from the greenhouse warming potential, the higher atmospheric CH_4 inventory may also lead to a reduction of the tropospheric oxidising capacity due to the depletion of OH (Hein et al., 1997). Evaluation of the strengths of various sources and sinks of CH_4 is therefore very important.

The methanogens are strict anaerobes, however, and can only be active in reducing environments such as those found within biogenic particles and in the guts of marine organisms (Wolfe, 1971). Similarly, as the CH_4 oxidisers also require nitrogen for their growth, they need sufficiently high ambient combined nitrogen or low oxygen (O_2) levels, the latter to enable nitrogen fixation if the combined nitrogen levels are low (Rudd et al., 1976; Harrits and Hanson, 1980; Kiene, 1991). Such a dependence of CH_4 production and consumption to the ambient conditions results in high variability in its concentration in space and time. Thus, minor perturbations in environmental conditions can bring about potentially large changes in the oceanic CH_4 fluxes, underlining the need to understand the pathways of CH_4 cycling in the marine ecosystems.

The role of oceans as a source of methane to the atmosphere is very well understood. However, there has been only two reports till date on methane distribution in the Arabian Sea (Owens et al., 1991; Patra et al., 1998). Owens et al. (1991), highlighted the potential of this region as a source of atmospheric

methane. However their main stress was on the upwelling regions off Oman. Patra et al. (1998) reported high supersaturation of methane in the 100-200m range in the northern Arabian Sea and computed sea to air fluxes. The role of the acute oxygen deficiency in this region on methane distribution has not been adequately investigated. Moreover, there are no reports of any measurements on the shelf, estuaries or the coastal water bodies in the region.

1.3. Study Area:

The northern Indian Ocean consists of the Arabian Sea in the west and the Bay of Bengal in the east, separated by the Indian sub-continent (Fig.1.2). The hydrography of the region is well documented. Both these seas are bounded by land on three sides and are open only to the South, as a result of this, subtropical convergence is not found in the northern Indian Ocean. It is believed that the circulation at depth is weak and the intermediate depth waters are renewed slowly (Dietrich, 1973). The Arabian Sea houses one of the world's largest and most intense oceanic oxygen deficient environments. It has been postulated that the poor renewal of the intermediate waters in the Arabian Sea may be responsible for the development of oxygen deficient conditions culminating in denitrification (Wyrtki, 1973; Sen Gupta and Naqvi, 1984).

However, the more recent work has shown that these waters are renewed at a faster rate than believed earlier (Naqvi 1987; Somasundar and Naqvi, 1988; Olson et al., 1993). Thus the development of oxygen deficient conditions may result from an excessive oxygen consumption combined with the low oxygen content of waters responsible for renewal (Swallow, 1984). However, the mechanisms leading to this condition, remain largely unknown.

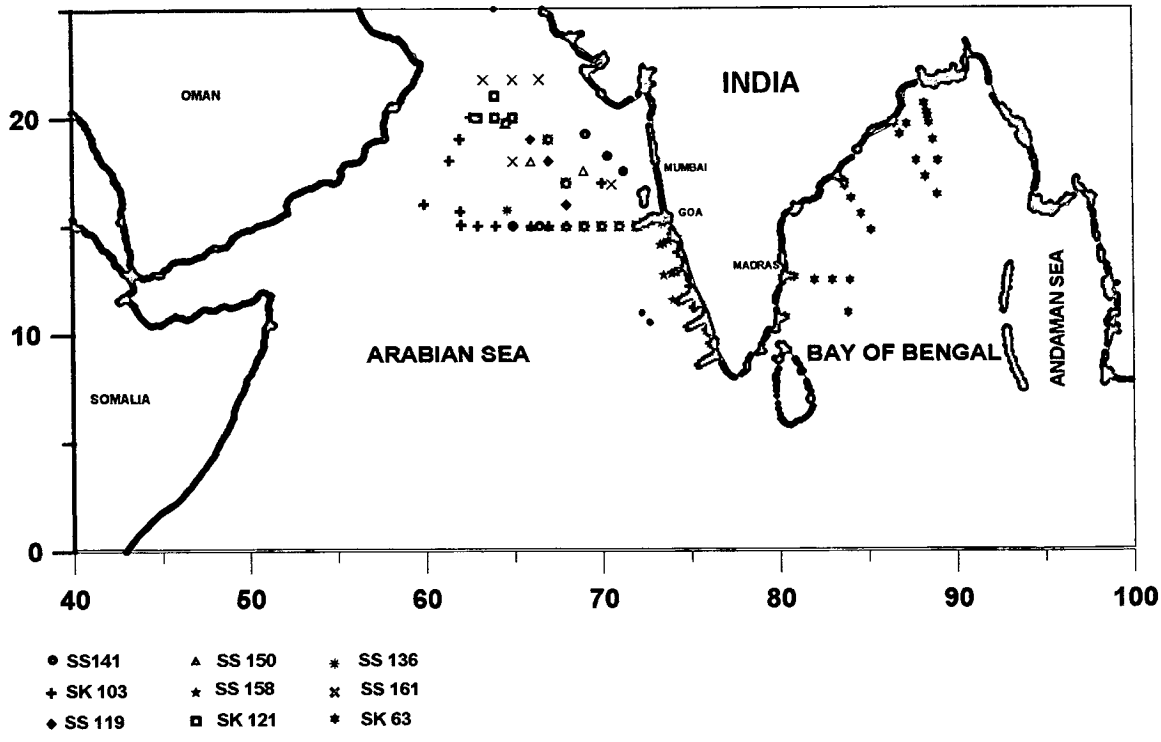

Fig.1.2. Figure showing the sampling positions

As a consequence of the low oxygen levels in the Arabian Sea, the cycling of redox sensitive elements are expected to be different from the more-common oxic environments. Large deficiencies in the inorganic combined nitrogen occur within the intermediate waters of the northern Arabian Sea (Sen Gupta et al., 1976; Deuser et al., 1978; Naqvi et al., 1982; Naqvi, 1986, 1987). Naqvi (1987) estimated that that denitrification in the Arabian Sea accounts for about a third of the global oceanic water column denitrification. Denitrification leads to both the production and consumption of nitrous oxide and so its turnover is expected to be rapid in the Arabian Sea.

1.4. Hydrographic features of the Arabian Sea:

The Arabian Sea between Lats 0° and 25° N and Longs. 50° and 80° E, occupies an area of about $6.225X10^{6}$ Km^{2} (Qasim, 1977). Robinson (1966) demarcated Arabian Sea from Laccadive Sea as the latter is more like the Bay of Bengal in terms of circulation. According to Schott's (1935) description, the southern boundary of the Arabian Sea runs from the Indian coast near Goa, along the west coast of the Laccadive islands to the equator; then further south up to Mombasa at 5° S. The Arabian Sea is connected to the Persian Gulf through the Gulf of Oman by the Hormuz Strait and to the Red Sea by the Strait of Bab-el-Mandab.

The Carlsberg Ridge, a north-western extension of the Mid Indian Ridge, divides the Arabian Sea into two major basins the Arabian Basin and the Somali Basin. The maximum depths in these basins are 3600 and 5300 m, respectively (Robinson, 1966). All along the Arabian coast the continental shelf remains very narrow; around Makran Coast the shelf averages 37 km width and gradually decrease towards the west. The shelf is the widest off the Gulf of Khambhat, about 352 km and north of this up to Karachi it remains about 185 km wide. From the Gulf of Cambay the shelf narrows down to 56 km near 11°N and widens to about 120 km off the southern-most part of India.

As evaporation exceeds precipitation and runoff, the Arabian Sea has a negative water balance and results in high surface salinity. This forms a shallow salinity maximum throughout the Arabian Sea surface layer and is identified as the Arabian Sea high-salinity water (Rochford, 1964) (Fig. 1.3). This excess evaporation is maximum closer to the Arabian coast and decreases steadily towards Southeast. Towards the southwest coast of India the balance reverses as here the annual precipitation marginally exceeds evaporation (Venkateswaran, 1956). High salinity water from the Persian Gulf and Red Sea

enters the Arabian Sea via the Gulf of Aden and the Gulf of Oman. To balance this outflow, fresh lower salinity surface waters enter both these gulfs (Grasshoff, 1969, 1975; Morcos, 1970; Hartmann et al., 1971) by Mediterranean type water exchange. The high salinity water from the Persian Gulf (PGW) sinks to approximately 300 m to find its own density level in the Arabian Sea (Fig. 1.3.). This water mass, characterised by Wyrtki (1971) by a σ_θ value of 26.6, spreads to the south along the west coast of India and loses its signature gradually towards the south (Ramesh Babu et al., 1980).

The Red Sea (RSW) outflow is characterised by a σ_θ value of 27.2 and is observed to flow between 500 and 800 m (Wyrtki, 1971) (Fig.1.3). This water mass, found south of 17°N, spreads southward and can be traced as far as Madagascar Channel (Ramesh Babu et al., 1980). During the SW monsoon there is a temporary subsurface inflow to and surface outflow from the Red Sea (Bethoux, 1988).

Large changes of water characteristics are mostly confined to the upper and intermediate layers and the deep waters are found to have very similar thermohaline properties throughout the Arabian Sea (Fig.1.3). The bottom water mass is considered to be a mixture of the North Indian high salinity intermediate water and the bottom water of circumpolar origin. Penetration of the Antarctic intermediate water (AAIW) as a low salinity layer into the southern Arabian Sea at ~800m have been reported (Tchernia et al., 1958; Naqvi, 1986). Ivanenkov and Gubin (1960) have described the deep and bottom water masses as the North Indian deep water and North Indian bottom water, respectively.

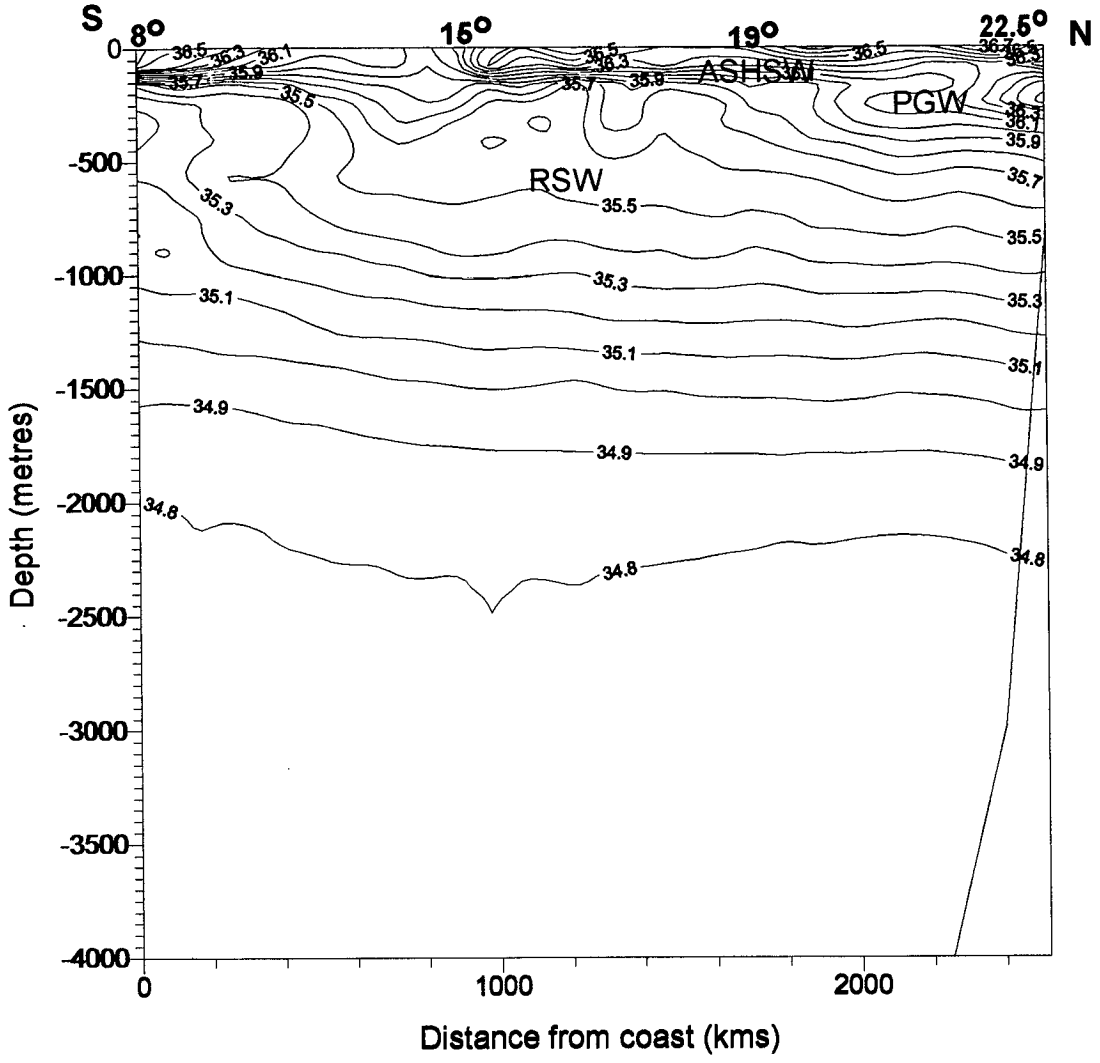

Fig.1.3. Salinity distribution along a N-S section in the Arabian Sea

Surface currents in the northern Indian Ocean undergo a biannual reversal, which is closely associated with the monsoons. During the north-east monsoon (NE) the flow is from east to west, north of the equator and forms the NE monsoon current (Fig. 1.4). The surface circulation is generally counter-clockwise during this season. The circulation pattern during this period is similar to that in the north Pacific and the Atlantic Oceans. This flow starts in November. It is most intense during February and subsides by April (Wyrtki, 1973). Along the West coast of India, a branch of this flow moves northwards and brings in

low salinity surface water from the Bay of Bengal from November to January. Off Somalia the NE monsoon current turns south and merges with the South Equatorial Current.

With the onset of the southwest (SW) monsoon the current reversal takes place and the surface flow generally turns clockwise (Fig.1.4). The reversal starts in February and is complete by May. A strong northward flow off Somalia forming the Somali current is strongest during July. Off Sumatra the South Equatorial Current merges with the monsoon current and this then joins the Somali Current in the west and thus completes the gyre. Intense upwelling takes place along Somali and Arabian coast as a result of strong winds reaching speeds up to 30 knots (Smith and Bottero, 1977). There are also reports of upwelling along Southwest India (Banse, 1959, 1968; Sastry and D'Souza, 1972; Wyrtki, 1973; Shetye et al., 1990). This region has not been well explored and hence a major emphasis has been made during the course of this study to explore this region during the SW monsoon. Contrary to the earlier reports strong upwelling was observed on two occasions during SW monsoon of 1995 and 1997 with low surface temperature and high nitrate (Figs. 5.14, 5.15, 5.9, 5.13).

1.5. Hydrographic features of the Bay of Bengal:

The Bay of Bengal receives annually around 2700 km^3 runoff from large number of major rivers (Dr. Sen Gupta, unpublished data) resulting in nearly estuarine conditions. A major portion of the discharge (72%) into the Bay occurs during June to October as a consequence of the SW monsoon. There exists a sharp salinity gradient in the upper 100 m water column, with surface salinity of 32 ppt during non-monsoon season (Shetye et al., 1993). By the end of the SW monsoon the surface water to about 40 m has an isothermal structure. Salinity dominates the vertical stratification in this region in the upper 100 m in contrast

to other parts of world oceans where the temperature variation plays a major role in determining the upper water stratification.

With the onset of monsoon the river discharge spreads on the surface as a 200-300km wide low salinity tongue and moves south parallel to the coast (Fig. 1.4), without hugging the coastline (Shetye et al., 1991b). Simultaneously, a narrow band of upwelled more saline and cooler water flows swiftly northward hugging the coastline. This can, partially, be offset by the large river runoff. By November the SW monsoon withdraws and the NE monsoon sets in. The discharge decreases and as the wind pattern changes, a well developed equatorward current is seen all along the western boundary of the Bay (Cutler and Swallow, 1984). The low salinity water is confined to a 50 km

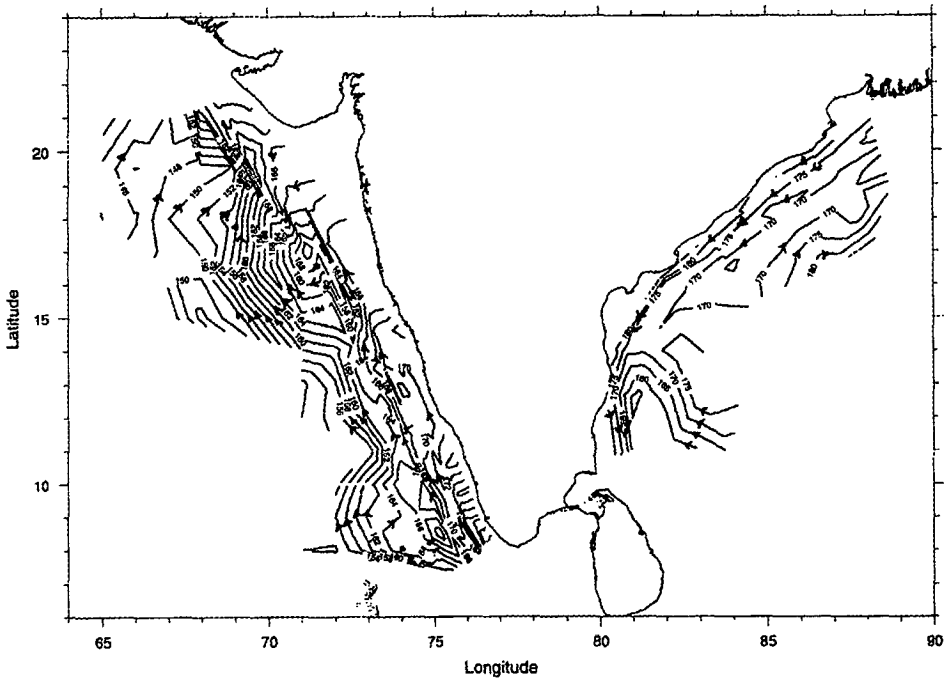

Fig.1.4 Dynamic Topography (dyn. cm) of the sea surface relative to 1000db during NE monsoon (Source: Shetye et al 1991a; Shetye et al 1993).

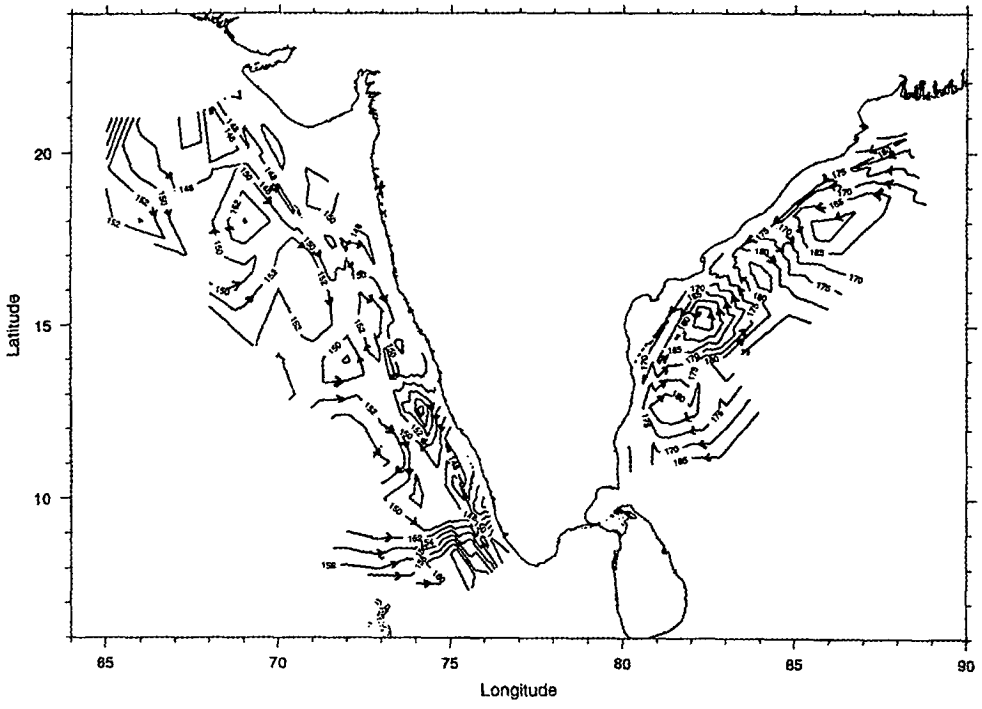

Fig.1.5. Dynamic Topography (dyn. cm) of the sea surface relative to 1000db during SW monsoon (Source: Shetye et al 1990; Shetye et al 1991b).

(Please note that different contour intervals have been used for Arabian Sea and Bay of Bengal to improve clarity)

wide band along the coast, with sinking and is carried all the way to the SW coast of India. With the onset of NE monsoon the surface cools down suddenly to 25°C and a subsurface maximum in temperature is seen. Normally this would lead to a convective mixing, but due to the salinity gradient this does not take place. The southward flow along the western boundary is best developed in November (Fig. 1.5) and by January this disintegrates (Shetye et al., 1993). During February a poleward western boundary current is the most conspicuous feature of surface circulation. This is analogous to the permanent Gulf Stream in the N. Atlantic and the Kuroshio in the N. Pacific. This persists during March - April and weakens in May and disappears by August (Shetye et al., 1993). The low salinity water accumulated in the surface of the Bay during SW monsoon gets mixes up with the underlying waters during this season. Salinity in other

parts of the Bay also gets reduced with the gyre circulating this low salinity water around. Generally speaking depth to depth, salinity in the Bay is lower than that in the Arabian Sea throughout the Arabian Sea

1.6. Objectives of the present Study:

1. *To study the temporal and spatial variability of the suboxic conditions and associated nitrogen cycling in the northern Indian Ocean.*

Due to the extremely delicate biogeochemical balance that exists in the Arabian Sea, this region is expected to be among the first to respond to future human-induced environmental and climatic changes. In order to evaluate the magnitude of such changes, the natural variability in the suboxic system must be known. The Arabian Sea is one of the three major oceanic sites where an acute oxygen deficiency within a large body of intermediate waters causes large scale microbially-mediated reduction of nitrate ions to molecular nitrogen (denitrification). Appreciable seasonal changes in the denitrification regime had been previously reported. One of the main objectives of this study was to evaluate the extent of this seasonality. A series of cruises were organised to investigate biogeochemical cycling within the Arabian Sea suboxic zone. Hydrochemical and hydrographic data were collected to get a measure of seasonal and interannual variabilities (for which purpose the very same stations were occupied during all the cruises).

2. *To investigate the nitrous oxide (N_2O) cycling in the Arabian Sea.*

The N_2O cycling in aquatic environments is greatly affected by the ambient O_2 levels. At O_2 concentrations approaching but not reaching suboxia large N_2O accumulation occurs, but when the O_2 concentrations are low enough to trigger denitrification, N_2O is itself utilised as an oxidant by bacteria. The Arabian Sea contains a variety of environments with varying O_2 levels. This makes the Arabian Sea an ideal site for studying the cycling of N_2O. Moreover, the Arabian

Sea also experiences unique mixing in the upper layer caused by the cooling of surface waters brought about by the cold, dry northeast monsoon winds blowing over the sea from the land. This results in the injection of new nutrients to the surface layer enhancing biological productivity. The thermocline water also has high levels of N_2O. Therefore, large emissions of this greenhouse gas to the atmosphere are expected to occur during the winter season.

3. *To understand cycling of methane in the Arabian Sea.*

Previous studies have shown that CH_4 levels in the surface waters of the Arabian Sea are higher than the oceanic average. It has been proposed that the high CH_4 supersaturation in surface waters could be sustained at least in part by the release of CH_4 from sediments along the Indian continental margin. On the other hand, the Arabian Sea which houses one of the most intense and thickest O_2 minima in the world oceans is expected to favour *in situ* production of CH_4 in the upper water column. Also, the coast of the Indian subcontinent is indented by numerous backwaters and estuaries endowed with extensive growth of mangroves. The contribution of these wetlands, potentially important sites of CH_4 production, to CH_4 cycling in the coastal zone has not been investigated.

4. *To estimate the fluxes of N_2O and CH_4 from the northern Indian Ocean and the coastal environments to the atmosphere during various seasons.*

Estimation of concentrations of climatically important gases such as N_2O and CH_4 and their fluxes across the air-sea interface from the Indian Ocean and their seasonal variability is important to budget the contribution by the tropical oceans to the global greenhouse effect. The work carried out previously demonstrated that air-sea fluxes of N_2O and CO_2 vary significantly with time. One of the major objectives of the present study is to estimate the seasonal flux of N_2O and CH_4 from the northern Indian Ocean and its coastal environments in detail. As previous samplings were confined largely to the non-monsoon months

and only to the open ocean, the data collected during the course of this work are expected to greatly improve estimates of the overall fluxes of N_2O and CH_4 from the Arabian Sea.

5. *To study the role of upwelling regions in the cycling of N_2O and CH_4*

Of the three centres of seasonal (southwest monsoon) upwelling in the northwestern Indian Ocean, located off the coasts of Somalia, Arabia and Southwest India, the one off the Indian coast has been least investigated, in spite of its unique physical forcing and unusual hydrography. Studies were undertaken during the monsoons of 1995 and 1997 to understand the biogeochemical cycling in this region. The eastern boundary upwelling zones have been known to be sites for rapid turnover of N_2O, due to the prevailing low oxygen levels in these regions. Hence detailed observations were made to study the upwelling related low oxygen environments off the SW coast of India to study the cycling of N_2O and its production mechanism. Contribution of CH_4 to these waters was also studied in detail, so as to understand its source in these regions.

6. *To apply stable isotopic tracers (natural abundance) as a tool to understand the mechanism of production and consumption of N_2O and to understand the implications of ocean-atmosphere exchange of N_2O in global cycling.*

The isotopic data on various dissolved nitrogen species can provide useful insights into the pathways of nitrogen transformations. Hence, measurements of $^{15}N/^{14}N$ in dissolved molecular nitrogen (N_2), nitrate (NO_3^-) and nitrous oxide (N_2O) and $^{18}O/^{16}O$ in N_2O, have been made in water column at several locations in the Arabian Sea. These measurements were aimed at understanding the microbially-mediated transformations in various nitrogen species so as to understand the pathway of cycling, especially the production and consumption of N_2O.

Moreover, the downward flux of ^{15}N- and ^{18}O-rich stratospheric N_2O requires large inputs of isotopically light N_2O to the troposphere, and it has been suggested that exchanges with the ocean, where light N_2O may be produced through nitrification, could help achieve the isotopic mass balance. One of the major emphasis of the present study is to understand the role of the oceans in balancing the stratospheric back flux and its implication in the global N_2O cycling.

2. Materials and methods:

The data presented were collected mainly on board FORV *Sagar Sampada* and partly on board ORV *Sagar Kanya*. While planning the cruises special emphasis were made on studying the low oxygen environments of the Arabian Sea. A wide range of geographical areas (Fig 1.2) and seasons were covered to include samples from regions where various processes such as upwelling, winter cooling, denitrification etc., were in progress. The details of the geographical positions occupied on each cruise and the sampling dates are presented in Table 2.1. The observations made on each of these cruises are given in Table 2.2.

In order to study the biogeochemical cycling of nitrous oxide and methane, observations were made during eight different cruises of ORV_*Sagar Kanya* and FORV *Sagar Sampada*. Nitrous oxide and supporting data on nutrients were invariably collected on all these cruises. Concurrent data on the two gases were collected only on two cruises. To quantify the fluxes from the coastal regions, seasonal surveys were made from the near- shore regions and estuaries using fishing trawlers. The boats used for the coastal and estuarine surveys were not equipped with analytical instruments. Water samples collected with 5-litre Niskin samplers were stored in an ice box and analysed immediately on arrival in the shore laboratory the same day.

2.1. Sampling and Analytical Procedures:

Temperature and salinity data were collected using a CTD (Seabird Electronics Inc., USA) system on both the ships. The salinity data was calibrated using a Guildline Autosal 8400. The Autosal in turn was calibrated using IAPSO standard. Similarly reversing thermometers were fixed to the Niskin bottles fitted

on the CTD rosette assembly and were triggered at discrete depths to calibrate the CTD System temperature data. Potential temperature and density were calculated using algorithms of Fofonoff (1977), the International Equation of State of Millero et al. (1980) and Bryden's (1973) formulations of adiabatic temperature gradient.

Table 2.1. Source of data.

Cruise	Station No	Date of Sampling	Lat °N	Lat mins	Long °E	Long min
SK 63	H13	14-Mar-91	17	59.80	88	59.90
SK 63	H12	15-Mar-91	18	57.00	88	44.00
SK 63	H10	15-Mar-91	19	43.60	88	30.40
SK 63	H03	16-Mar-91	20	37.30	88	14.90
SK 63	H6	16-Mar-91	20	13.91	88	23.50
SK 63	H8	16-Mar-91	20	2.10	88	26.60
SK 63	G1	17-Mar-91	19	50.80	86	26.20
SK 63	G3	17-Mar-91	19	42.30	86	34.00
SK 63	G7	18-Mar-91	19	13.10	86	51.60
SK 63	G9	18-Mar-91	19	41.00	87	15.30
SK 63	G10	19-Mar-91	18	0.20	87	47.30
SK 63	G11	19-Mar-91	17	15.60	88	17.30
SK 63	F11	19-Mar-91	16	27.14	88	56.85
SK 63	E13	23-Mar-91	14	47.92	85	12.60
SK 63	E12	24-Mar-91	15	32.64	84	39.21
SK 63	E10	24-Mar-91	16	16.40	84	6.10
SK 63	E8	25-Mar-91	16	50.79	83	44.33
SK 63	E6	25-Mar-91	17	2.64	83	44.37
SK 63	E4	26-Mar-91	17	11.04	83	24.57
SK 63	E2	26-Mar-91	17	17.62	83	19.91
SK 63	B1	02-Apr-91	12	43.05	80	18.66
SK 63	B2	02-Apr-91	12	42.84	80	28.58
SK 63	B4	02-Apr-91	12	40.47	80	39.43
SK 63	B6	02-Apr-91	12	38.86	80	50.94
SK 63	B8	02-Apr-91	12	36.51	80	10.18
SK 63	B11	03-Apr-91	12	29.86	83	0.31
SK 63	B10	03-Apr-91	12	30.37	81	59.46

SK 63	B12	04-Apr-91	12	29.43	84	0.33
SK 63	A12	04-Apr-91	10	59.67	83	54.05
SK 63	A5	07-Apr-91	10	47.90	80	20.84
SK 63	A4	07-Apr-91	10	46.64	80	17.76
SK 63	A3	07-Apr-91	10	45.40	80	12.25
SK 63	A2	07-Apr-91	10	42.82	80	6.18
SK 63	A1	07-Apr-91	10	40.95	80	1.03
SS 106	I14	28-Jan-93	15	0.00	68	0.00
SK 87	11	16-Sept-93	19	0.00	66	0.00
SK 87	13	17-Sept-93	21	0.00	66	0.00
SS 119	3201	11-Apr-94	17	0.00	68	0.00
SS 119	3202	13-Apr-94	18	0.00	67	0.00
SS 119	3204	14-Apr-94	19	45.00	64	37.00
SS 119	3203	14-Apr-94	19	0.00	66	0.00
SS 119	3205	18-Apr-94	19	0.00	67	0.16
SS 119	3206	19-Apr-94	15	59.90	68	0.01
SS 128	3247	19-Jan-95	15	22.00	73	19.00
SS 128	3251	20-Jan-95	15	16.00	72	41.00
SS 128	3249	20-Jan-95	15	21.00	72	49.00
SS 128	3248	20-Jan-95	15	23.00	73	7.00
SS 128	3254	20-Jan-95	15	0.00	72	1.00
SS 128	3253	20-Jan-95	15	9.00	72	24.00
SS 128	3252	20-Jan-95	15	12.00	72	32.00
SS 128	3250	20-Jan-95	15	17.00	72	45.00
SS 128	3255	21-Jan-95	15	0.00	71	0.00
SS 128	3256	22-Jan-95	14	57.00	70	3.00
SS 128	3257	22-Jan-95	14	50.00	69	0.00
SS 128	3258	23-Jan-95	15	58.00	67	58.80
SS 128	3259	23-Jan-95	14	55.00	66	53.00
SS 128	3260	25-Jan-95	17	0.00	67	58.80
SK 103	1	26-Jun-95	15	22.08	73	18.66
SK 103	3	27-Jun-95	15	22.32	72	49.92
SK 103	5	27-Jun-95	15	16.38	72	41.22
SK 103	8	27-Jun-95	14	59.64	71	59.58
SK 103	6	27-Jun-95	15	12.12	72	33.00
SK 103	7	27-Jun-95	15	8.40	72	24.30
SK 103	4	27-Jun-95	15	18.18	72	46.02
SK 103	2	27-Jun-95	15	22.92	73	6.90
SK 103	10	28-Jun-95	15	0.00	70	0.00
SK 103	9	28-Jun-95	15	0.12	71	0.00
SK 103	11	29-Jun-95	15	0.42	69	0.78
SK 103	12	29-Jun-95	15	0.00	68	0.12

SK 103	13	30-Jun-95	15	0.30	67	0.30
SK 103	14	30-Jun-95	15	0.12	66	0.12
SK 103	16	01-Jul-95	15	0.12	64	0.42
SK 103	15	01-Jul-95	15	0.66	64	59.52
SK 103	17	02-Jul-95	15	0.30	63	0.12
SK 103	18	02-Jul-95	15	3.00	62	3.96
SK 103	22	03-Jul-95	18	0.90	61	25.08
SK 103	19	03-Jul-95	15	40.63	62	0.99
SK 103	20	03-Jul-95	16	0.00	59	57.40
SK 103	23	04-Jul-95	19	0.54	62	0.54
SK 103	25	05-Jul-95	19	45.12	64	37.32
SK 103	24	05-Jul-95	20	1.56	62	36.78
SK 103	26	06-Jul-95	19	0.00	67	0.00
SK 103	27	07-Jul-95	17	0.00	68	0.54
SK 103	28	08-Jul-95	16	59.64	70	1.02
SK 103	32	10-Jul-95	8	46.86	75	48.12
SK 103	30	10-Jul-95	8	34.86	75	25.98
SK 103	31	10-Jul-95	8	42.00	75	37.92
SK 103	39	11-Jul-95	10	37.92	75	36.24
SK 103	35	11-Jul-95	8	59.16	76	19.14
SK 103	36	11-Jul-95	9	34.80	76	6.84
SK 103	37	11-Jul-95	10	11.04	75	53.34
SK 103	34	11-Jul-95	8	55.68	76	8.46
SK 103	38	11-Jul-95	10	47.04	75	41.16
SK 103	33	11-Jul-95	8	50.46	75	57.78
SK 103	41	12-Jul-95	10	30.00	75	15.00
SK 103	42	12-Jul-95	10	23.94	75	2.10
SK 103	40	12-Jul-95	10	34.08	75	25.08
SK 103	46	12-Jul-95	11	26.88	75	30.00
SK 103	45	12-Jul-95	11	21.84	75	22.20
SK 103	44	12-Jul-95	11	13.98	75	11.22
SK 103	43	12-Jul-95	10	20.10	74	51.06
SK 103	49	13-Jul-95	11	44.52	74	49.56
SK 103	52	13-Jul-95	11	30.84	74	20.10
SK 103	51	13-Jul-95	11	36.06	74	34.38
SK 103	50	13-Jul-95	11	38.04	74	39.06
SK 103	55	13-Jul-95	14	37.68	73	58.74
SK 103	47	13-Jul-95	11	51.12	75	9.00
SK 103	54	13-Jul-95	13	46.20	74	18.42
SK 103	48	13-Jul-95	11	46.98	75	1.92
SK 103	53	13-Jul-95	12	12.42	74	57.18
SS 136	3319	10-Sep-95	17	0.00	67	59.00

SS 136	3320	12-Sep-95	19	0.00	66	59.00
SS 136	3321	14-Sep-95	15	44.00	64	40.00
SS 136	3322	17-Sep-95	14	59.55	68	0.29
SS 136	3323	17-Sep-95	14	59.30	69	1.83
SS 136	3324	18-Sep-95	14	59.06	70	1.60
SS 136	3326	18-Sep-95	15	0.00	72	0.20
SS 136	3325	18-Sep-95	15	0.29	71	0.88
SS 136	3329	19-Sep-95	15	21.72	72	49.95
SS 136	3331	19-Sep-95	15	8.05	73	23.72
SS 136	3328	19-Sep-95	15	18.08	72	40.87
SS 136	3327	19-Sep-95	15	8.05	72	23.72
SS 136	3330	19-Sep-95	15	22.80	73	6.80
SS 141	3430	26-Apr-96	15	21.30	73	19.30
SS 141	3434	27-Apr-96	15	25.10	72	56.40
SS 141	3436	27-Apr-96	15	12.25	72	33.30
SS 141	3435	27-Apr-96	15	15.40	72	41.60
SS 141	3433	27-Apr-96	15	16.00	72	46.10
SS 141	3432	27-Apr-96	15	22.70	72	49.80
SS 141	3431	27-Apr-96	15	22.50	73	6.30
SS 141	3439	28-Apr-96	14	59.70	71	0.00
SS 141	3437	28-Apr-96	15	8.20	72	24.70
SS 141	3438	28-Apr-96	15	0.00	72	0.00
SS 141	3442	29-Apr-96	15	24.70	73	48.60
SS 141	3440	29-Apr-96	14	59.80	70	0.30
SS 141	3441	29-Apr-96	14	59.60	69	0.20
SS 141	3443	03-May-96	15	0.00	66	30.20
SS 141	3444	04-May-96	15	0.00	65	0.00
SS 141	3445	06-May-96	16	58.90	16	58.90
SS 141	3446	08-May-96	18	59.80	67	0.20
SS 141	3447	09-May-96	19	45.00	64	37.00
SS 141	3448	11-May-96	19	14.10	69	7.10
SS 141	3449	12-May-96	18	13.80	70	21.70
SS 141	3450	12-May-96	17	31.20	71	16.00
SS 141	3453	13-May-96	16	23.50	72	26.20
SS 141	3454	13-May-96	16	8.20	72	25.50
SS 141	3455	13-May-96	16	1.00	72	25.70
SS 141	3452	13-May-96	16	29.80	72	17.60
SS 141	3451	13-May-96	16	37.40	72	32.10
SS 150	3781	21-Nov-96	15	22.60	72	49.80
SS 150	3783	21-Nov-96	15	7.90	72	24.70
SS 150	3782	21-Nov-96	15	14.90	72	45.20
SS 150	3779	21-Nov-96	15	21.12	73	19.38

SS 150	3780	21-Nov-96	15	22.50	73	6.50
SS 150	3785	22-Nov-96	14	59.20	70	58.70
SS 150	3784	22-Nov-96	14	59.40	71	59.50
SS 150	3786	23-Nov-96	14	59.40	69	59.80
SS 150	3787	23-Nov-96	14	59.90	68	59.80
SS 150	3788	24-Nov-96	15	0.00	67	59.80
SS 150	3789	24-Nov-96	15	0.00	67	0.20
SS 150	3790	25-Nov-96	14	59.80	66	0.00
SS 150	3791	26-Nov-96	16	59.40	67	59.30
SS 150	3792	27-Nov-96	17	59.20	66	0.50
SS 150	3793	28-Nov-96	19	43.20	64	34.40
SS-150	3794	29-Nov-96	19	0.70	66	57.50
SS 150	3795	01-Dec-96	17	33.70	68	59.40
SK 121	7	09-Feb-97	20	0.00	63	59.80
SK 121	6	09-Feb-97	19	59.90	65	0.00
SK 121	8	09-Feb-97	20	0.00	63	0.00
SK 121	9	10-Feb-97	21	0.00	64	0.00
SS 158	3910	24-Aug-97	8	41.69	75	37.85
SS 158	3909	24-Aug-97	8	34.79	75	26.25
SS 158	3915	25-Aug-97	9	1.55	76	24.20
SS 158	3912	25-Aug-97	8	50.29	75	57.75
SS 158	3913	25-Aug-97	8	55.70	76	8.06
SS 158	3914	25-Aug-97	8	59.11	76	18.92
SS 158	3911	25-Aug-97	8	46.70	75	48.10
SS 158	3918	26-Aug-97	10	13.81	76	1.00
SS 158	3917	26-Aug-97	10	11.23	75	52.44
SS 158	3919	26-Aug-97	10	46.80	75	41.05
SS 158	3920	26-Aug-97	10	37.60	75	36.08
SS 158	3916	26-Aug-97	9	34.55	76	6.79
SS 158	3921	26-Aug-97	10	33.68	75	24.27
SS 158	3922	27-Aug-97	10	30.00	75	15.00
SS 158	3923	27-Aug-97	10	24.00	75	2.10
SS 158	3924	27-Aug-97	10	20.10	74	51.10
SS 158	3926	28-Aug-97	11	28.21	75	28.48
SS 158	3928	28-Aug-97	11	52.06	75	15.05
SS 158	3929	28-Aug-97	11	49.87	75	8.12
SS 158	3925	28-Aug-97	11	14.00	75	11.20
SS 158	3927	28-Aug-97	11	46.29	75	17.34
SS 158	3931	28-Aug-97	11	43.84	74	44.05
SS 158	3930	28-Aug-97	11	47.48	74	55.00
SS 158	3932	29-Aug-97	11	40.18	74	28.94
SS 158	3933	29-Aug-97	11	33.72	74	0.26

SS 158	3934	30-Aug-97	12	43.88	73	29.29
SS 158	3939	30-Aug-97	13	7.60	74	37.91
SS 158	3936	30-Aug-97	12	52.39	74	6.46
SS 158	3938	30-Aug-97	13	0.33	74	33.47
SS 158	3937	30-Aug-97	12	52.39	74	12.98
SS 158	3935	30-Aug-97	12	48.32	73	56.76
SS 158	3940	31-Aug-97	14	7.80	73	18.23
SS 158	3945	31-Aug-97	14	28.02	74	15.12
SS 158	3942	31-Aug-97	14	19.63	73	45.90
SS 158	3941	31-Aug-97	14	11.72	73	29.53
SS 158	3944	31-Aug-97	14	28.07	74	10.11
SS 158	3943	31-Aug-97	14	23.87	74	0.15
SS 158	3946	01-Sep-97	15	8.33	72	24.42
SS 158	3947	01-Sep-97	15	16.04	72	41.42
SS 158	3949	01-Sep-97	15	22.64	73	7.13
SS 158	3950	01-Sep-97	15	21.65	73	19.16
SS 158	3951	01-Sep-97	15	20.54	73	37.86
SS 158	3948	01-Sep-97	15	22.41	72	49.88
SS 158	3953	02-Sep-97	15	13.30	73	47.00
SS 161	3995	04-Jan-98	14	59.96	68	59.67
SS 161	3997	05-Jan-98	14	59.55	70	59.58
SS 161	3996	05-Jan-98	15	0.06	69	59.13
SS 161	3998	06-Jan-98	15	1.06	72	0.37
SS 161	3999	06-Jan-98	15	8.17	72	23.63
SS 161	4000	06-Jan-98	15	20.95	72	49.92
SS 161	4001	06-Jan-98	15	21.09	73	18.87
SS 161	4002	07-Jan-98	15	20.85	73	39.84
SS 161	4003	10-Jan-98	17	0.00	67	59.95
SS 161	4004	13-Jan-98	17	59.70	64	59.61
SS 161	4005	14-Jan-98	19	43.70	64	37.08
SS 161	4006	15-Jan-98	19	59.96	62	59.99
SS 161	4008	16-Jan-98	21	44.83	64	59.90
SS 161	4007	16-Jan-98	21	44.70	63	21.05
SS 161	4009	17-Jan-98	21	45.10	66	30.15
SS 161	4010	18-Jan-98	18	59.75	67	0.22
SS 161	4011	20-Jan-98	16	56.08	70	34.47

Table 2.2.Observations made on various cruises.

Cruise	CTD	Nutrients	N_2O	CH_4	DO	N isotopes
SK 63	yes	yes	yes	no	yes	no
SS 106	yes	yes	no	no	yes	yes
SK 87	yes	yes	no	no	yes	yes
SS 119	yes	yes	yes	no	yes	yes
SS 128	yes	yes	no	no	yes	yes
SK 103	yes	yes	yes	no	yes	yes
SS 136	yes	yes	no	no	yes	yes
SS 141	yes	yes	yes	yes	yes	yes
SS 150	yes	yes	yes	no	yes	no
SK 121	yes	yes	yes	no	yes	no
SS 158	yes	yes	yes	yes	yes	no
SS 161	yes	yes	yes	no	yes	no

All samples for the chemical analysis were collected using Niskin samplers fixed on the rosette of the CTD system. First sub-samples were drawn for dissolved oxygen, followed by samples for nitrous oxide and methane, after this the samples for nutrients were collected. While sampling for the gas analysis, care was taken not to introduce any atmospheric contamination. While the dissolved oxygen samples were fixed with the Winkler reagents, the nitrous oxide and methane samples were fixed with saturated mercuric chloride solution (2ml per litre of sample) and were analysed within twenty-four hours of collection. However, methane analysis could be done only after reaching the shore laboratory and may have been subjected to some amount of error, although enough care was taken to stop the bacterial action by the addition of mercuric chloride and gas exchange through the lid by wrapping the bottles airtight with plastic sheets. Experiments have shown that poisoned seawater samples can be stored for atleast one year without producing any measurable change in methane over the concentration range of 0.5 to 6 nM (Tilbrook and Karl, 1995).

2.2. Nutrients:

Onboard *Sagar Sampada* the samples were analysed using a four channel Technicon autoanalyser, while on board *Sagar Kanya* the samples were analysed for nutrients using a six channel SKALAR autoanalyser 5100/1 (Grasshoff et al., 1983). The nutrient estimations were done immediately after collection, however if there was a delay in the analysis the samples were refrigerated and analysed within twelve hours of collection. For uniformity the standards were prepared in bulk and stored aseptically in ampoules. During the US JGOFS inter-calibration cruise these bulk nitrate and nitrite standards were compared with the standards from Scripps Institution of Oceanography Ocean Data Facility (SIO/ODF). These standards compared well with each other and the deviation between the two set of standards was $\pm$ 0.04% (Codispoti and Morrison, 1995).

Nitrite was estimated by the method described by Bendschneider and Robinson,(1952).

Nitrate was analysed by the cadmium - mercury amalgam method of Morris and Riley (1963) as modified by Grasshoff (1964).

Inorganic Phosphate by the method described by Murphy and Riley (1962).

Dissolved oxygen was estimated by the Winkler method as modified by Carpenter (1965).

2.3. Analysis of Dissolved Nitrous Oxide:

The estimation of nitrous oxide was done by the multiple phase equilibration technique as described by Mcauliff (1971). In an airtight 60 ml plastic syringe, which had been flushed with helium, 25ml of the seawater sample was drawn without any atmospheric contact. To this sample 25ml helium was injected, without any atmospheric contamination and equilibrated for 5

minutes by vigorous shaking. The head space was then injected into a 3ml loop via a 10cm length (1cm diameter) drierite column and this 3ml was in turn injected into the main stream of the GC- system using a 6-Port high temperature rotary Carle valve. Argon - Methane gas mixture (95/5 - vol/vol) with a flow rate of 20ml min^{-1} was used as the carrier gas. The GC used was a Hewlett Packard 5890 Series II Gas Chromatograph equipped with an Electron Capture Detector (ECD) containing 10mCi ^{63}Ni foil operated at 300 °C. A stainless steel column packed with Porapak-Q (mesh 80/100) maintained at 80 °C was used for separation of N_2O. The sample was extracted twice more with 25ml aliquots of helium and similarly injected into the GC. The GC signal was obtained in the form of peak area, by interfacing the GC to an integrator. The precision of the analysis was ~4%. A standard mixture of 510ppb N_2O in nitrogen (Gas standards, Alltech Associated Inc., IL. USA) and several dilutions of this was used for calibration. Standards were run at the beginning and end of every set of samples and to check the drift in the equipment conditions a number of air samples were run in between. The column was conditioned periodically by baking it at 150 °C with the carrier gas flowing through to remove traces of impurities which might accumulate in the column over a period of analysis. Percent saturation was computed with reference to the solubility given in Weiss and Price (1980). The gas transfer velocity to compute the flux across the ocean - atmosphere boundary was obtained from the model of Wanninkhof (1992).

2.4. Nitrous oxide data processing:

The log of the peak area of each extraction is plotted against the extraction number and the slope (z) and intercept (I) of each sample is computed. The initial concentration (C_{N2O}) is obtained from the equation,

$$C_{N2O} = I / (z-1) \qquad (2.1)$$

2.5. Analysis of Dissolved Methane:

A 100ml glass syringe was used instead of the 60ml syringe as in N_2O analysis. 50ml of seawater sample was drawn into the syringe without atmospheric contamination and equilibrated with an equal volume of helium. A larger sample volume was used in the analysis of methane to efficiently flush the 5ml sample loop used in this case. The larger loop was used to increase the sensitivity of the analysis. Otherwise the analysis and quantification followed was the same as that of nitrous oxide. A Hewlett Packard 5890 Series II Gas Chromatograph equipped with a Flame Ionisation Detector (FID) operated at 250°C was used. A stainless steel column (1.5 m length, 3.2 mm diameter) packed with molecular sieve 5A (mesh 80/100, Alltech Associates, Inc., USA) maintained at a temperature of 40°C was used for separation of methane, with nitrogen as the carrier gas. The instrument response, monitored through frequent injections of air samples, was quite linear within the range of concentrations encountered during the course of this study. Several dilutions of a standard (Scotty II Analysed Gases) procured from Supelco, Inc., USA were used for calibration. All carrier gases and combustion gases used in the analysis were of ultra-pure grade supplied by Bhoruka gases Bangalore or Speciality gases, Bombay. The precision of the method expressed as the coefficient of variation based on replicate (n=10) analysis of one sample was $\pm$ 0.8 %. Equilibrium solubility of CH_4, calculated according to Wiesenburg and Guinasso (1979), was combined with the observed concentration to determine the air sea concentration gradient, which in turn was multiplied by the transfer velocity to get the CH_4 flux across the air-sea interface. The gas transfer velocity was obtained from the model of Wanninkhof (1992).

2.6. Nitrogen Isotopes:

Isotopic measurements on three dissolved nitrogen species (N_2, NO_3^- and N_2O) were made during four cruises of FORV *Sagar Sampada* (SS106, November 1992; SS119, April 1994; SS128, January 1995; and SS141, May

1996) and two cruises of ORV *Sagar Kanya* (SK87, September 1993; and SK103, June-July 1995) at the stations shown in Fig. 6.1. However, concurrent measurements on all these species were made only at one station (3204/SS119). While the $^{15}N/^{14}N$ ratio was measured in N_2 and NO_3^-, both $^{15}N/^{14}N$ and $^{18}O/^{16}O$ were determined in N_2O.

Water samples for $^{15}N/^{14}N$ analysis in N_2 and/or NO_3^- were taken during SK87, SS119, SS128 and SS141 from 1.8-litre Niskin samplers mounted on the CTD (conductivity-temperature-depth) rosette. Utmost care was taken to avoid atmospheric contamination while sampling for N_2. Sub-samples (200-250 ml) were drawn immediately after recovery into evacuated, $HgCl_2$ poisoned 500-ml glass bottles. The N_2 extraction and analysis was done at the University of Washington using a Finnigan MAT 251 mass spectrometer (Brandes *et al*, 1998). Reproducibility was within $\pm$0.05 ‰. Subsamples (1 litre) for NO_3^- were stored after poisoning with 1 ml saturated $HgCl_2$ for analysis at the University of Washington following the method described by Brandes and Devol (1997). Briefly, it involved reduction of NO_3^- to NH_4^+ using Devarda's alloy. The NH_4^+ was distilled and sorbed into ion sieve. The sorbed material was then filtered onto quartz QM-A filters and sealed into evacuated quartz combustion tubes containing Cu and CuO. Ampoule contents were converted into N_2 with a micro-Dumas combustion method, extracted into liquid N_2-cooled cold fingers containing molecular sieve and analysed for $^{15}N/^{14}N$ using a Finnigan MAT 251 mass spectrometer. The results, reproducible to $\pm$0.2 ‰ were corrected for an isotopic shift of -0.9 ‰ to account for the reagent blank.

Samples for the N_2O isotope analysis were collected using specially modified 20-litre Go-flo samplers mounted on a hydrowire (during SS106 and SK87) or a CTD rosette sampler (during SS119 and SK103). The modified samplers enabled extraction of N_2O, without transferring the water to another vessel, with high-purity argon that was recirculated after removal of moisture and

CO_2 and adsorption of N_2O on molecular sieve (MS 5A) packed in stainless steel columns. Extraction was carried out (Fig.2.1) for 90 minutes at an Ar flow rate of ~1.5 l min^{-1} (Yoshinari *et al*, manuscript in preparation). After thermal desorption in the shore laboratory, N_2O was purified by gas chromatography and its isotopic composition ($^{15}N/^{14}N$ and $^{18}O/^{16}O$) measured at Woods Hole Oceanographic Institution by continuous-flow isotope-ratio monitoring using a Finnigan MAT 251 mass spectrometer (Yoshinari *et al*, 1997). Reproducibility was better than $\pm$0.3 ‰ for both isotopes.

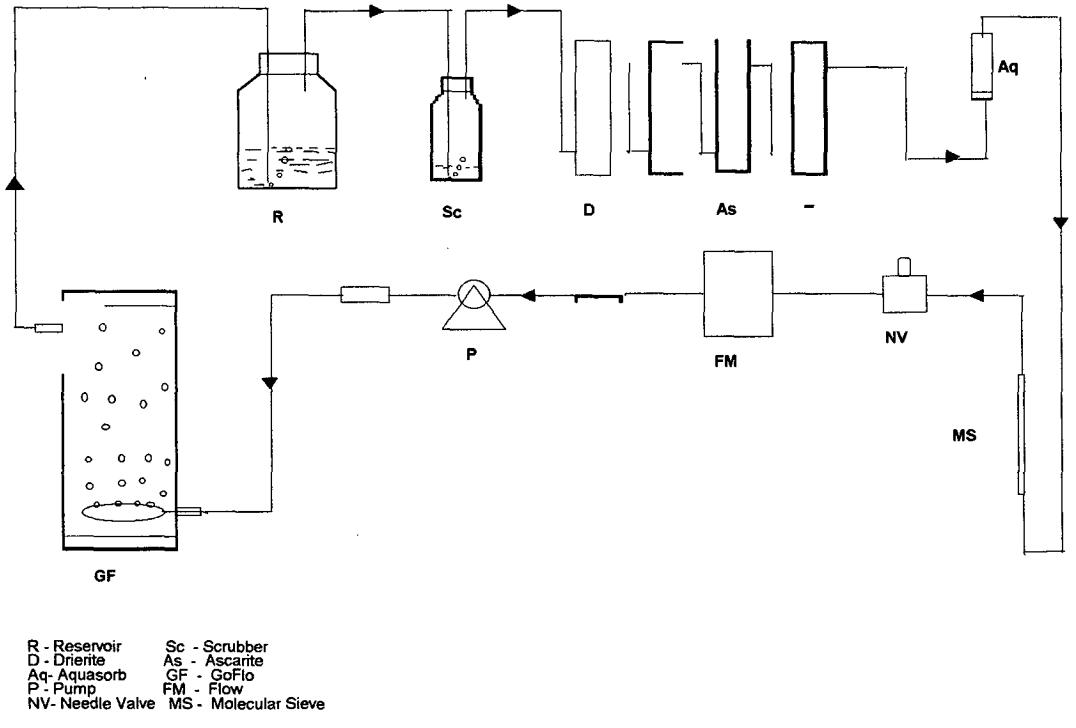

Fig. 2.1 Schematic diagram of system to quantitatively recover dissolved N_2O in seawater

3. Distribution of Methane in the Northern Indian Ocean:

3.1. Introduction:

As compared to the terrestrial sources, the emission rate of CH_4 to the atmosphere from the oceans appears to be quite modest, ranging from 0.40 Tg yr^{-1} (1 Tg = 10^{12} g) by Bates et al. (1996) to 11-18 Tg yr^{-1} by Bange et al. (1994). These represent 0.1-4% of the total atmospheric flux of CH_4 from all natural and anthropogenic sources (Crutzen, 1991). However, the atmospheric emission of CH_4 from the oceans are not uniformly distributed geographically with the continental shelves and estuaries, which occupy a small area of the world oceans, accounting for as much as 75% of the total oceanic CH_4 emission (Bange et al., 1994).

Previous studies on CH_4 in the northwestern Indian Ocean have revealed that its concentrations in surface waters and consequently its flux to the atmosphere from this region are several folds higher than the oceanic averages (Owens et al., 1991; Patra et al., 1998). It has been proposed that the high CH_4 supersaturation in surface waters could be sustained at least in part by the release of CH_4 from sediments along the Indian continental margin (Karisiddaiah and Veerayya, 1994, 1996). On the other hand, the Arabian Sea is a highly productive area which also contains one of the most intense and thickest O_2 minima in the world oceans the upper portion of which (~150-500 m) is strongly reducing (Qasim, 1982; Sen Gupta and Naqvi, 1984; Naqvi, 1994). These conditions are expected to favour *in situ* production of CH_4 in the upper water column (Owens et al., 1991). Finally, the coast of the Indian subcontinent is indented by numerous backwaters and estuaries endowed with extensive growth of mangroves. The contribution of these wetlands, potentially important sites of CH_4 production, to CH_4 cycling in the coastal zone has not been investigated. An

assessment of the relative importance of these sources in regulating the CH_4 distribution in this region forms the principal objective of the present study.

Most of the data used in this study were collected during two cruises of FORV *Sagar Sampada* (SS141 and SS158) undertaken in April-May, 1996 and August-September, 1997, corresponding to the premonsoon and southwest monsoon seasons, respectively. Some observations were also made in the estuary (in both seasons) and along a short shallow section just north of the mouth of the river Mandovi in Goa during the monsoon (September 1997). Station locations are shown in Fig.3.1. The stations occupied during SS141 formed an east-west transect off Goa extending well into the suboxic (denitrifying) zone of the open central Arabian Sea (Naqvi, 1991). This section was repeated, up to the shelf break, during SS158 as well. However, the primary objective of the latter cruise was to investigate the effect of upwelling off the southwest Indian coast (Banse, 1968), and for this purpose four additional cross-shelf sections were worked at between Quilon in Kerala and Karwar in Karnataka.

Results and Discussion

3.2. Methane Distribution in Waters over the Continental Shelf:

Concentrations of CH_4 recorded in coastal surface waters during the monsoon cruise ranged from 2.6 to 20.3 nM, corresponding to saturations of 140-1091%. The near-bottom shelf waters at some stations were characterised by significant CH_4 enrichment relative to the surface; at other stations particularly those forming the shallowest parts of the sections the maximal concentrations were found at the surface or mid-depth (Fig. 3.2a-e). The most conspicuous feature seen in all the sections is the strong onshore-offshore gradients at all the depths with the concentrations decreasing rapidly offshore.

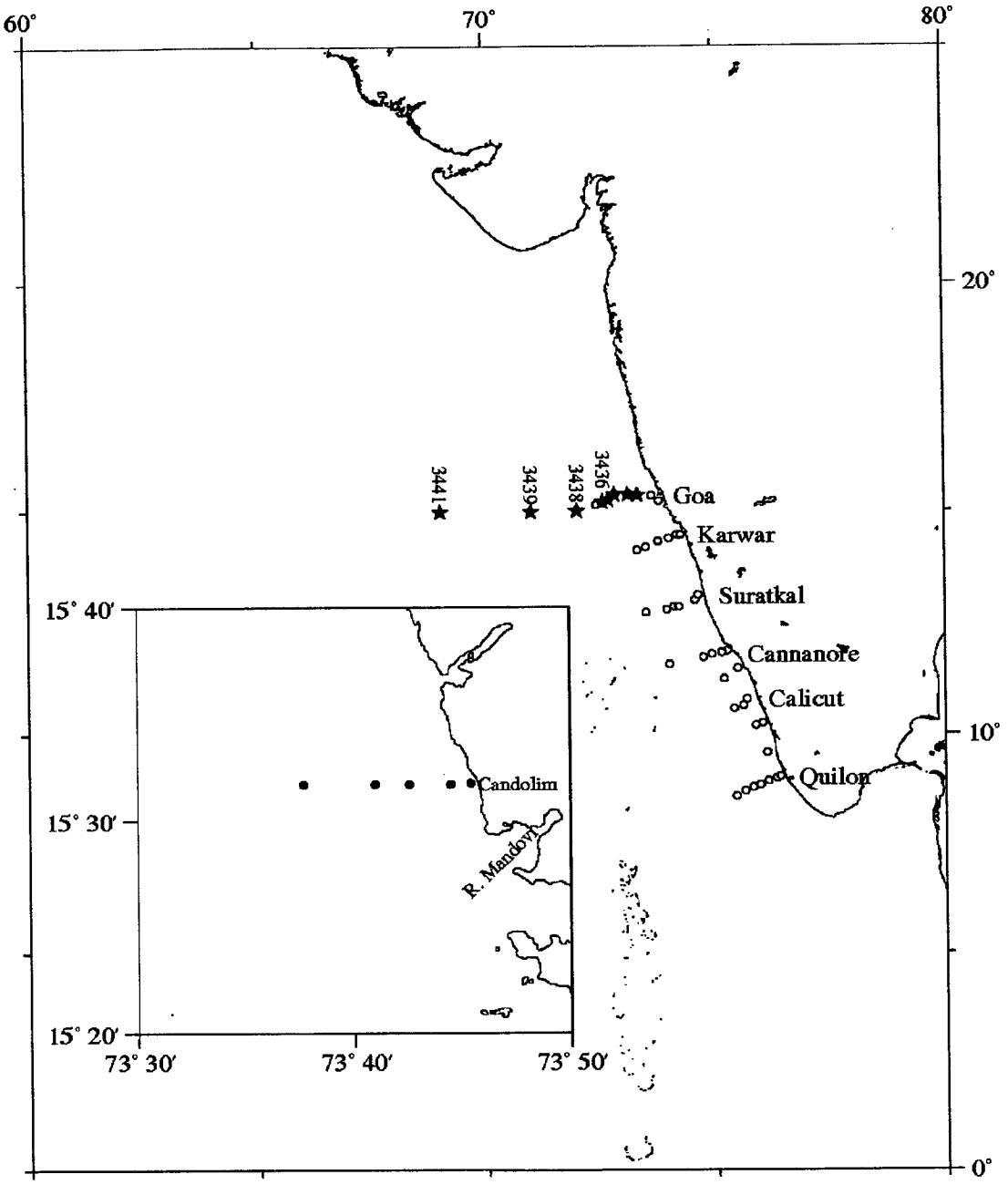

Fig.3.1. Station location for methane studies

The three possible factors that could combine to produce the observed distribution are (a) supply from the sediments, (b) production in the water column, and (c) inputs from the coastal wetlands.

3.3. Sedimentary Supply:

Sedimentary supply of CH_4 may occur through bacterial degradation of organic matter (biological source) at shallow depths in sediments and also by thermal cracking of kerogens (geological source) (Floodgate and Judd, 1992). Seepage from the geological source may be limited to specific regions, but the biological source is expected to be more widespread given an adequate supply of organic matter and an availability of suitable reducing sites. Conditions conducive for the biological production of CH_4 in the sediments and at the sediment-water interface appear to exist along the shelf off the west coast of India due to copious supply of organic carbon to the sediments from land as well as overlying water column (Paropkari et al., 1987) where, as will be seen later, very high rates of primary production are supported by coastal upwelling during the monsoon. Moreover, the upwelled water covering the shelf sediments is extremely depleted in O_2 (Banse, 1968). The supply and preservation of organic matter in the present inner shelf region should have been even higher during the late Pleistocene-early Holocene when the sea level was lower and the monsoon had greatly intensified in response to the precession-related peak in the northern hemisphere summer insolation centred around 11,000 years Before Present (Van Campo, 1986).

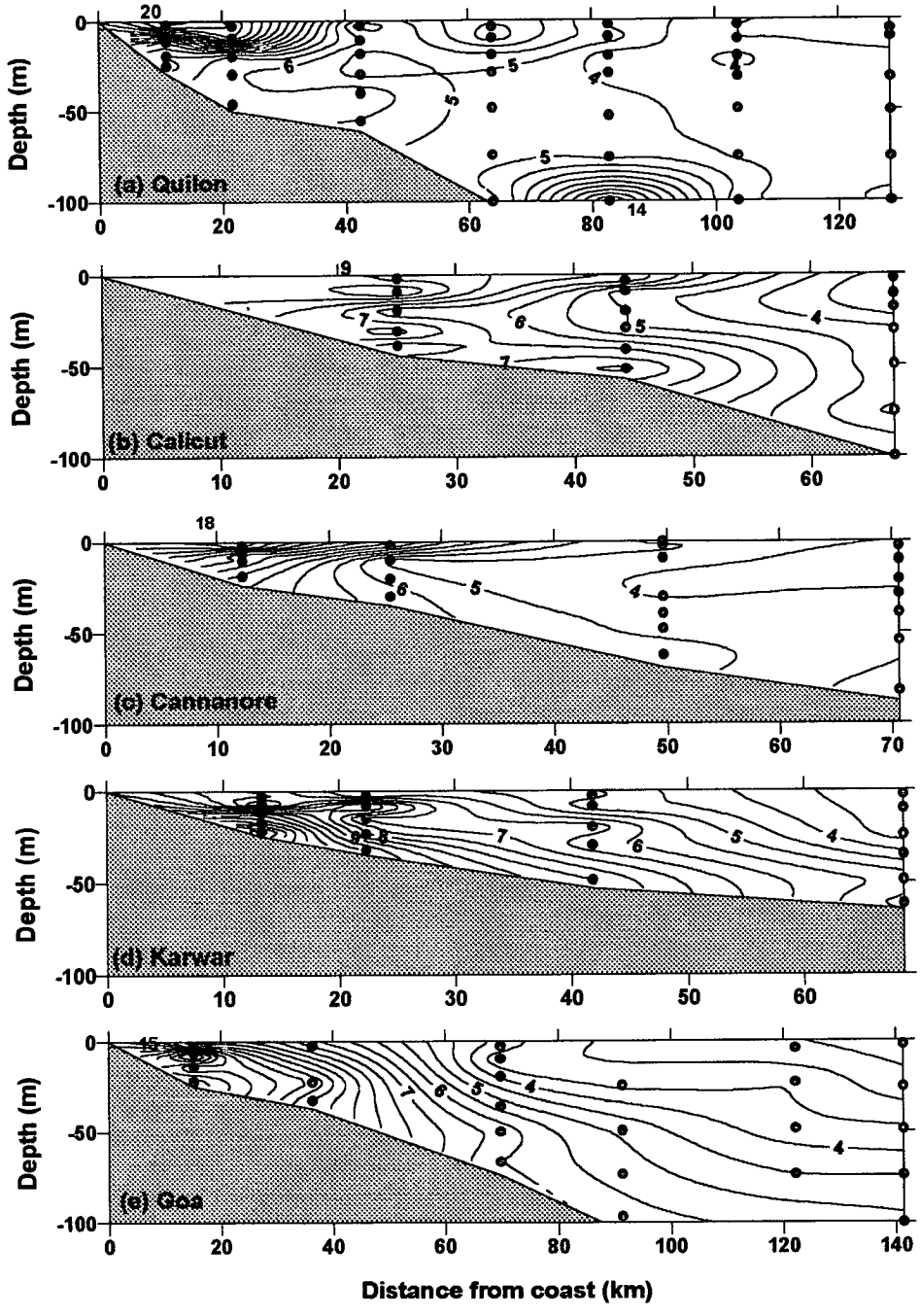

Fig.3.2. Distribution of methane (nM) during SW monsoon along five transects on the shelf off SW India.

Karisiddaiah and Veerayya (1994, 1996) have hypothesised that this organic matter could have served as the main biogenic source for the accumulation of CH_4 within the shallow inner shelf sediments. Presence of such gas-charged sediments a few metres below the seafloor, inferred from the

occurrence of acoustic maskings during seismic surveys, is also supported by limited chemical measurements in sediments (Siddiquie et al., 1981). The total inventory of CH_4 trapped in the gas charged sediment of the inner continental shelf off western India has been estimated as 2.6 Tg (Karisiddaiah and Veerayya, 1994, 1996). These authors also proposed that the diffusion of CH_4 from the sediments to the overlying water column, estimated as 0.039 Tg y^{-1} [very nearly the same as the net atmospheric flux from the Arabian Sea reported by Owens et al. (1991)], could be important in sustaining high CH_4 saturation in the Arabian Sea surface waters. However, given the above estimates the sedimentary CH_4 inventory would be depleted in just (2.6/0.039=) 67 years, and so the estimated sedimentary CH_4 flux, if real, must be supported presently by a high rate of methanogenesis. It is pointed out here that while some near-bottom CH_4 enrichment is generally seen off Goa both during the monsoon (Fig. 3.2e) and premonsoon (Fig.3.3) seasons, with lower levels occurring during the latter period, these concentrations (5-6 nM) are in no way anomalously high. Indeed, as it will be shown later, these are generally lower than the maximal CH_4 concentrations in the open Arabian Sea (also see Owens et al., 1991; Patra et al., 1998). It is possible that the supply from the gas-charged sediments is episodic or that the seepage occurs at specific locations. Moreover, the diffused gas may be rapidly consumed by micro-organisms through aerobic (Rudd and Taylor, 1980) and anaerobic (Alperin and Reeburgh, 1984) oxidation. In any case, the present results clearly show that the sedimentary inputs from the eastern Arabian Sea do not produce large CH_4 anomalies in the overlying water column such as those seen in areas of known hydrocarbon seepage (e.g. Cynar and Yayanos, 1991).

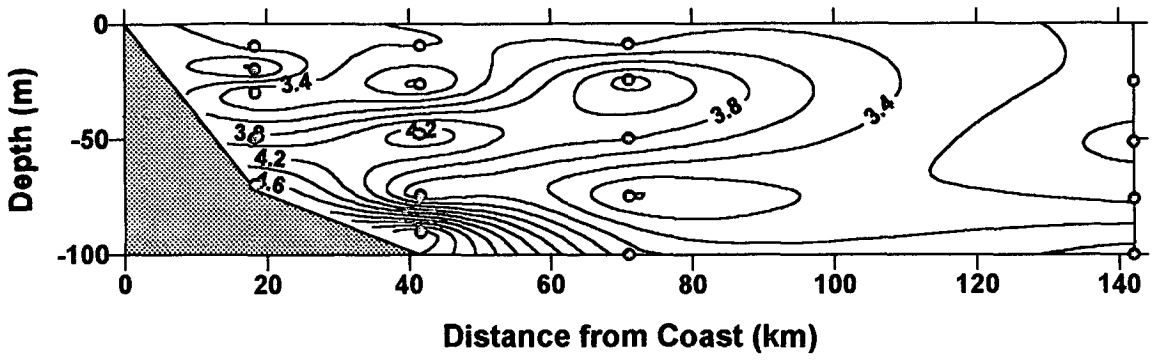

Fig. 3.3. Methane distribution off Goa during premonsoon.

3.4. Land Drainage and In-situ Production

As stated above, the coastal zone off the central and southwest coasts of India experiences intense upwelling during the monsoon. The physical processes that cause this upwelling appear to be complex. Studies by Shetye et al. (1990) led them to conclude that it was largely forced by local winds. But it is now generally recognised that while the wind stress may be an important contributing factor, particularly in the southern region, it cannot by itself account for the observed upwelling intensity, and that a remote forcing by winds in the Bay of Bengal may be equally, if not more, important (McCreary et al., 1993). In addition to the unique physical forcing, the other interesting aspect of the hydrography of this region is that the upwelled water is invariably capped by a thin (5-10 m) lens of fresher water which originates in part from the local precipitation and in part from runoff from the narrow coastal plain that receives heavy monsoon rainfall. The combination of upwelling and precipitation plus land runoff results in the property

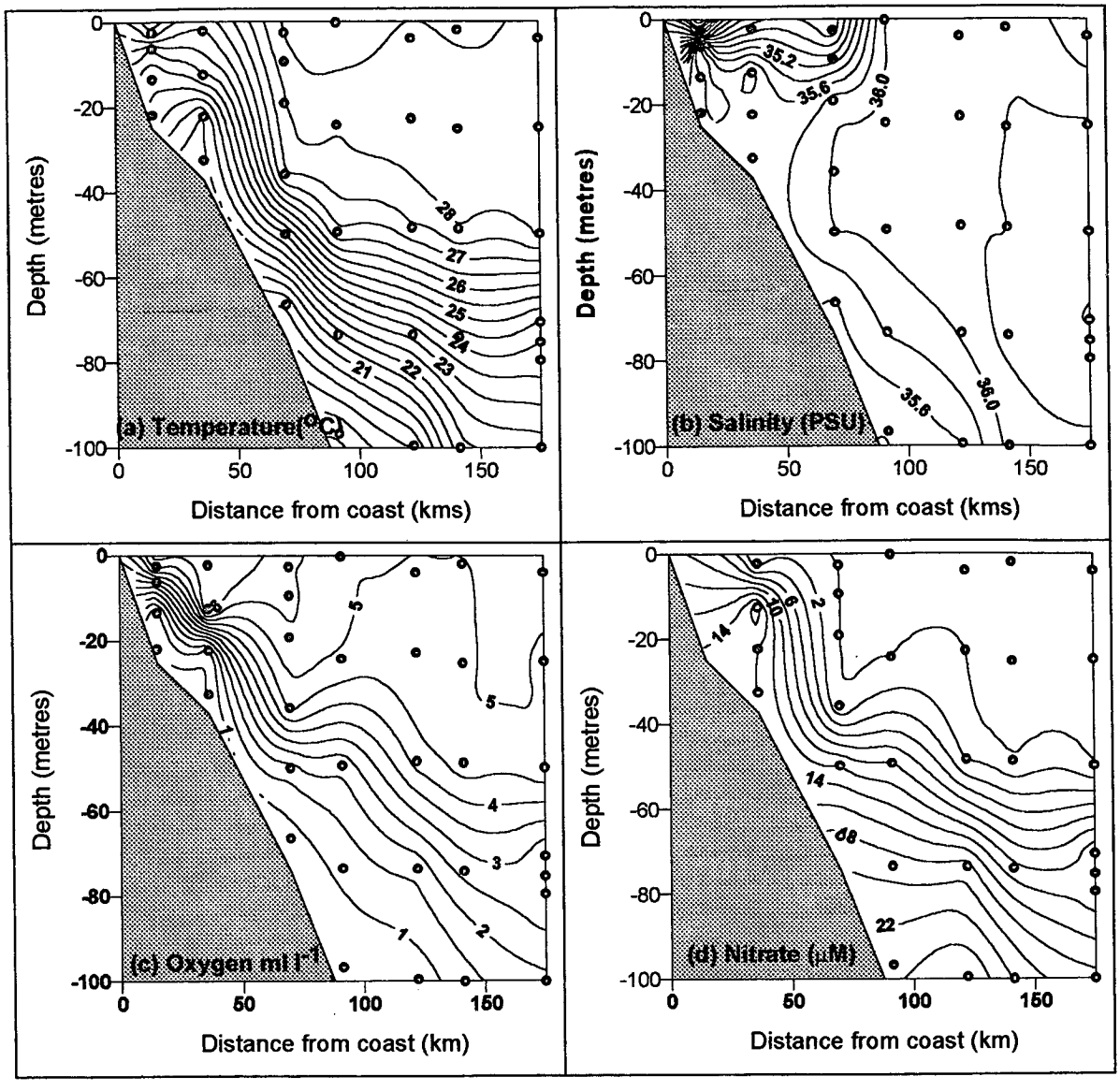

Fig. 3.4. Distribution of temperature, salinity, dissolved oxygen and nitrate off Candolim (Goa) during the SW monsoon.

distributions shown in Fig.3.4a-d along the transect off Goa which is typical of all transects occupied during SS 158. Large vertical and horizontal gradients in all the properties are conspicuous in these sections. The low-salinity lens extending ~80 km from the coast of Goa was characterised by sharply decreasing CH_4 concentrations offshore indicating that the CH_4-rich surface waters originated from the land or at the land-ocean boundary. In order to investigate this

phenomenon in detail, observations were carried out at five closely-spaced stations along a short transect perpendicular to Candolim beach just north of the mouth of the river Mandovi (Fig.3.1 inset). As expected, the highest CH_4 concentration (47.6 nM corresponding to a saturation of 2521%) was associated with the lowest salinity (25.3) (Fig.3.5a). Further support for the large riverine inputs of CH_4 is provided by the data collected within the estuary during the same season (Fig. 3.6). The average CH_4 concentration at the river mouth was 57.9±12.7 nM

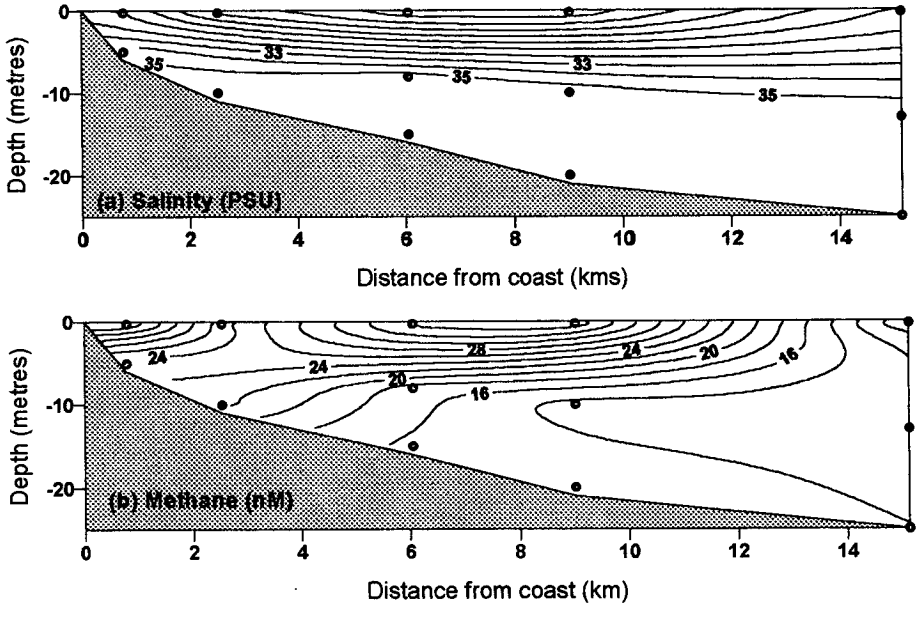

Fig.3.5. Distribution of (a) salinity and (b) methane (nM) off Candolim (Goa) during the SW-monsoon

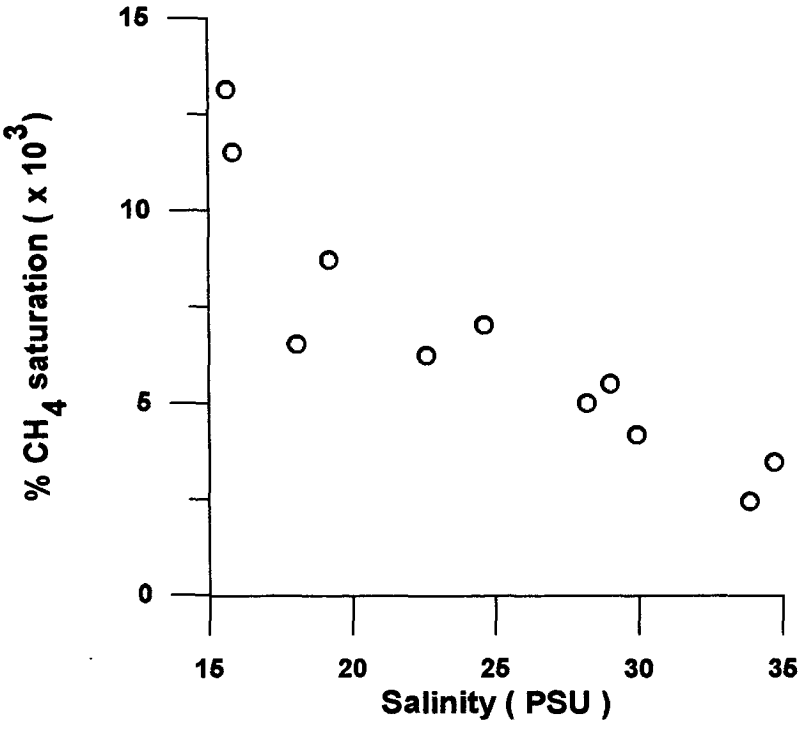

Fig.3.6. Plot of methane saturation (%) versus salinity in the Mandovi estuary (Goa)

(3334±712% saturation); these are almost twice the corresponding values during the premonsoon (32.6±25.2 nM and 1818±1396%, respectively). The highest values were recorded at the freshwater-end of the estuary (248.1nM and 13133%) decreasing almost conservatively towards the seawater-end (Fig. 3.6) during the monsoon season. Thus, it is evident that large amounts of CH_4 are added to coastal waters from the adjacent wetland ecosystems, which comprise extensive mangroves, during the wet season. However the effect of this is not felt a long distance offshore.

The fresher water "lid" occurring during the monsoon season causes strong stratification and prevents the upwelled water from reaching the sea surface, except at very shallow depths and presumably under very turbulent conditions. However, since the thermocline is very shallow, the upwelled waters, which are highly enriched with nutrients, should still be well lit by the Sun (Fig.

3.4d) supporting high rates of biological production. Measurements of primary productivity made at seven coastal stations during SS 158 by the ^{14}C uptake method yielded an average value of ~300 mgC m^{-3} d^{-1} at the surface and about twice as much at ~10 m depth (J. Kurien, unpublished data). The consequently high biological demand in the stratified subsurface layer in conjunction with the already low O_2 content of the upwelled water leads to the development of suboxic conditions in the water column very close to the sea surface (Fig. 3.4c). The high primary production is expected to support rich zooplankton biomass and provide conducive conditions for *in situ* production of CH_4 in the water column as well as at the sediment water interface through availability of suitable sites for methanogenesis. The suboxic conditions would further aid the development of microenvironments within particles within which CH_4 could be produced (Karl and Tilbrook, 1994). Moreover, the shallow depths and high turbulence would keep these particles in suspension (the CTD-light transmission data showed the occurrence of thick bottom nepheloid layers at all these stations), resulting in their recycling and presumably greater release of CH_4 from their interiors. This might account for the generally high CH_4 concentrations with frequent subsurface maxima observed during the monsoon. However, it should also be pointed out that as the CH_4 oxidation is favoured by high combined nitrogen levels (Rudd et al., 1976; Harrits and Hanson, 1980), its rate is also expected to be high in the upper layers of the eastern Arabian Sea during the monsoon. This together with a vigorous air-sea exchange aided by strong winds may be responsible for the rapid offshore decline in CH_4 concentration.

3.5. Methane Distribution in the Open Arabian Sea

Profiles of CH_4 at four open ocean stations in the central Arabian sea are shown in Fig.3.7. Two CH_4 maxima were observed in almost all the profiles. The weakly-developed primary maximum was located in the upper 50 metres while the more pronounced secondary maximum was found between 150 and 200 m depths. CH_4 concentrations invariably decreased below 200 m at all the stations.

Oceanic surface waters are supersaturated with respect to atmospheric CH_4 the world over presumably due to its production through *in situ* biological processes (Sieburth, 1987). Since the bacterial production of CH_4 cannot take place in oxic environments (Wolfe, 1971), it is believed to be formed mostly within the reducing interiors of particles; evidence for existence of such a source has been provided by Owens et al. (1991), Karl and Tilbrook (1994) and Marty et al. (1997) through incubation experiments. However, since CH_4 is oxidised by bacteria and also lost to the atmosphere through gas exchange, the shape of its vertical profile must be determined by the balance between *in situ* biological production and consumption, and its inputs and removal by physical processes of diffusion, advection and gas exchange. Thus a "typical" CH_4 profile in the ocean with a subsurface peak normally found within the pycnocline (e.g., Brooks and Sackett, 1973; Scranton and Farrington, 1977; Brooks et al., 1981; Burke et al., 1983; Owens et al., 1991; Patra et al., 1998) can be explained by a decrease in CH_4 production rate with depth (Karl and Tilbrook, 1994) coupled with a high loss rate in the surface layer which could overwhelm the high potential CH_4 production rate at shallow depths (Burke et al., 1983). Possible departures from this "typical" profile in the Arabian Sea might be caused by its unique geographical setting (leading to, for example, a greater quasi-horizontal transport) and the resultant unusual biogeochemistry (for example, widespread suboxia at mid-depths) that distinguishes this region from most other parts of the open ocean.

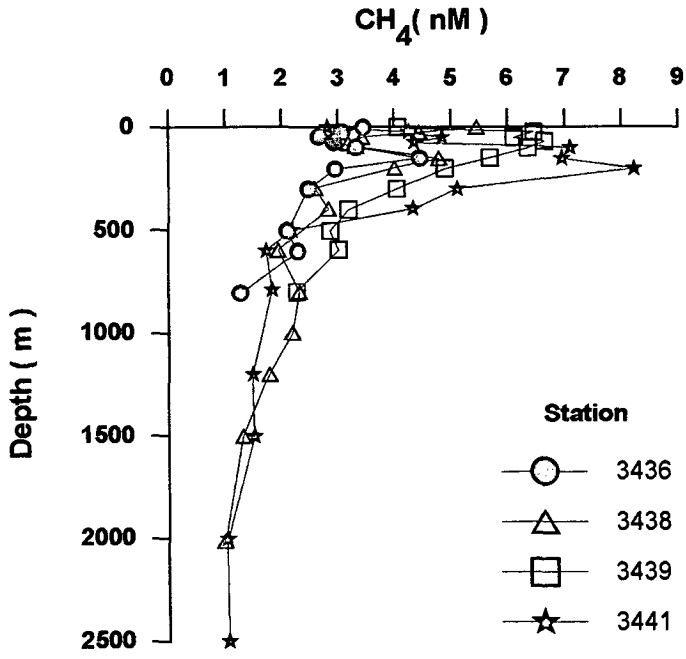

Fig.3.7. Vertical profiles of methane at four open ocean sites

For most parts, however, the vertical distribution of CH_4 in the Arabian Sea is qualitatively typical of the open ocean. The subsurface CH_4 maximum (the deeper maximum in this case) is, of course, the most important feature generally occurring close to the top of the pronounced O_2 minimum (Fig.3.8; also see Owen et al. (1991) and Patra et al. (1998)). The available data seem to suggest that the CH_4 concentration at this maximum may be affected by the intensity of the O_2 minimum and associated denitrification in this layer. Of the four open ocean stations occupied during the course of this study, the highest concentration (~4 μM) of nitrite (NO_2^-), an indicator of the denitrification intensity - see Naqvi (1991) was recorded at the most offshore Sta. 3741; the concentration of CH_4 at this station was also maximal at this site similar intensification of the CH_4 maximum within the denitrifying layer, not recognised previously, could be seen in the earlier data sets as well. For example, Fig. 2 of Owens et al. (1991) shows a deepening and intensification of the CH_4 maximum at Stas. 5-7 which were located within the denitrifying zone (Mantoura et al.,

1993). Similar trend is discernible at Stas. 6-15 in Patra et al.'s (1998) Fig. 2. Finally, the two stations (4 and 5) worked by Burke et al. (1983) in the eastern tropical North Pacific's suboxic zone also show elevated CH_4 levels within the suboxic layer, although the absolute CH_4 concentrations were lower than those in the more oxygenated waters at Sta. 3 which was located in the frontal zone immediately to the north of Sta. 5. There are two possible explanations for this relationship. First, the denitrifying layers are invariably associated with pronounced suspended particle maxima (e.g., Fig. 3.8) in the two regions (Garfield et al., 1983; Naqvi et al., 1993). Bacteria, which show a biomass maximum at these depths (Ducklow, 1993; Ward et al., 1998) are believed to constitute a very significant part

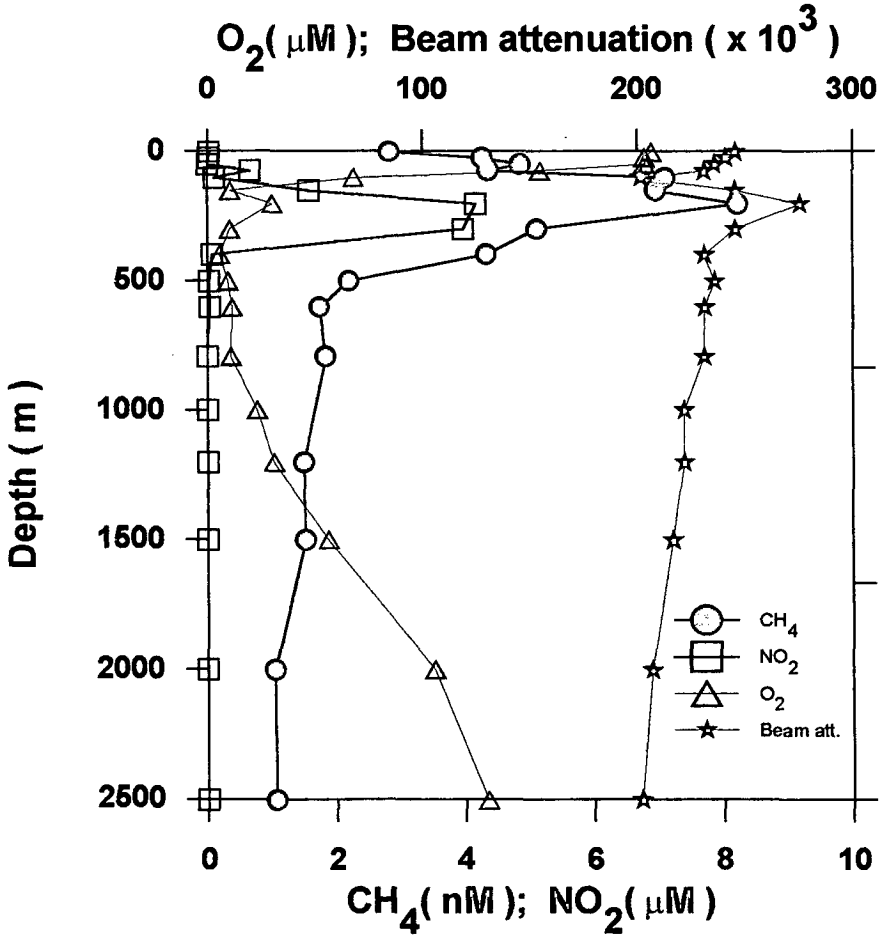

Fig. 3.8. Vertical profiles of methane, DO, NO_2, and beam attenuation at station 3441 (15°N 69°E)

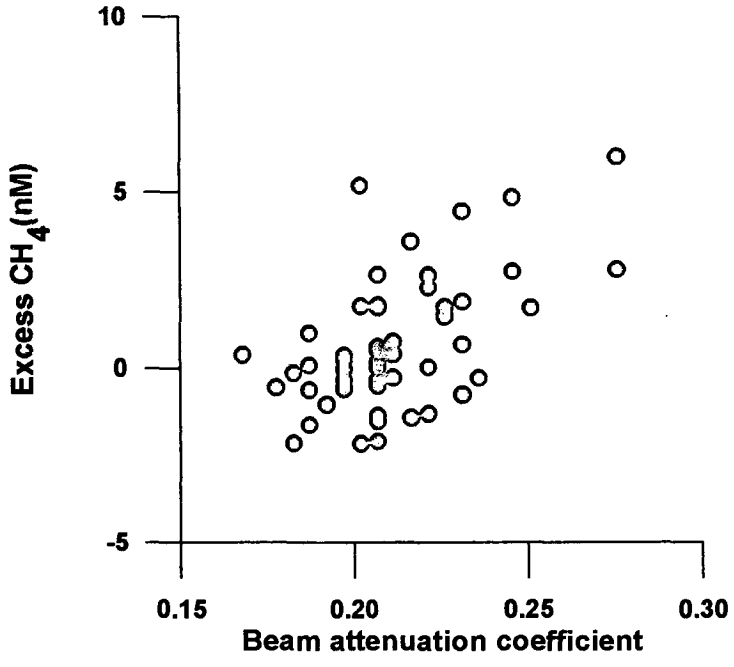

Fig.3.9. Plot of excess methane versus beam attenuation coefficient in the suboxic zone

of this "particulate" matter. But elevated CH_4 levels may be expected if some of these "particles" support methanogenesis. A relationship between water turbidity (represented by the beam attenuation coefficient) and CH_4 is suggested by the present data (Fig. 3.9), but the relationship is not always one-to-one in that peaks in the beam attenuation coefficients and CH_4 do not always coincide (also see Burke et al., 1983). The second, more likely, explanation is that, owing to the extremely low O_2 contents of the NO_2^- bearing waters (<0.02 ml/l as measured colorimetrically by S.W.A. Naqvi during the US JGOFS Process Study), the activity of CH_4 oxidisers may be greatly constrained. This view is reinforced by the rapid decreases in CH_4 concentration just above the suboxic (denitrifying) zone where the O_2 concentrations rise rapidly (Fig. 3.8). In any case, it would appear that the main subsurface CH_4 maximum in the Arabian Sea, as in other oceanic environments, is produced *in situ* (Owens et al., 1991) rather than being formed as a result of advection from the shelf. The latter

possibility was favoured by Patra et al. (1998) who proposed that the CH_4 maximum was associated with the Arabian Sea high salinity surface water (ASHSW) formed in the northern Arabian Sea. However, this hypothesis is not subscribed on several counts. First, it requires unreasonably high volume of ASHSW production. Secondly, the depth of CH_4 maximum in the central Arabian Sea is too deep for the ASHSW. Thirdly, as stated earlier, the maximal CH_4 concentrations in the central Arabian Sea are actually higher than those found in the near bottom waters of the continental margin off India making it unlikely that the CH_4 is supplied into the ocean interior from the marginal sediments.

The cause of the shallower CH_4 maximum observed during the present study [which was also occasionally observed by Patra et al. (1998)] is less certain. One possibility is that the waters with higher CH_4 concentrations may be sandwiched between two layers where the rate of CH_4 loss is higher: above this horizon (at the sea surface) CH_4 may be lost rapidly through exchange with the atmosphere while below it (within the thermocline) its oxidation may be favoured by high combined nitrogen concentrations. At or just above the subsurface chlorophyll maximum (SCM), however, high O_2 and relatively low nitrate (NO_3^-) concentrations may severely constrain bacterial oxidation of CH_4. Alternately, a higher rate of CH_4 production may occur at the SCM either due to phytoplankton metabolism (Scranton and Brewer, 1977) or in the guts of zooplankton (Scranton and Brewer 1977; Alldredge and Cohen 1987; Paerl and Prufert, 1987), which are expected to be concentrated in this layer for grazing. However, the correlation between the CH_4 maximum and SCM is quite patchy (Owens et al., 1991; Patra et al., 1998).

An interesting aspect of the present data is that the shallower CH_4 maximum was right at the surface at stations sampled at night. As diurnal variation at the same location could not be studied, all the surface saturation values were plotted against the sampling time (Fig. 3.10). It is possible that the

suggested trend, with the lowest saturation around noon and the highest around midnight may be real eventhough there is considerable scatter in the data, probably arising from the variable population density of the plankton. This aspect of CH_4 distribution warrants detailed investigation.

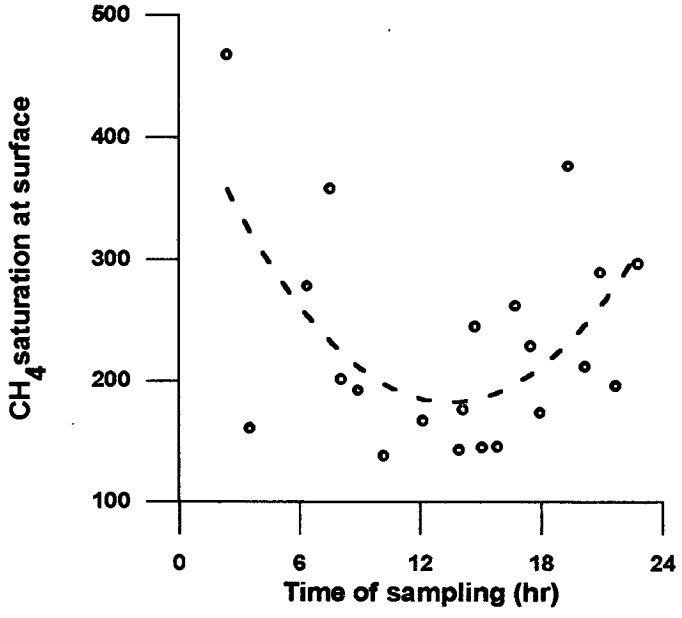

Fig.3.10. Plot of surface methane saturation in the open ocean versus time of sampling

4.6. Conclusion:

In conformity with previous reports the results obtained during the course of this study also show higher-than-average CH_4 emissions from the Arabian Sea with a pronounced seasonal variability. While the waters over the continental shelf are significantly more enriched with CH_4 relative to the open ocean, particularly during the monsoon season when fairly intense upwelling takes place off the central and southwest coasts of India leading to the development of suboxic conditions at shallow depths, near-bottom methane anomalies such as those reported from other regions of known hydrocarbon seepage, are not seen in this region. Instead the maximal CH_4 concentrations are frequently seen either at the surface, associated with the low-salinity water

mass which caps the upwelled water, or at mid-depth, indicating that the major sources of high CH_4 saturation are the *in situ* production and supply from the land-sea interface. Extremely high CH_4 concentrations are observed in the Mandovi estuary presumably due to intense production in coastal wetlands. However, the large onshore-offshore gradients occurring during the wet season indicate rapid loss due to air-sea exchange and CH_4 oxidation.

The pronounced subsurface CH_4 maximum in the open ocean appears to occur within the upper portion of the suboxic (denitrifying) water close to the intermediate nepheloid layer supporting the view that the maximum is produced *in situ* from particulate matter at a depth where the vanishingly low O_2 levels might suppress the oxidative loss. An advective origin of the maximum, suggested previously, is not supported by the data. In addition, another weaker maximum is also seen in the upper well-oxygenated layer. It is speculated that this feature is formed either due to plankton metabolism or through a lower rate of CH_4 loss relative to the overlying or underlying waters. The shallower maximum may also show diurnal changes, but this aspects needs to be confirmed by future studies.

4. Nitrate Deficit

4.1. Introduction:

The Arabian Sea houses one of the world's largest oceanic oxygen deficient environments. Both the Arabian Sea and the Bay of Bengal are enclosed on three sides and are open only to the south. As a result of this, subtropical convergence does not exist in the northern Indian Ocean. It has long been believed that the circulation at depth was weak and the intermediate depth waters were renewed slowly (Dietrich, 1973), and this was regarded as the main factor responsible for the development of oxygen deficient conditions culminating in denitrification (Wyrtki, 1973; Sen Gupta and Naqvi, 1984). However, more recent works have shown that the intermediate waters are renewed at a much faster rate than believed earlier (Naqvi 1987, Somasundar and Naqvi, 1988; Olson et al., 1993). Thus the development of oxygen deficient conditions may be due to excessive oxygen consumption combined with the low oxygen content of waters responsible for renewal (Swallow, 1984; Naqvi 1987). However, the mechanisms of the rapid mid-depth ventilation remain largely unknown. It is difficult to study the circulation in the intermediate waters using direct current measurements. One way of studying this process is by using chemical tracers such as nitrite and nitrate deficits. The nitrate deficit, a measure of the extent of gaseous nitrogen production through denitrification, can be estimated using 'NO' (Naqvi and Sen Gupta, 1985). Introduced by Broecker (1974), NO is a conservative biogeochemical tracer, originating from the Redfield stoichiometry (Redfield et al., 1963),

$$(CH_2O)_{103}(NH_3)_{16}(H_3PO_4)+135\ O_2 \rightarrow 103\ CO_2+16HNO_3+H_3PO_4+119H_2O \quad (4.1)$$

Which suggests that roughly one mole of nitrate is regenerated for every nine moles of oxygen consumed in the aerobic degradation of phytobiomass, in the sea.

The results of computation of nitrate deficits combined with nitrite are used here to investigate the renewal of intermediate waters in the northern Arabian Sea and the role of circulation in supplying oxygen to the suboxic environment. Data were collected along mostly zonal sections at 15°N during SK103 (July 95), SS 141 (May 96), SS 150 (November 96) and SS 161 (January 98). Repeated observations were also made at three locations (Fig. 4.1) - 19° N 67°E (Location A), 19.75°N 64.62°E (Location B), and 17°N 68°E (Location C). The cruises during which these stations were occupied are listed in Table 4.1. Combining data collected during the course of this work with those obtained during the US JGOFS, temporal changes in the suboxic environment could be studied at a reasonable resolution from April 1994 to November 1996 at location A.

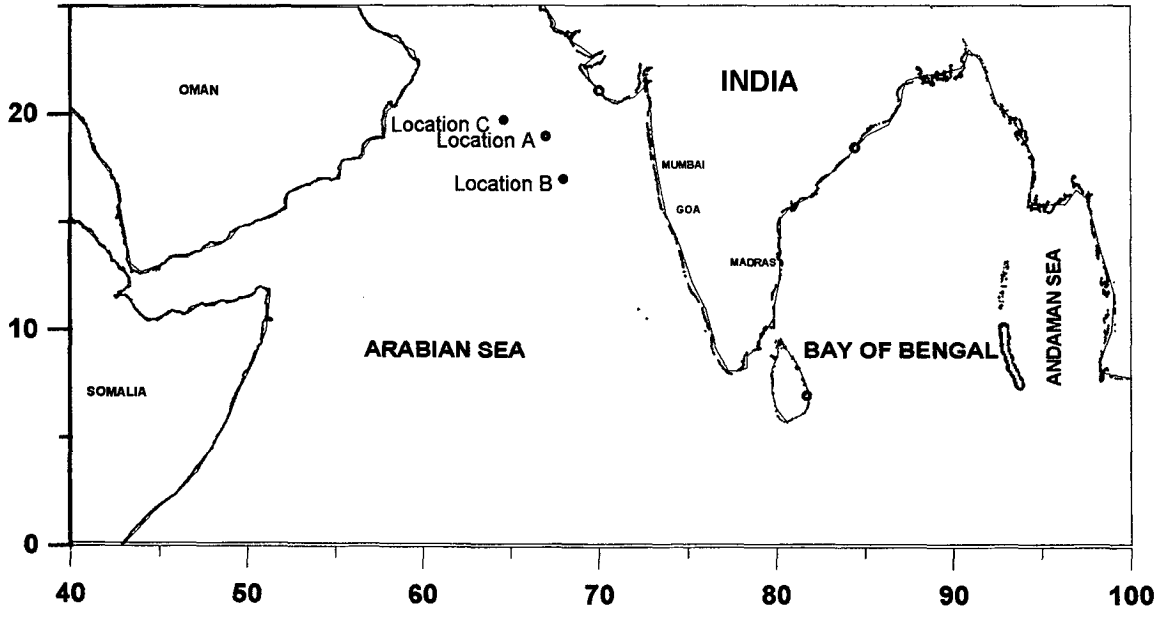

Fig.4.1. Sampling positions

Table 4.1. Cruises during which observations were also made at locations A, B and C.

Location	Positions	Cruises
A	19°N 67°E	SK103, SS119, SS136, SS141, SS150, SS161 USJGOFS- 39,43, 45, 49, 50, 53, 54
B	19.72°N 64.62°E	SK103, SS119, SS136, SS141, SS150, SS161
C	17°N 68E	SK103, SS119, SS136, SS150, SS161

4.2. NO Computation:

For calculation of NO, as suggested by Naqvi et al. (1990) a value of 9.1 for - $\Delta O_2/\Delta NO_3$ was used instead of 8.65 employed by Naqvi and Sen Gupta (1985):

$$NO = O_2 + 9.1(NO_3+NO_2) \qquad (4.2).$$

To determine the relationship between 'NO' and potential temperature(θ), the method of Naqvi et al. (1990) was followed. All the data collected along and south of 15°N during different cruises were pooled together and NO was plotted against θ (Fig 4.2). The observed relationship is linear in two ranges with a discontinuity at $\theta \simeq 12$°C. All samples with potential temperatures ≤ 9 were

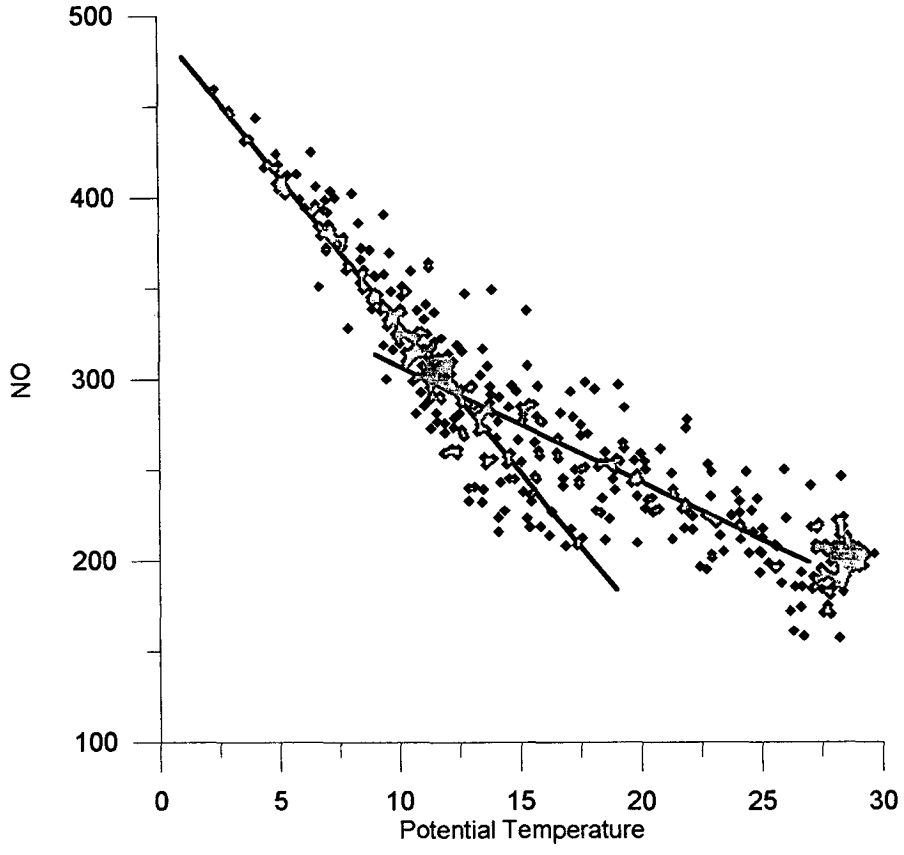

Fig. 4.2 NO-θ Plot for stations along and south of 15°N

considered to quantify the relationships of NO with θ in the deep waters. The relationship between NO and θ is visibly linear below this level. As only ca 5% of the deficits produced in the overlying waters will diffuse through its lower boundary (Naqvi, 1987) the corresponding error can be ignored. For $17 \leq \theta \leq 27$ data collected from stations south of the active denitrification zone were used. Stations which were located south of 15°N and which did not show any detectable secondary nitrite were only utilised for this purpose. Samples with $\theta > 17$ were not considered, because it was felt that above this level horizontal mixing with low nitrate water may modify NO. The relationship was fairly linear in the selected range. The least square regressions are given by the equations:

$$NO = -8.532\theta + 418.564 \quad 17 \leq \theta \leq 27 \qquad (4.3)$$

$$NO = -16.137\theta + 493.505 \quad \theta \leq 9\ °C \qquad (4.4)$$

The point of intersection of the two line at θ = 9.854 was treated as a physical discontinuity . Thereby, expected NO was computed for all the samples using equation (4.3) for $\theta \geq 9.854$ °C and equation (4.4) for $\theta < 9.854$ °C. Nitrate deficits (ΔN) were computed from the equation,

$$\Delta N = (NO-O_2)/9.1 - (NO_3+NO_2) \qquad (4.5)$$

4.3. Results and Discussion:

Overall the deficits were found to be the lowest during the Pre-SW monsoon and the highest during the NE monsoon seasons. Along 15°N, maximum deficit was observed in the depth range of 200 and 300m, during all the observations except in November, where it was centred around 200m. The highest deficits were observed during November, followed by July. The section during January extended only up to a distance of 500 km and here the highest deficit observed was 7.5 μM NO_3; the highest ΔN for November was 13μM NO_3 and during May and July it was 7 and 8 μM NO_3 respectively.

At the most north-western station, location B, high values of ΔN were found at depths varying between 300 and 450m, at different times of the year. Further east at location A, the highest deficit was almost invariably around 300m, without much inter- annual or intra-annual variations. At location C although the temporal variation is high, the depth of maximum ΔN varied within a narrow range (250 - 300 m). Again at all these locations, the lowest deficit was observed between April and July after which an increase in ΔN was noticed. The deficits at location A was higher than the other two locations, the deficits here was invariably over 9 μM NO_3. However during the NE monsoon period the deficits went further up, as much as 14 μM NO_3.

4.4. East-West Sectional Distribution During SW Monsoon Season:

During the SW monsoon there appears to be a break in the ΔN distribution centred around 200 km from the coast and extending up to the shelf (Fig. 4.3.a). This feature is also reflected in the nitrite field (Fig.4.3.b). These low NO_2^-, low ΔN waters are fresher (S>35.4) indicating their origin in the south. Previously, Naqvi et al. (1990) reported the advection of a water mass from the south with its core centred around 400 m some 200 km from the coast. Shetye et al. (1990) described a shallow (75 - 100m) equatorward surface current during the SW monsoon season (June -August). Below this, they saw signatures of downwelling indicating a poleward undercurrent hugging the continental slope. This undercurrent is a common feature of coastal circulation in the eastern Pacific and Atlantic ocean (Wooster and Reid, 1963; McCreary, 1981). Similar features can also be seen in the 15° N section during the SW-monsoon in the present study (Fig.4.3.c.), with the high salinity water mass in the upper ~150m hugging the coast. However the poleward undercurrent is restricted to the SW monsoon season off the west coast of India (Shetye et al., 1990). The thermal structure is characterised by upsloping isotherms indicating upwelling (Fig.4.3.d.). Below this watermass, the poleward undercurrent described by Shetye et al. (1990) can be identified, marked by downwelling (isotherms at 150, 250 and 400m) and low salinity. The upper water coming from the north has relatively high ΔN and high NO_2^-. The undercurrent bringing in O_2 - rich waters from outside the denitrification zone (Fig.4.3.e.) obviously accounts for the low ΔN and NO_2^-, values off the continental margin below the upper 150m.

4.5. East-West Sectional Distribution During NE Monsoon Season:

Shetye et al. (1991a) described the circulation in the eastern Arabian Sea during the NE monsoon and found in accordance to the previous studies, a reversal of the coastal currents relative to those during the SW monsoon season. The Equatorial Surface Water flow northward along the west coast of India. This fresher, lighter and warmer watermass is about 400 km wide and 200 m deep around 10°N. The current narrows northward and at around 22°N the flow, restricted mainly to the continental slope, is 100 km wide and 400 m deep (Shetye et al., 1991a). Below the poleward surface flow (at depths> ~250 m), an equatorward undercurrent along the continental slope has been suggested to exist. Some of these features can be seen in fig. 4.4.c and 4.4.d. A watermass with lower salinity (S<35.5) above 400 m depth extending off the continental margin to a distance of about 400 km is clearly discernible (Fig.4.4.c.). The nitrite (Fig.4.4.b.) and nitrate deficit plots (Fig.4.4.a.) also confirm that this water mass originates from the south as in this water mass the low nitrate deficits are associated with no nitrite up to about 400 km from the coast.

Although, November is not a true representative of either the NE or SW monsoon, (the reversal of currents start by October), it would appear that the poleward undercurrent may continue for some time after the SW monsoon. Using the data collected during January-February, Naqvi et al. (1990) reported that the nitrate deficits and nitrite extended nearly up to the shelf during this season. During the observations made in January 1998, nitrite extended nearly up to the coast (Fig. 4.5.b.) and nitrate deficits which could be seen only up to a distance of 400 kms from the coast during November (Fig.4.4.a.) extended up to the shelf (Fig.4.5.a.). The distribution during November could result from a time lag in reversal between surface and subsurface waters and/or the cumulative effect is seen well after the current during the SW monsoon has ceased to be active. However, the dissolved oxygen content of the upper mid-water

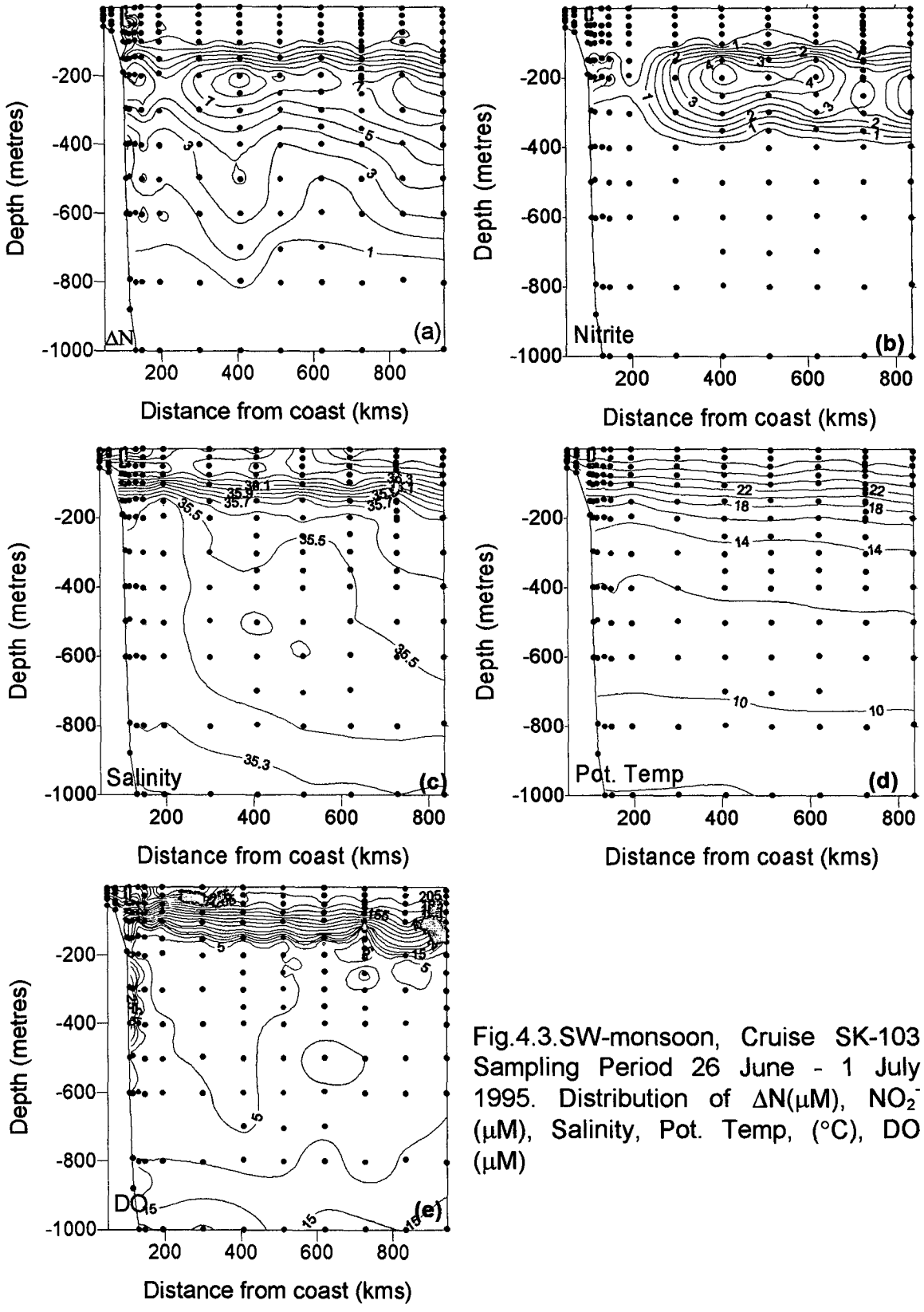

Fig.4.3.SW-monsoon, Cruise SK-103 Sampling Period 26 June - 1 July 1995. Distribution of ΔN(μM), NO_2^- (μM), Salinity, Pot. Temp, (°C), DO (μM)

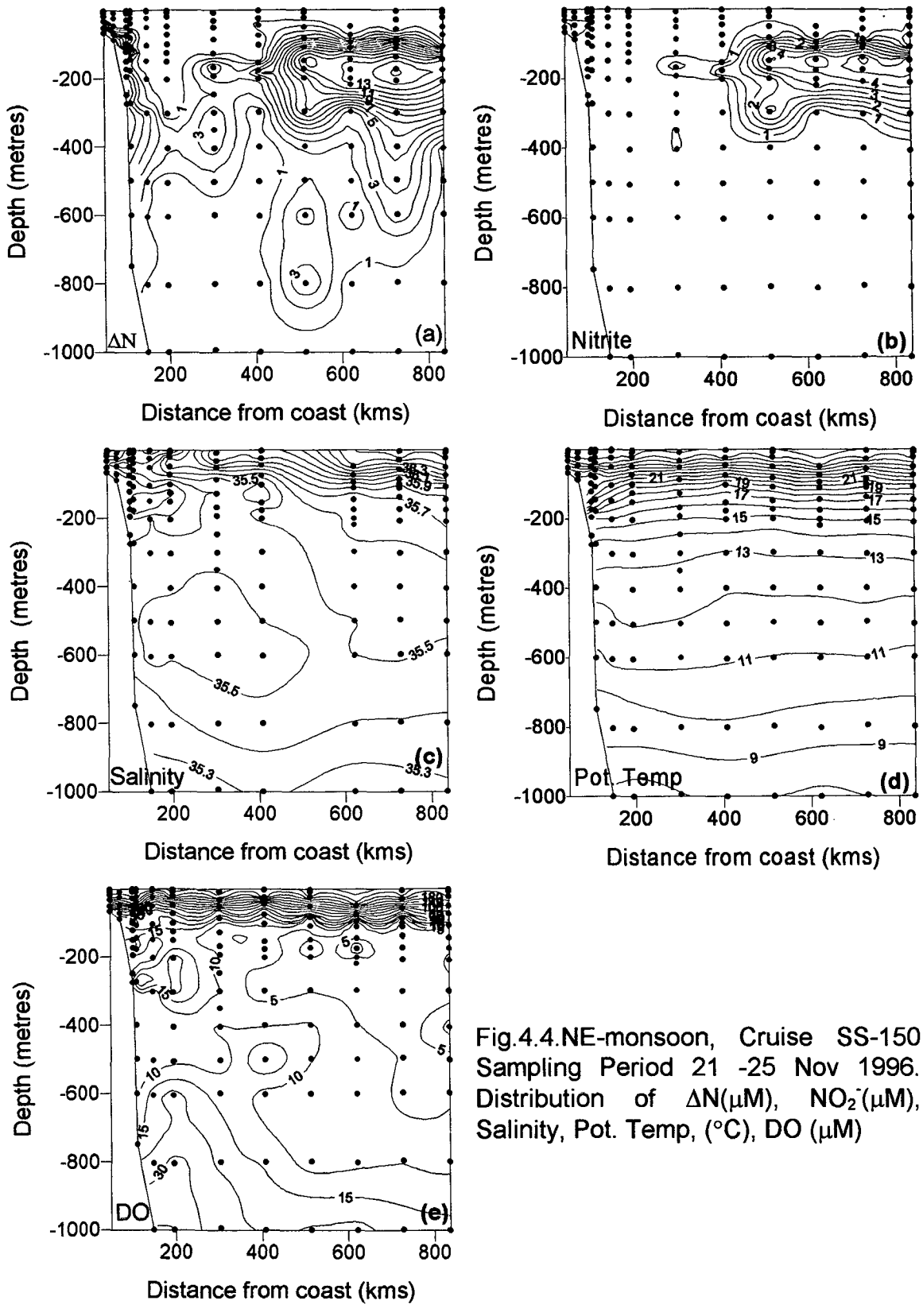

Fig.4.4.NE-monsoon, Cruise SS-150 Sampling Period 21 -25 Nov 1996. Distribution of ΔN(μM), NO_2^-(μM), Salinity, Pot. Temp, (°C), DO (μM)

responsible for renewal is only marginally higher than the water existing in this region. The Winkler method of dissolved oxygen determination is not sensitive enough to detect changes below 5 μM; hence, it is usually difficult to demarcate this watermass based on the oxygen distribution (Fig 4.3.e, Fig 4.4.e, Fig.4.5.e. and Fig.4.6.e).

The 35.5 salinity isopleth extended up to 200 kms from the coast and is restricted to the depth range 150-350m, during January (Fig. 4.5.c.), while in November it extended to a larger area as mentioned above (Fig.4.4.c.). As the season progresses, these waters could be more influenced by the adjacent watermass, where denitrification is quite intense. Beyond this region that comes under the influence of coastal currents and more towards the north, the rate of denitrification is expected to be much higher (Naqvi 1991a, 1994, and also the data presented here). As the data are available only up to 500 kms from the coast, it could not be confirmed whether deficits in excess of 10 μM NO_3 observed during November were present in January as well. However, an increase in deficits could be seen around 400-500 kms (Fig.4.5.a.) similar to that of the November distribution (Fig.4.4.a.).

Along the shelf a narrow band of nitrate deficit is observed during November (Fig.4.4.a.). The most plausible explanation of this is the near-bottom water-column denitrification that may occur at the end of the SW monsoon all along the shallow shelf. During cruise SS158 (September) denitrification was observed along the shelf, between Quilon and Goa (observations were not made beyond these locations). The productivity in the coastal waters is very high due to upwelling during the SW monsoon. And as these waters are already low in oxygen, the large amount of organic matter produced would greatly enhance the oxygen demand and create conditions conducive for denitrification.

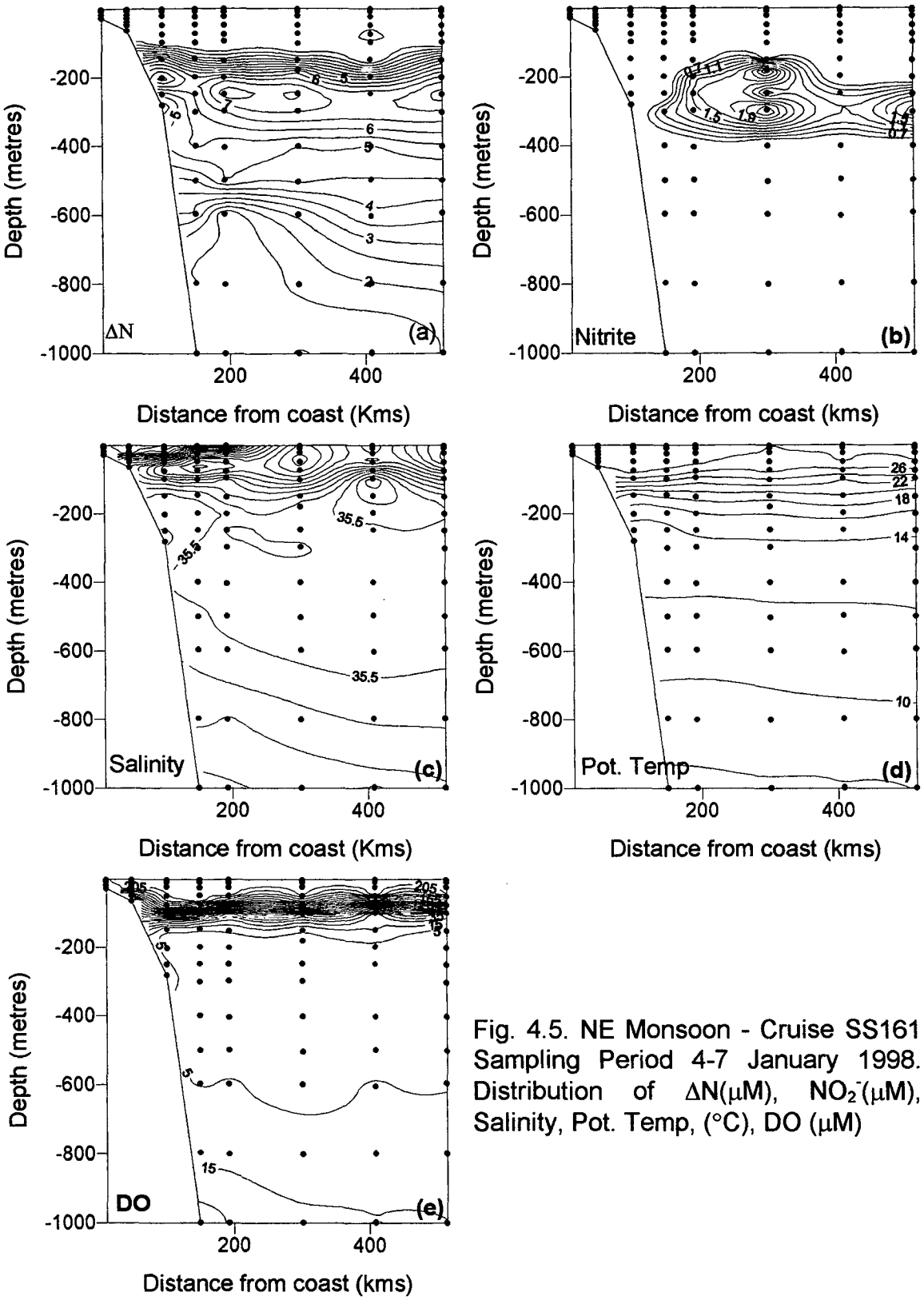

Fig. 4.5. NE Monsoon - Cruise SS161 Sampling Period 4-7 January 1998. Distribution of ΔN(μM), NO_2^-(μM), Salinity, Pot. Temp, (°C), DO (μM)

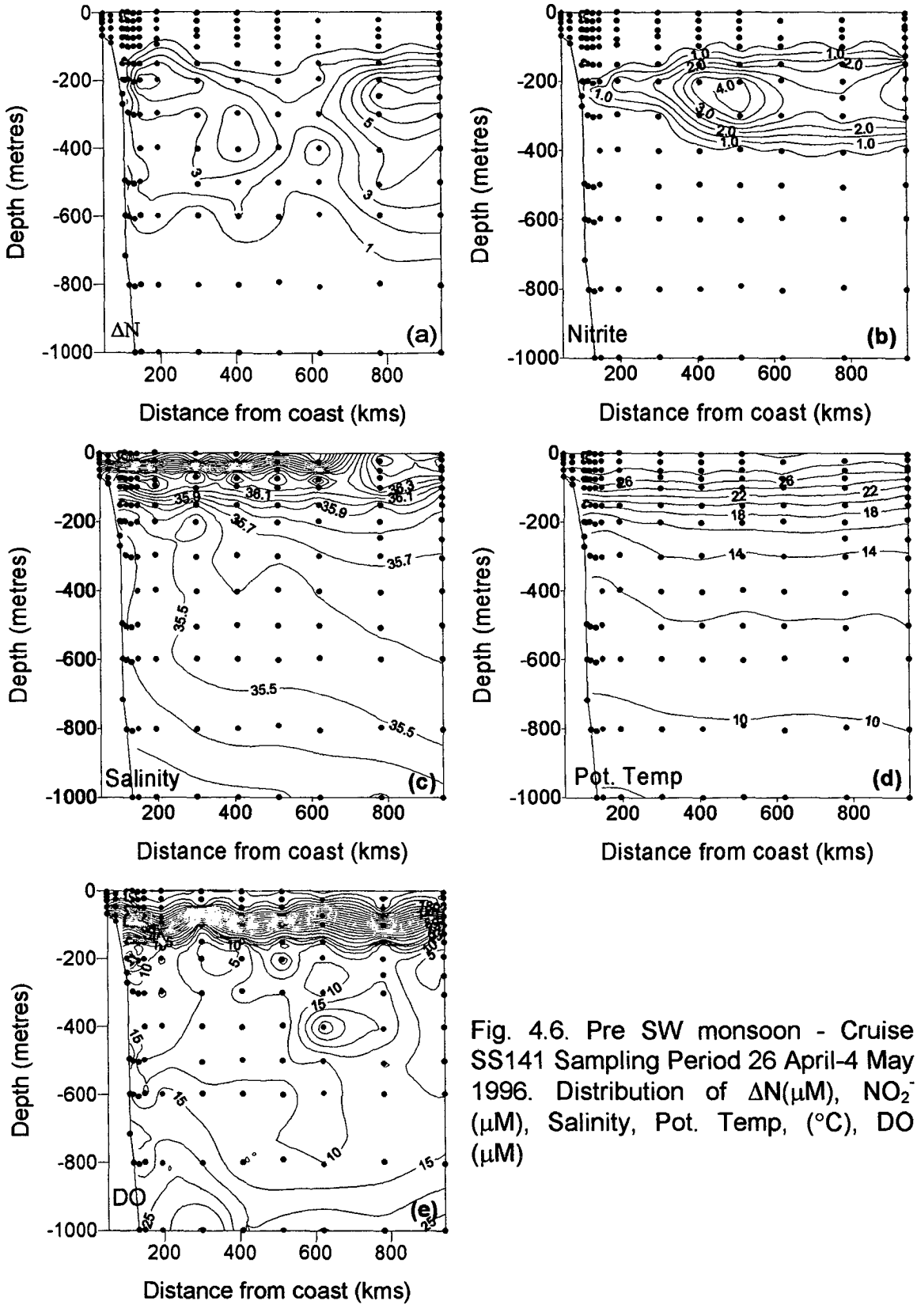

Fig. 4.6. Pre SW monsoon - Cruise SS141 Sampling Period 26 April-4 May 1996. Distribution of ΔN(μM), NO_2^- (μM), Salinity, Pot. Temp, (°C), DO (μM)

4.6. East-West Sectional Distribution During Pre-SW Monsoon Season:

During May the salinity structure (Fig.4.6.c.) is more or less like the SW monsoon season albeit a little less defined. The poleward undercurrent which is seen up to a distance of 200 km from the coast during the SW monsoon (S<35.4) (Fig.4.3.c.) is just beginning to show close to the coast (Fig.4.6.c.) The isotherms in surface waters (Fig.4.6.d.) close to the coast do not show any signal of upwelling yet but the waters below 200 m do show signs of downwelling as in the monsoon. This suggests that this is a transition phase. Fig. 4.6.b. shows the penetration of nitrite up to the shelf as seen during the monsoon season. The deficits are lower than the SW monsoon season (Fig.4.6.a.). Significant deficit associated with the equatorward surface flow has not developed yet. Closer to the coast the deficits are lower than during the SW monsoon season. The higher deficits closer to the coast during SW monsoon arises partly from the equatorward flow of the surface waters and also partly from the upwelling process. Hence, as both these processes are weak or absent the deficit near the coast are lower than during the SW monsoon season. Maximum denitrification is found to occur around 500 km from the coast (using nitrite as an indicator, Fig.4.6.b.), while the corresponding ΔN is only between 2 and 3 μM NO_3, (Fig.4.6.a.) which would suggest that denitrification is just settling in with the change in conditions.

4.7. Temporal Variations at the Three Northern Locations:

The results suggest that within the core of the denitrifying regime, at location A, the denitrification process is intense throughout the year (Fig 4.7.a and Fig.4.7.b.). The extent of denitrification appears to be maximal during the NE monsoon season with the deficits exceeding 10μM NO_3 (Fig.4.7.a.). Location B, lies at the periphery, of the denitrification zone as demarcated by Naqvi

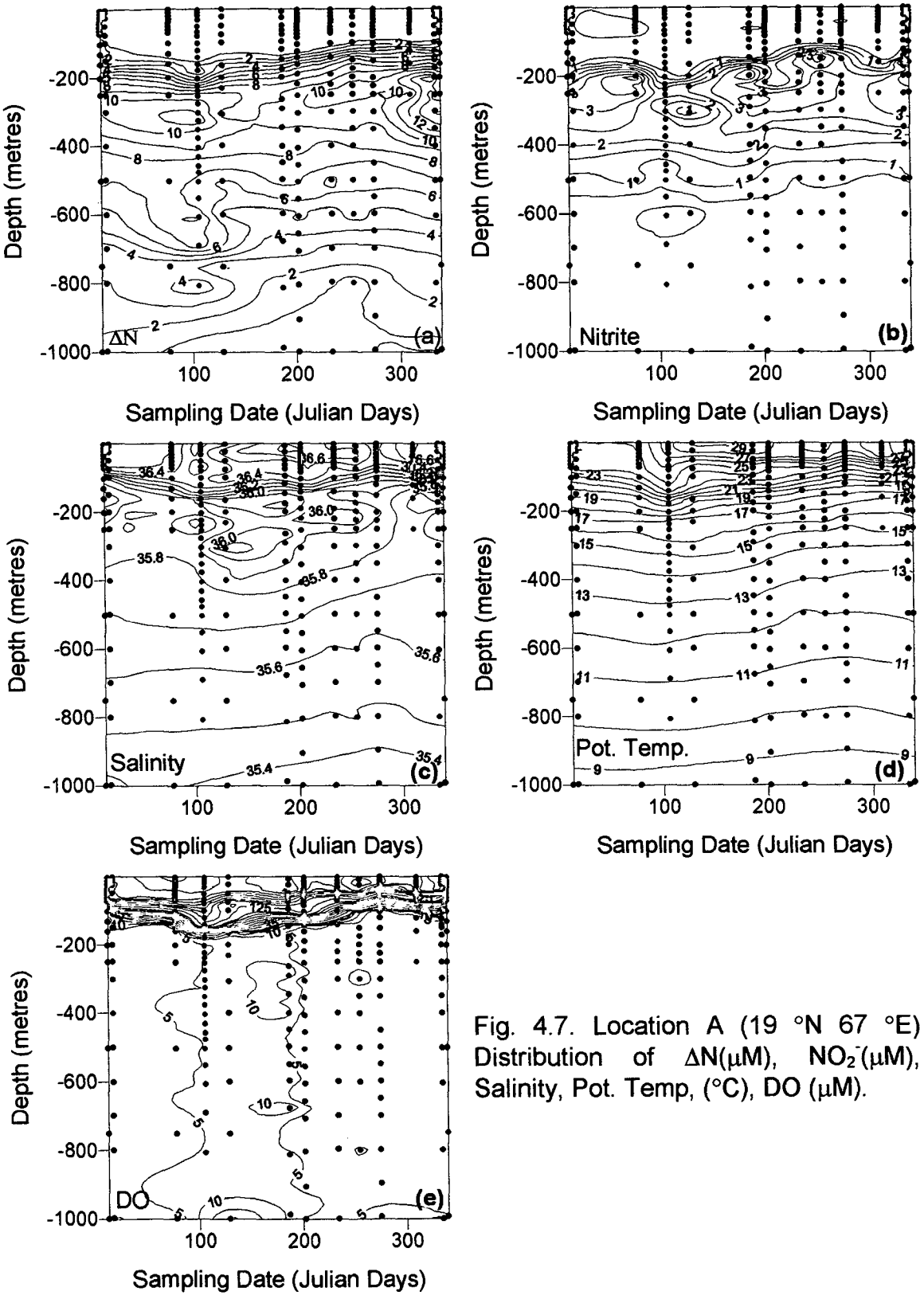

Fig. 4.7. Location A (19 °N 67 °E) Distribution of ΔN(μM), NO_2^-(μM), Salinity, Pot. Temp, (°C), DO (μM).

(1991a) and so the denitrification signals show a much larger temporal variability (Fig.4.8.a. and Fig.4.8.b.). The deficit starts increasing at the end of the SW monsoon season and high values persist till the end of the NE monsoon (Fig.4.8.a.). It falls thereafter to the lowest values during the pre- and early southwest monsoon periods.

Winter cooling process is expected to induce mixing at intermediate depth in the northern Arabian Sea and thereby supply oxygen to the oxygen deficient mid-depth waters. Effect of winter cooling process was observed at location A during January -February 1998, with surface water NO_3 levels going up to 3 μM. However the deficit distribution at location A (Fig.4.7.a.) did not show any noticeable changes in the denitrifying condition associated with the winter cooling, as the ΔN values were still over 10 μM and NO_2 was over 3.0 μM. As a result of nutrients being pumped into the euphotic zone by winter cooling the productivity also increases. And the sinking of the organic matter would further increase the oxygen demand. So this is a situation where there is a higher oxygen supply as well as a higher demand.

The annual deficit cycle seems to follow the primary productivity pattern (Bhattathiri et al., 1996), suggesting a link between deficit and productivity. An important question which arises here is, what makes the two sites different? The two locations are almost at the same latitude, and hence the productivity and physical forcing (mixing due to winter cooling) are not expected to be much different. The most plausible factor that may cause the observed differences is the advection of the Persian Gulf Water (PGW). This water originally has a fairly high oxygen content but as it mixes with the Arabian Sea low-oxygen water almost penetrating its core, the oxygen content falls rapidly (Wyrtki, 1971). However, even the very limited oxygenation associated with the advection of this water has a profound influence on the redox condition. Location B lying more

towards the west is expected to be more influenced by this water mass as compared to location A.

The salinity structure is characterised by a well pronounced salinity maximum (> 36.0) throughout the year at location B (Fig.4.8.c.), while at location A, isopleths of 36.0 salinity could only be seen in patches during the pre- SW monsoon season (Fig.4.7.c.) in the 200 to 300m depth range. This watermass is found very close to the depth at which the denitrifying activity is maximum. Indeed, the association of denitrification with the PGW has been proposed by some previous workers (Deuser et al., 1978). However, the present results show that denitrification seems to be either weak or entirely absent during the pre-SW monsoon season and early SW monsoon season (Fig.4.8.b.), due to supply of oxygen by the PGW (Fig.4.8.e.). During the remaining part of the year reducing condition seem to prevail and the deficits are higher. As the productivity is high during both the summer monsoon and winter periods the oxygen levels of PGW is not sufficient to sustain the oxidation of the high organic load. At location A (Fig.4.7.a.) the only occasion where the deficit goes below 9 μM NO_3 in the O_2 minimum layer is when salinity exceeds 36.0. At location B, the shift in the depth of the ΔN maximum is a result of the influence of PGW. Active denitrification seem to take place only from the middle of the SW monsoon to the end of NE monsoon, as secondary nitrite was observed only during these periods (Fig.4.8.b.). From May to September associated with the high saline water at the mid-depths the oxygen levels are marginally higher (Fig.4.8.e). However, during September although the high saline water is present the secondary nitrite also starts to build up probably as a result of higher rates of sinking organic matter from the higher productivity during the monsoon season.

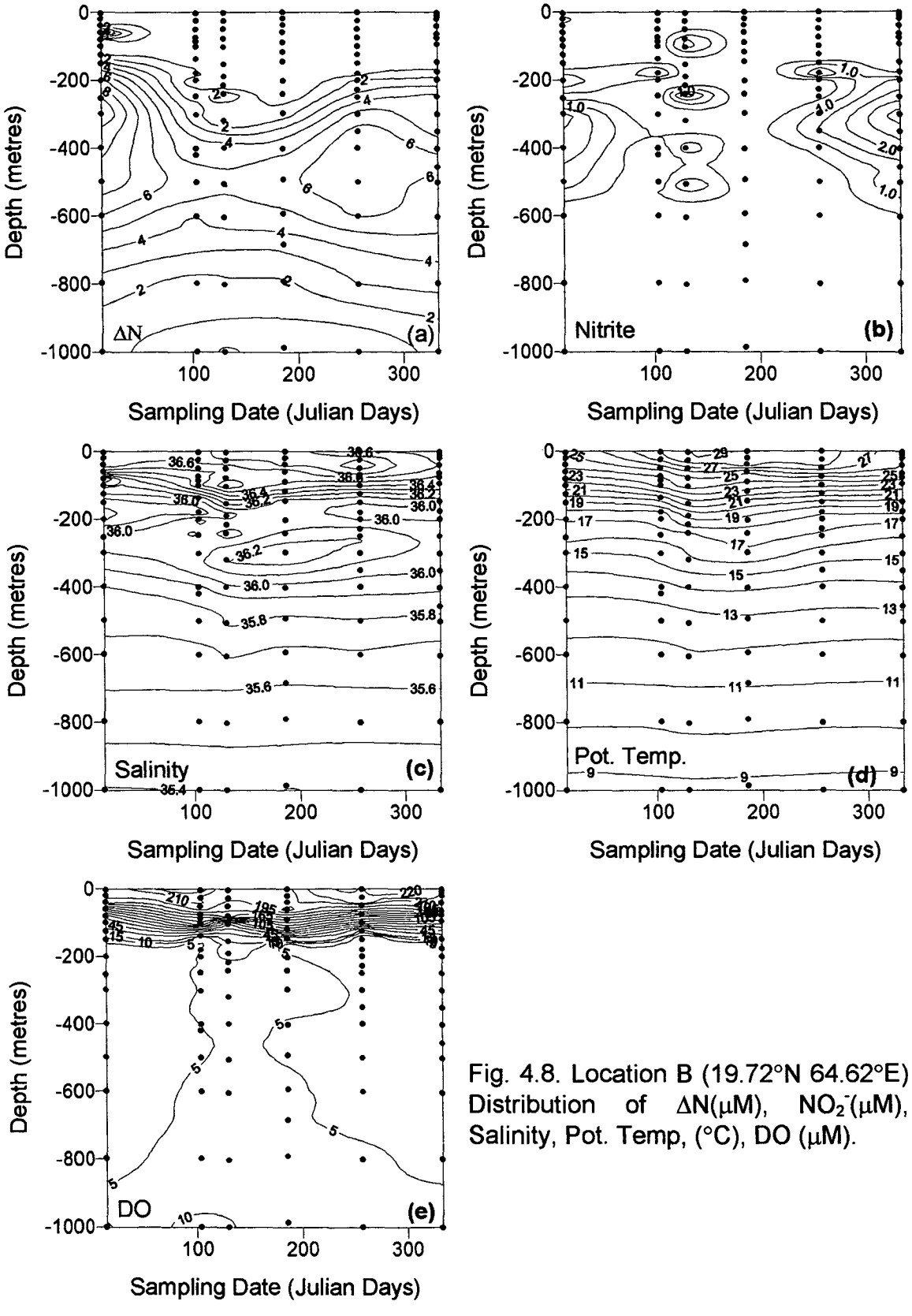

Fig. 4.8. Location B (19.72°N 64.62°E) Distribution of ΔN(μM), NO_2^-(μM), Salinity, Pot. Temp, (°C), DO (μM).

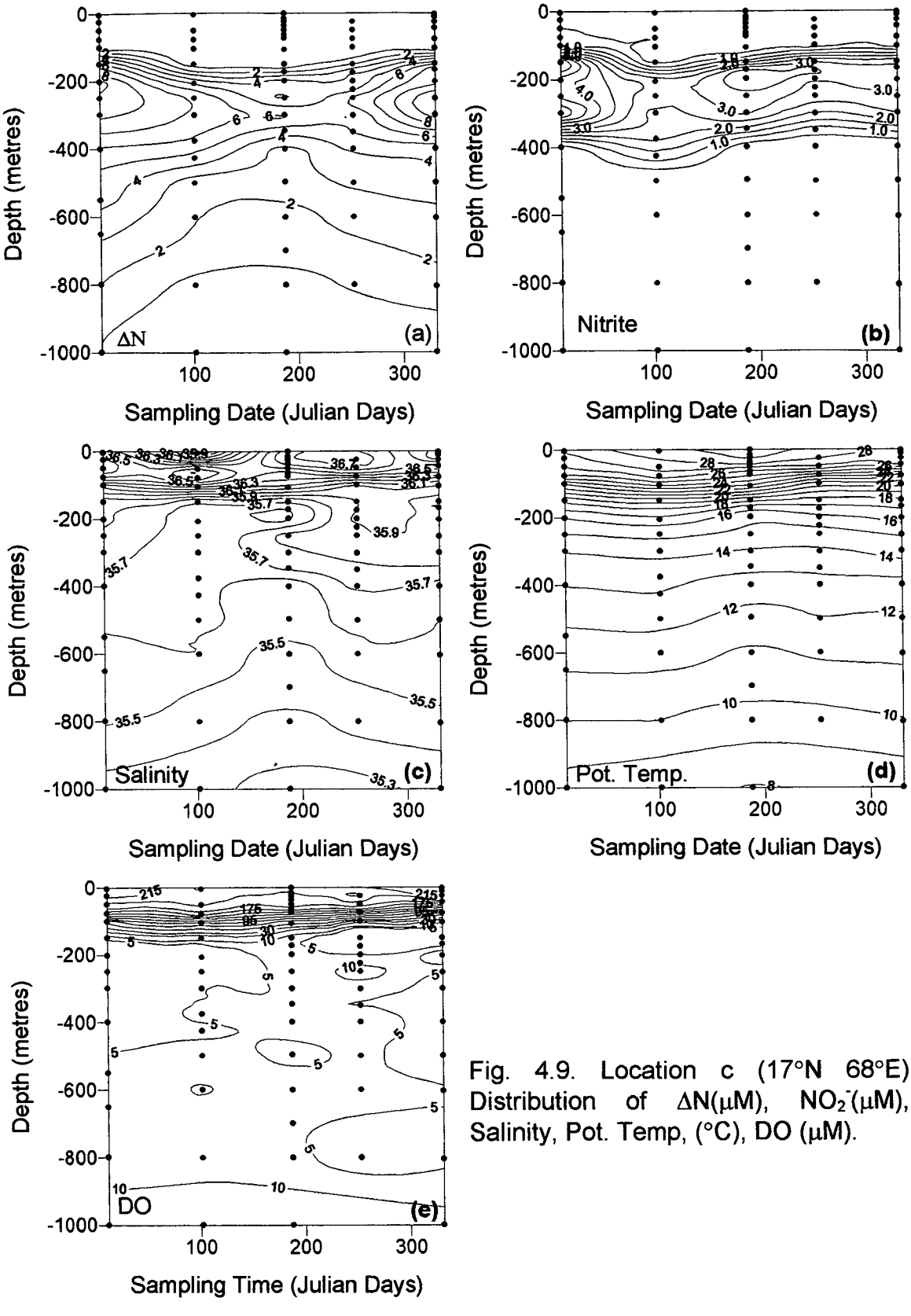

Fig. 4.9. Location c (17°N 68°E) Distribution of ΔN(μM), NO_2^-(μM), Salinity, Pot. Temp, (°C), DO (μM).

Although Location C experiences denitrifying conditions throughout the year (Fig 4.9.b.) the deficits are lesser than at location A, as this location lies more south it receives more O_2 supply relative to location A. The high salinity PGW is not clear in this location (Fig 4.9.c.). However as this location lies farther south west than location A and crosses the dense denitrifying region (e.g. Location A) the chances of it retaining any of its original oxygen content is very poor as even at location A it was on only one occasion the deficit went marginally low (to 9 μM NO_3). At location C also, the highest deficits were observed from the middle of the SW monsoon to the end of NE monsoon., with deficits reaching a maximum of 9 μM NO_3.

4.8. Conclusions:

The results suggest that the intensity and the spatial distribution of denitrification has a seasonal cycle. The nitrate deficits start increasing at the end of the SW monsoon. This trend is seen till the end of NE monsoon after which a decrease in deficit occurs with the lowest values occurring during pre-SW monsoon and at the beginning of the SW monsoon. Primary productivity of the Arabian Sea seems to have an influence on the denitrifying cycle. Reversing coastal currents supply limited amounts of oxygen to part of the oxygen deficient zones, thereby decreasing the intensity of denitrification in the waters close to the coast.

Results of repeated samplings at fixed sites show large temporal variations. The intensity of denitrification is less towards the central and western parts of the Arabian Sea, because of the advection of PGW, as this water flowing at a critical depth is a source of oxygen to the suboxic zone. When the productivity is very high the oxygen content of the PGW is not sufficient to prevent the onset of denitrification.

5. Distribution of Nitrous oxide in the Northern Indian Ocean:

5.1. Introduction:

The inventory of combined nitrogen in the oceans is regulated by several processes. Inputs of nitrogen to the oceans occur mainly through river runoff, atmospheric deposition and nitrogen fixation, while its loss is principally through conversion of combined nitrogen into N_2 (Codispoti and Christensen, 1985). This process, known as denitrification, takes place when the O_2 concentrations are close to zero and bacteria utilise NO_3^- instead of O_2 as an oxidant for decomposing organic matter (Richards, 1965). Conditions conducive for denitrification commonly develop within the coastal sediments. In the water column, however, the oceanic currents supply enough O_2 at all depths to prevent the development of anoxia in most oceanic areas. However, there are three regions where some unusual oceanographic processes cause the O_2 demand to exceed its supply leading to an almost complete O_2 depletion (suboxia) at mid-depths (Deuser, 1975).

Two of these sites are located in the eastern tropical North and South Pacific, while the third is found in the Arabian Sea. Although these regions account for only ~2% of the total oceanic area, they are extremely important from the biogeochemical and climatic points of view. This is because the high and temporally variable rate of denitrification in these regions has the potential to greatly alter the oceanic combined nitrogen inventory. This in turn may cause variations in the rate of photosynthetic carbon fixation and thereby in the rate at which carbon dioxide (CO_2) is sequestered from the atmosphere. Thus the oceanic O_2-deficient zones probably contribute very significantly to global climatic changes (McElroy, 1983; Codispoti et al., 1996a). Another important way in which these environments affect the atmospheric composition is through production of trace gases, particularly nitrous oxide (N_2O). Recent studies show that the oceans may account for about half of the total inputs of N_2O to the

atmosphere from all natural sources, and that a large fraction of the oceanic efflux comes from the O_2-deficient zones particularly the Arabian Sea (Codispoti and Christensen, 1985; Law and Owens, 1990; Naqvi and Noronha, 1991; Bange et al., 1996).

5.2. N_2O Distribution in the Suboxic Zone:

In the denitrifying zone of the northern and central Arabian Sea N_2O profiles are characterised by two maxima separated by a minimum. However, outside this region in the Arabian Sea and in the Bay of Bengal, only one broad maximum is observed (Fig 5.1). This is evident in the vertical sections of N_2O along 15°N section during three seasons (SW monsoon, NE monsoon and Pre-SW monsoon) presented in Figs.5.2a, b, c. Overall the distribution of N_2O was closely related to the distribution of dissolved oxygen (Fig.4.3.e, 4.5.e, 4.6.e). The N_2O minimum coincided with the O_2 minimum; above and below this the concentrations increased. Within the core of the denitrifying layer, the concentrations of N_2O were generally below saturation. The N_2O minima also coincided with the maxima in ΔN and nitrite (Figs. 4.3.a,b, 4.5.a,b, 4.6.a,b). The N_2O concentrations within the mid-depth minimum generally decreased offshore.

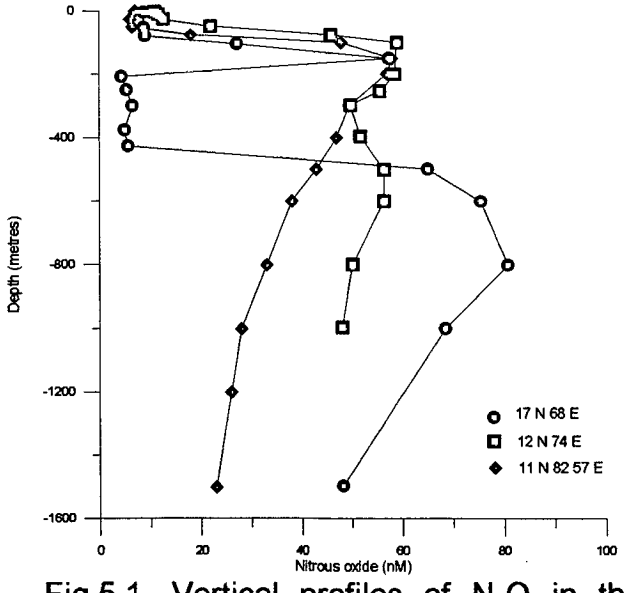

Fig.5.1. Vertical profiles of N_2O in the northern Arabian Sea, southern Arabian Sea and Bay of Bengal

The above pattern in the distribution of N_2O arises from the mid-depth O_2 depletion in these waters. Under normal conditions, when O_2 levels have not reached low enough to trigger denitrification, N_2O and O_2 concentrations are negatively correlated (Yoshinari, 1976). However, when the environment becomes reducing, N_2O becomes an electron acceptor and gets reduced to N_2 (Payne, 1981). The correlation between N_2O and O_2 observed in the oxic waters does not extend to such waters. The distribution of N_2O in the northern Arabian Sea observed in the present study is consistent with the results of Naqvi and Noronha (1991), which in turn, are similar to those reported from the oxygen poor environment of the eastern tropical Pacific Ocean (Cohen and Gordon, 1978; Elkins et al., 1978).

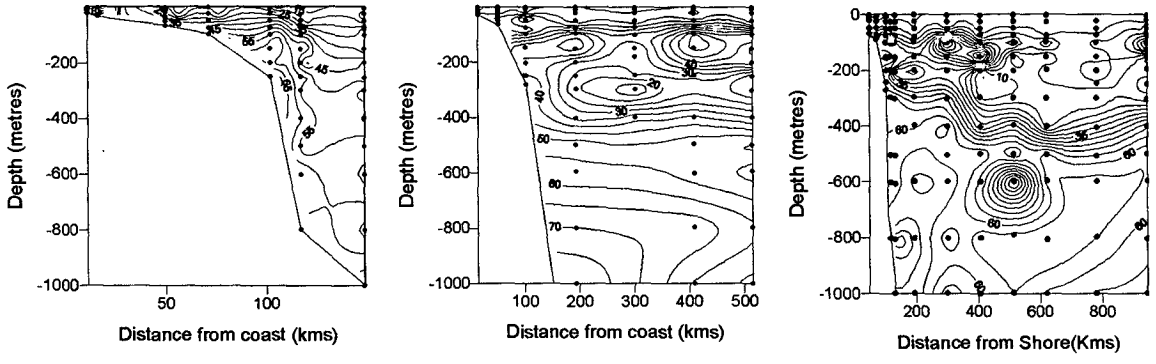

Fig 5.2. Zonal sections of nitrous oxide (nM) distribution during (a) SW-monsoon (cruise SS158), b) NE-monsoon (cruise SS161) and c) pre-SW monsoon(cruise SS158).

Overall the seasonal variation of N_2O followed that of denitrification as represented by nitrate deficit and discussed in Chapter 4. During the SW Monsoon season in the shelf region (Fig. 5.2a) within 200 km of the coast, N_2O concentrations reached a maximum of 60 nM at the primary maximum (depth ~ 100m) but during the other two seasons (Fig 5.2 b,c) it reached a maximum of only 30nM. As a result of upwelling along the SW coast of India during the SW

monsoon, deeper waters rich in N_2O rise up the shelf, and this phenomenon probably accounts for the observed higher N_2O levels during this season.

Although the N_2O level goes down to undersaturation occasionally at mid- depths along 15°N during pre-SW monsoon, the undersaturation is not too large (saturation ~90%). However, around 400 to 500 km from the coast, at ~250 m depths, the saturation level does go down to 60%, which is the lowest for the whole section. This undersaturation was concomitant with NO_2^- > 4μM, but ΔN did not show any marked increase. This scenario supports the view that denitrification was in an early stage as reported in Chapter 4. It is widely accepted that the minimum in N_2O within the core of denitrifying layer occurs due to the consumption of N_2O during denitrification (Cohen and Gordon, 1978; Elkins et al., 1978) because N_2O negatively correlates with nitrite and ΔN within this layer.

During the NE monsoon the deficits are higher than the pre-SW monsoon season, but N_2O does not go down to undersaturation levels. In chapter 4 it was stated that as the season progresses during NE monsoon, the waters closer to the coast (~200 km from the coast) could be more influenced by the adjacent watermass, where denitrification is quite intense. N_2O distribution also supports this view. Data are available only up to a distance of 500 km from the coast. However, the available data distribution also conforms to the ΔN distribution. As the ΔN values do not go very low, N_2O concentrations also do not go down to undersaturation levels, although there is considerable decrease in N_2O concentrations within the OMZ. The concentrations do not go down to undersaturation levels unless the ΔN values are over 10μM and invariably these extreme undersaturations are accompanied by high nitrite. This suggests that N_2O gets consumed during intense denitrification, which leads to extreme undersaturations. The minimum in N_2O at the mid-depth with low saturation would probably reflect the stage of denitrification. 19°N and beyond the ΔN

values were higher and was accompanied by extreme undersaturation in N_2O. This will be discussed in detail later in this chapter.

Above and below the denitrifying layer the concentration of N_2O was high. Generally, the concentration of N_2O in the upper or primary maximum was not as high as that at deeper maximum. Inputs of N_2O in the deeper layers are principally through nitrification process, while the primary N_2O maxima could be a resultant of both nitrification and denitrification processes. As this primary N_2O maximum is below the thermocline, active upward diffusion of N_2O across the barrier is reduced leading to the accumulation of N_2O in this layer. In the mixed layer, due to upward diffusion and flux of N_2O to the atmosphere there exists a trend of decreasing N_2O concentration towards the surface. Below 800m the concentration of N_2O is almost the same throughout the year.

Naqvi and Noronha (1991) reported a consistent and substantial decrease in N_2O concentrations at the deeper maximum towards the continental margin and suggested that the marginal sediments in contact with the low-oxygen water in the Arabian Sea could be a significant sink of N_2O. However during the course of this study no such loss of N_2O to the shelf sediments was observed. Even during the NE monsoon season, although nitrate deficits were observed along the shelf bottom waters (Fig. 5.2b) no noticeable loss of N_2O was observed, close to the continental margin.

5.3. Temporal Variations:

Repeated measurements of N_2O concentration were made at the three locations A, B and C (Fig.4.1). In the mixed layer N_2O concentrations ranged between 8 and 14 nM at locations A and B (Fig.5.3a,b), while at location C (Fig.5.3c), which lies further south the concentration in the mixed layer was between 7 and 13 nM. Below this, just above the O_2 minimum layer, the

concentrations reached over 50 nM. In the O_2 minimum layer the concentration fell below 10 nM throughout the year at location A while at location B the mid-depth minimum with concentration below 10 nM was observed only during the NE monsoon season. At location A, the depth range of the N_2O minimum was generally stable (~200-500 m), but some temporal variability best represented by the occurrence of a deeper maximum during the pre-southwest monsoon season, was discernible. N_2O distribution at location C was similar to that at location A except that the

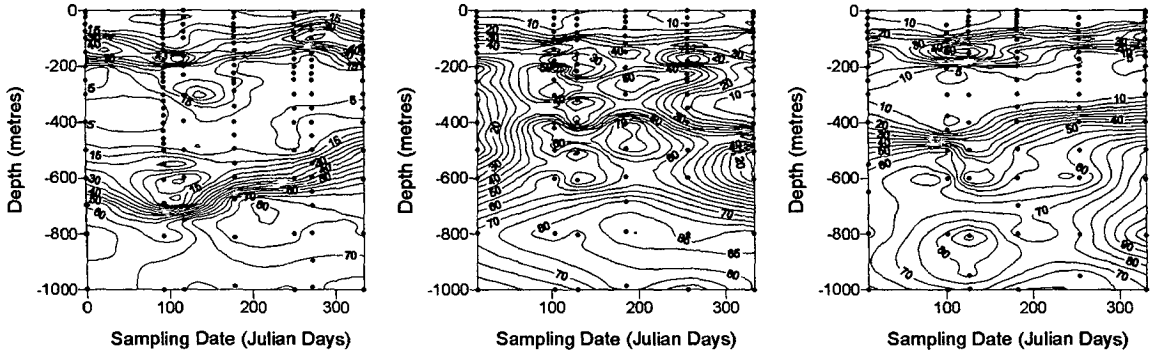

Fig.5.3. Nitrous oxide distribution at a) Location A (19°N, 67°E), b) Location B (19.72°N, 64.62°E), and Location C (17°N, 68°E)

thickness of the N_2O minimum was much smaller at C. Below 800 m depth the concentration rose above 80 nM at all the three locations and there was no noticeable seasonal variation.

The above pattern of the distribution of N_2O in the OMZ also reflects the distribution of ΔN as discussed in Chapter 4. Location A experiences intense denitrifying conditions throughout the year, which presumably caused the consumption of N_2O leading to under-saturation. For the period starting from the later part of the SW monsoon to the end of NE monsoon, the saturation was below 30%. At location B, where denitrification was less intense due to supply of O_2 by PGW (Chapter.4), the N_2O saturation fell below 100% only during the NE monsoon season. During the rest of the year in conformity with the observed

trends in NO_2^- and ΔN at this location the mid depth waters were supersaturated with this gas.

Although location C experienced denitrifying conditions throughout the year, these were not as severe as those at location A. Here the ΔN values exceeded 7 μM during the NE monsoon season. Similarly, the saturation of N_2O also went below 50% only during the NE monsoon season. The observed differences in reducing conditions between the two sites appear to follow the productivity pattern. During the winter monsoon the northern part of the Arabian sea experiences enhanced productivity due to winter cooling (Bhattathiri et al., 1996). As stated earlier the extreme N_2O undersaturation was invariably accompanied by ΔN values in excess of 10 μM. Thus the northward increase in biological productivity in conjunction with lower O_2 supply, except at location C, may explain the progressively higher ΔN and lower N_2O saturation from 15°N to location A.

5.4. Winter Cooling and N_2O:

To study the diffusive flux of N_2O across the thermocline and the effect of winter cooling on the distribution of N_2O, time series observations were made at 21°N 64 °E during cruise SK121. This site was chosen because it is located within the zone of convective overturning and deep mixed layer during winter, as a result of heat loss and evaporation from surface waters caused by the cool dry winds blowing from the land from northeast to southwest (Kumar and Prasad 1996). The surface waters were highly saturated with N_2O, but the saturation varied over a factor of 3 (130-439%), undergoing several increases and decreases during the period of observations (Fig. 5.4). Significantly, NO_3^- and NO_2^- also followed similar pattern in the surface waters. Apart from the finer short time variations in the time scale, the surface distribution of N_2O, NO_3^- and NO_2^- also exhibited an overall decreasing trend in phase with the wind speed. The

convective mixing due to winter cooling ensures inputs of nutrients to the surface waters from the subsurface layer. This mixing can also greatly influence the flux of trace gases to the atmosphere. During the course of the fourteen day observation, the mixed layer depth oscillated between 80 and 110 m (Fig.5.5a). The productivity of this region increased in response to the injection of nutrients into the photic layer (Bhattathiri et al., 1996). Apparently in response to the large quantities of available food, extensive swarming of the filter-feeding salps (Tunicates) occurred during the period of observations.

To start with the mixed layer depth was ~80m (Fig.5.5a and b) but with the passage of time the mixed layer depth increased and simultaneously there was nitrate injection into the mixed layer (Fig.5.5c). As NO_3^- was sampled at a high resolution in the time axis, the fine scale changes can be clearly seen. Along with NO_3^- other dissolved constituents with a positive gradient below the thermocline also get injected into the mixed layer. As the primary

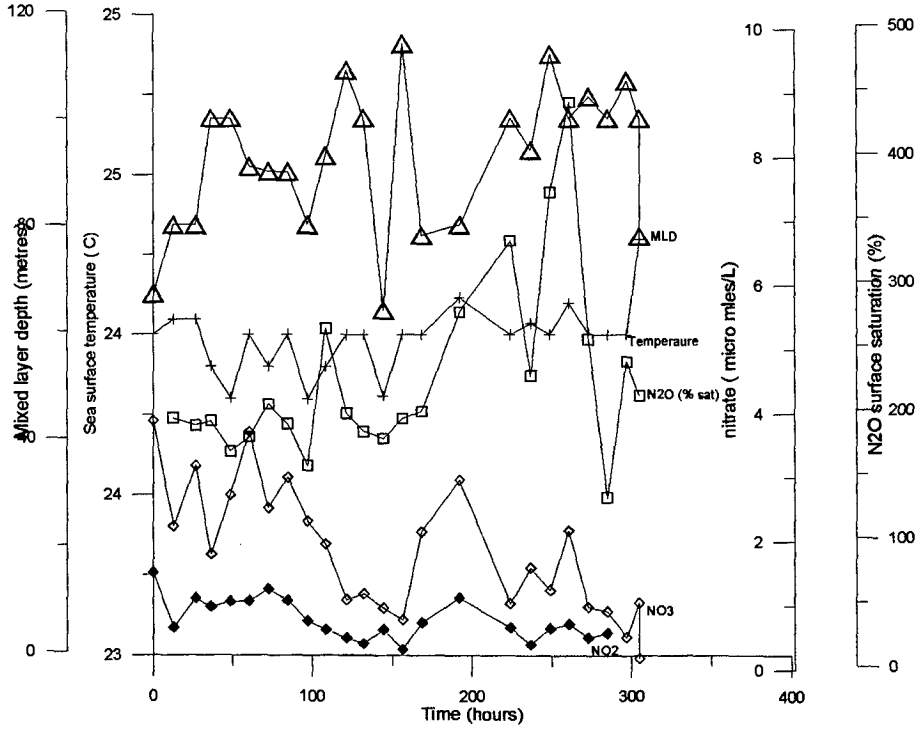

Fig.5.4. Distribution of N_2O surface saturation (%), NO_3^-(μM), NO_2^-(μM), sst (°C) and MLD (m) at 21°N 64°E during winter cooling during a 14 day period.

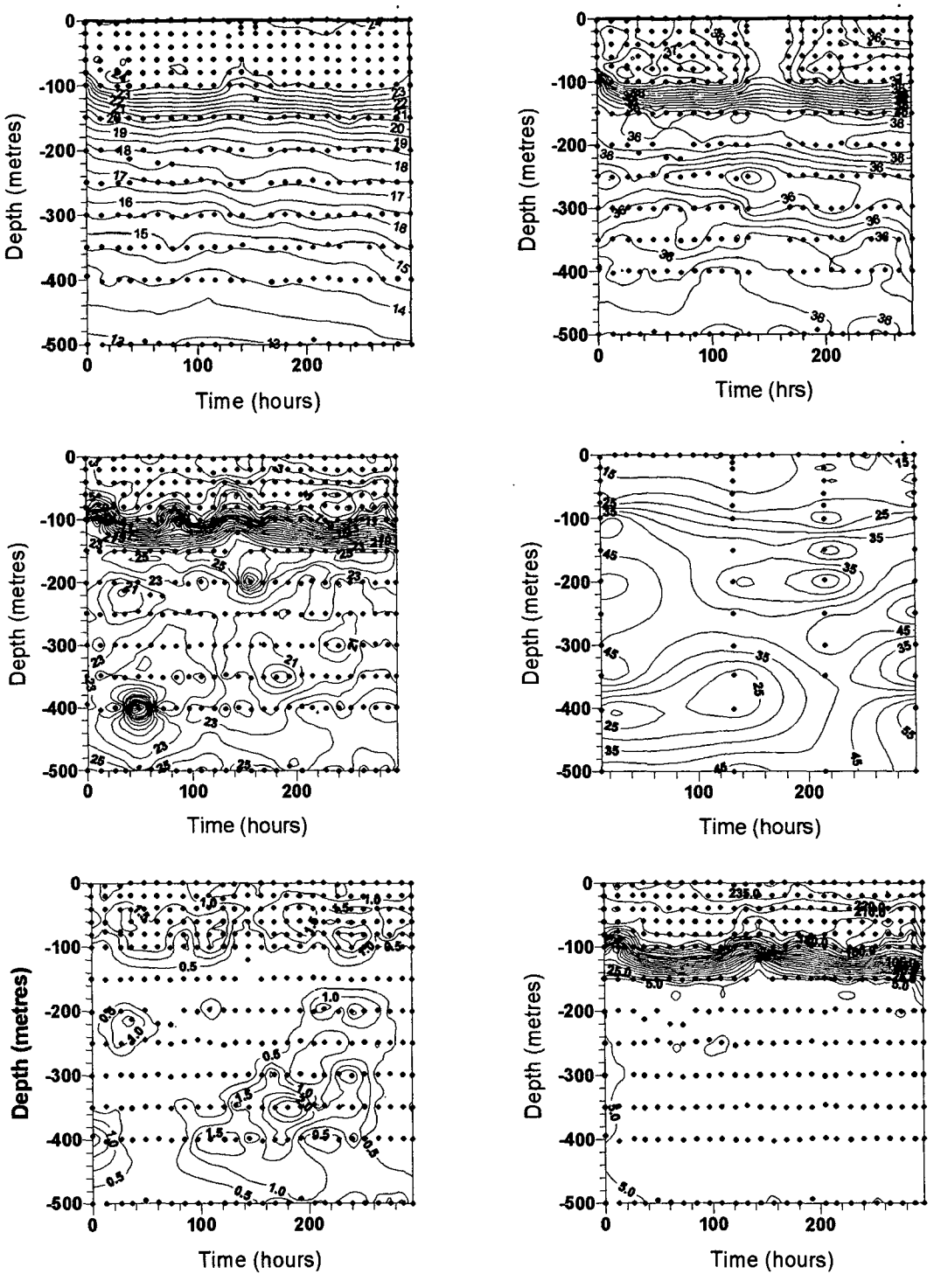

Fig.5.5. Observations at 21°N 64°E during SK-121 (February 1997) (a) Temperature (°C) (b) Salinity (c) NO_3(μM) (d) Nitrous Oxide (nM) (e) Nitrite (μM) (f) DO (μM)

maximum of N_2O is below the mixed layer and because of a positive gradient, N_2O is also pumped into the mixed layer (Fig 5.5d). On the seventh day of the observation the mixed layer became shallower (~80 m) and then started deepening again, resulting in the same sequence of events described above. The fluctuations in the mixed layer depth, within a short time span brings about large changes in the environmental conditions leading to high nutrient flux into the mixed layer. This sustains high rates of primary production. This process also results in enhanced flux of N_2O across the mixed layer which eventually reaches the atmosphere.

The overall decrease in the distribution of NO_3^- would suggest that the observations were initiated somewhere in the middle of the season and the process was on the waning phase. It would be appropriate to mention here that the large population of salps that were floating around the region at the start of the observations had declined to a large extent by the end of the observations. The swarming of salps in the same area was also observed during March 1991 (Sen Gupta et al., 1993)

5.5. Nitrite and N_2O relationship:

To investigate the relationship between N_2O and nitrite, all the data collected from north of 15°N were pooled and plotted (Fig 5.6). With a few exceptions, the high nitrite concentrations were associated with low N_2O, and high N_2O was mostly associated with low nitrite concentration. Within the oxygen minimum zone there was no correlation between NO_2^- and N_2O. High NO_2^- with low N_2O would indicate intense denitrification, as this was only observed at the core of the O_2-minimum. Intense denitrification in the northern Arabian Sea seem to be always accompanied by extreme N_2O under-saturation and high nitrite.

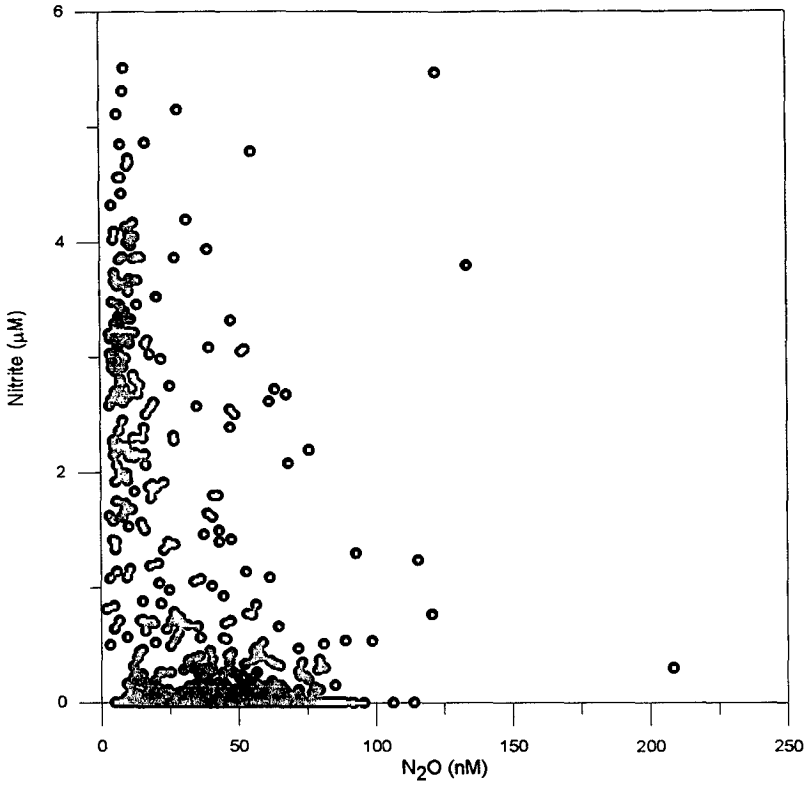

Fig.5.6. Plot of NO_2^- versus N_2O in the northern Arabian Sea

During the initial stages of denitrification there could be a stage where high N_2O may coexist with significant NO_2^- levels. With the increase in denitrifying activity, however, N_2O gets consumed, while the nitrite builds up. Accumulation of various substrates during denitrification may also depend on the type of denitrifying organism involved. Yoshinari (1980) demonstrated that *Vibrio succinogenes*, can reduce N_2O to N_2; but cannot reduce NO_3^- to N_2, it can reduce NO_3^- only to NH_4^+. On the other hand, it has also been observed that, at oxygen concentrations slightly above those prevailing within the core of the suboxic zone, a net production of N_2O may occur through denitrification under carbon limiting conditions (Betlach and Tiedje, 1981). Laboratory studies with non-marine ammonium oxidizers have revealed, an increase in the yield of N_2O with decreasing O_2 concentrations (Ritchie and Nicholas, 1972).

5.6. O_2 and N_2O relationship in the Arabian Sea:

The relationship between N_2O and O_2 is shown in Fig.5.7, by plotting the apparent oxygen utilisation (AOU) against ΔN_2O, the apparent production of N_2O. ΔN_2O is the excess N_2O concentration over its equilibrium concentration computed from the solubility equation of Weiss and Price (1980). All the samples that are likely to be affected by denitrification were discarded by screening out data pertaining to O_2 less than 10 μM.

Yoshida and Alexander, (1970), Elkins et al. (1978) and Butler et al. (1989) reported that the ΔN_2O/AOU relationship was dependent on temperature as well. The correlation between ΔN_2O and AOU improved with the inclusion of temperature, as more N_2O was produced per mole of O_2 consumed at higher temperatures. Hence including temperature as a variable the regression for the relationship between N_2O and AOU was computed as,

$$\Delta N_2O = 0.208 + (0.125 + 0.0029t)AOU \qquad (5.1)$$

The linear relationship between N_2O and AOU was found to exist in two ranges (Fig.5.7). Cline et al. (1987) observed linear trends in the N_2O - AOU relationship in three ranges in the equatorial Pacific. The slopes and the regression lines during the present study are similar to those reported by Naqvi and Noronha (1991). The observed linear relationships in two ranges, i.e. in the upper water column (depth $\leq$ 1000m) and in the lower water column (depth $\geq$ 1000m) may arise from the hydrochemical discontinuity in the vertical structure at about 10 °C as suggested by Naqvi et al. (1990) along with the temperature dependency of N_2O (Yoshida and Alexander, 1970; Elkins et al., 1978; Butler et al., 1989; fig. 4.2). These trends are in conformity with the results of Naqvi and Noronha (1991).

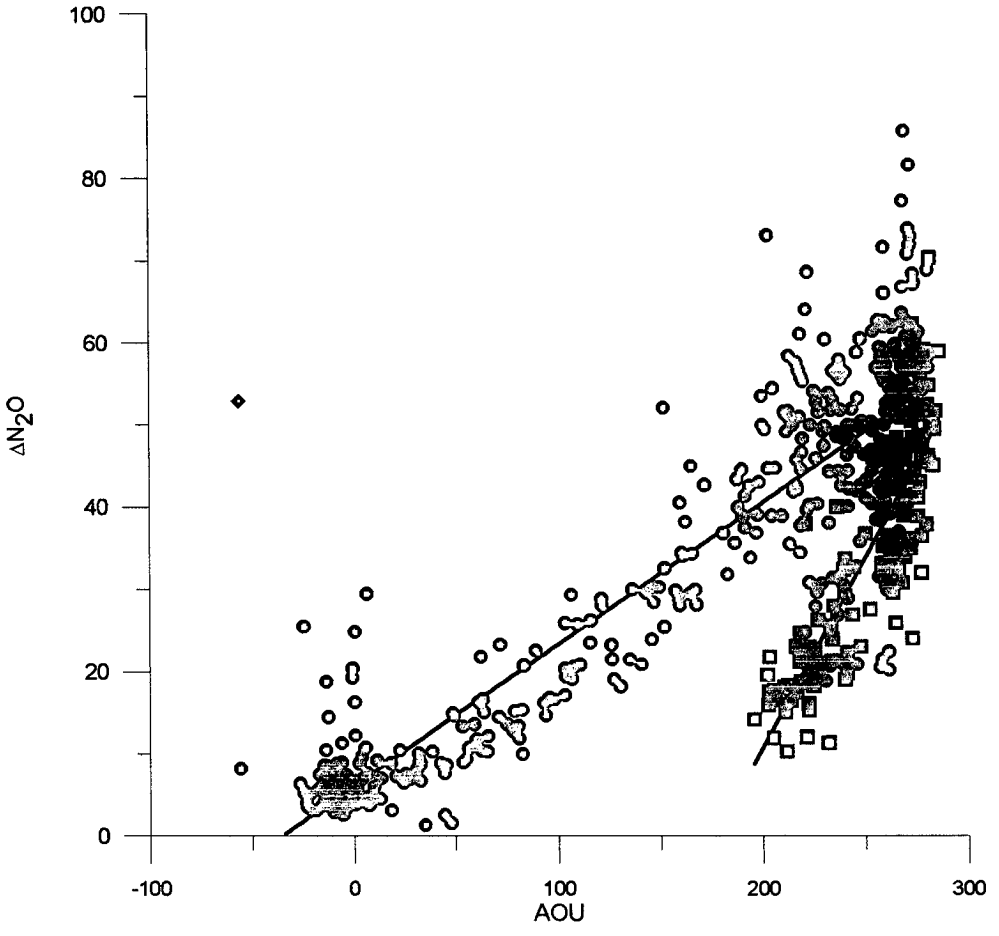

Fig.5.7. Relationship between the apparent N_2O production (ΔN_2O, nM) and apparent oxygen utilization (AOU, μM) for all samples with O_2 > 6μM. Circles and squares represent observations at depth <1000m and ≥1000m respectively. Straight lines give the linear least squares regression for the two depth ranges.

Within the core of the OMZ, ΔN_2O exhibited very high and low values within a narrow range of AOU. This indicates that the rates of both production and consumption of N_2O are very high within this layer. In this layer the relationship between AOU and ΔN_2O did not seem to hold. The increase in N_2O/AOU ratio to the core of the O_2 minimum is in agreement with the observation that the N_2O production rate increases at low concentrations of O_2 (Carlucci and McNally, 1969; Goreau et al., 1980; Cline et al., 1987; Naqvi and

Noronha, 1991). While N_2O production in aerobic waters by the nitrification pathway is expected to be only 0.3% of the NH_4^+ being oxidised, under low oxygen conditions, N_2O generation efficiencies may exceed 10% (Goreau et al., 1980; Capone, 1995). Similarly, N_2O production from denitrification pathway is also expected to increase when O_2 concentrations are low, as the N_2O generation efficiency may be greater where oxygen is present in small concentrations than when oxygen is highly depleted (Jorgensen et al., 1984). The low ΔN_2O within the OMZ arises from the consumption of N_2O under extreme depletion of O_2.

In the upper 1km of the water column the molar ΔN_2O/AOU ratio was 0.185×10^{-3} with a correlation coefficient of 0.893 (this does not include the data from the OMZ), while in the deeper layer the ratio was 0.462×10^{-3} with a correlation coefficient of 0.725. Naqvi and Noronha (1991) reported a ratio of 0.170×10^{-3} in the 0-1000m range. Elkins et al.(1978) measured a ratio of about 0.168×10^{-3} O_2 in the subtropical Pacific. Yoshinari, (1976), reported a ratio of 0.098×10^{-3} O_2 in the North Atlantic between 0 and 1000m. The ratio observed in the deep waters are much higher than the reported values from other regions suggesting a higher than average production of N_2O in the deep Arabian Sea. Naqvi and Noronha (1991) also reported a high ratio of 0.260×10^{-3} for the deep waters. Various other processes which result in the consumption or production of oxygen will affect the ΔN_2O - AOU relationship. In the surface mixed layer this relationship does not hold good because there is production of O_2 by photosynthesis. The relative concentrations of N_2O and O_2 may also be affected by the differential thermal fluxes across the air-sea interface (Keeling et al., 1993).

5.7. Distribution of Nitrous Oxide in the Coastal regions:

The eastern boundary upwelling zones have been known to be sites of rapid turnover of N_2O, due to the low oxygen levels in these regions. As long as

the oxygen levels do not fall below the threshold value to trigger denitrification, production of N_2O seems to be enhanced with decreasing O_2 levels within the water column. Codispoti and Christensen (1985) suggested that the eastern boundary upwelling regions which account for a meagre 1% of the total oceanic area could produce as much N_2O as the rest of the ocean. However, as these environments are also sites of active denitrification, within the water column as well as in sediments, it was suggested that whether they act as a net source or a sink for N_2O would depend on the oxygen distribution in the low range.

Distribution of N_2O along six cross-shelf sections during the SW monsoon - August 1997 (SS158) along the SW coast of India is shown in fig.5.8 a-f. Stations located closest to the shore had the highest N_2O concentration. The highest concentration recorded was 233nM, corresponding to a saturation of 3866%. This is the highest N_2O concentration reported from the water column in the world oceans. The concentrations were especially high along leg S-4; concentrations close to the shore decreased progressively both to the north and south of this leg.

In all the sections, the isotherms sloped upwards towards the coast indicating strong upwelling over the continental shelf (Fig. 5.9 a-f). The salinity sections also show high saline water rising up the continental slope (Fig. 5.10 a-f). Upwelling brings up N_2O-rich deep waters closer to the surface. These waters also have low oxygen contents (Fig. 5.11 a-f). The upwelling of these nutrient rich waters (Fig. 5.13 a-f) sustains very high rate of primary productivity in the inner shelf, ranging between 138 and 738 $mgC/m^3/day$ (J. Kurien unpublished).

At the stations located close to the shore (Fig. 5.11 a-f) the bottom waters had very low concentration of oxygen (~5uM or less) and had very high

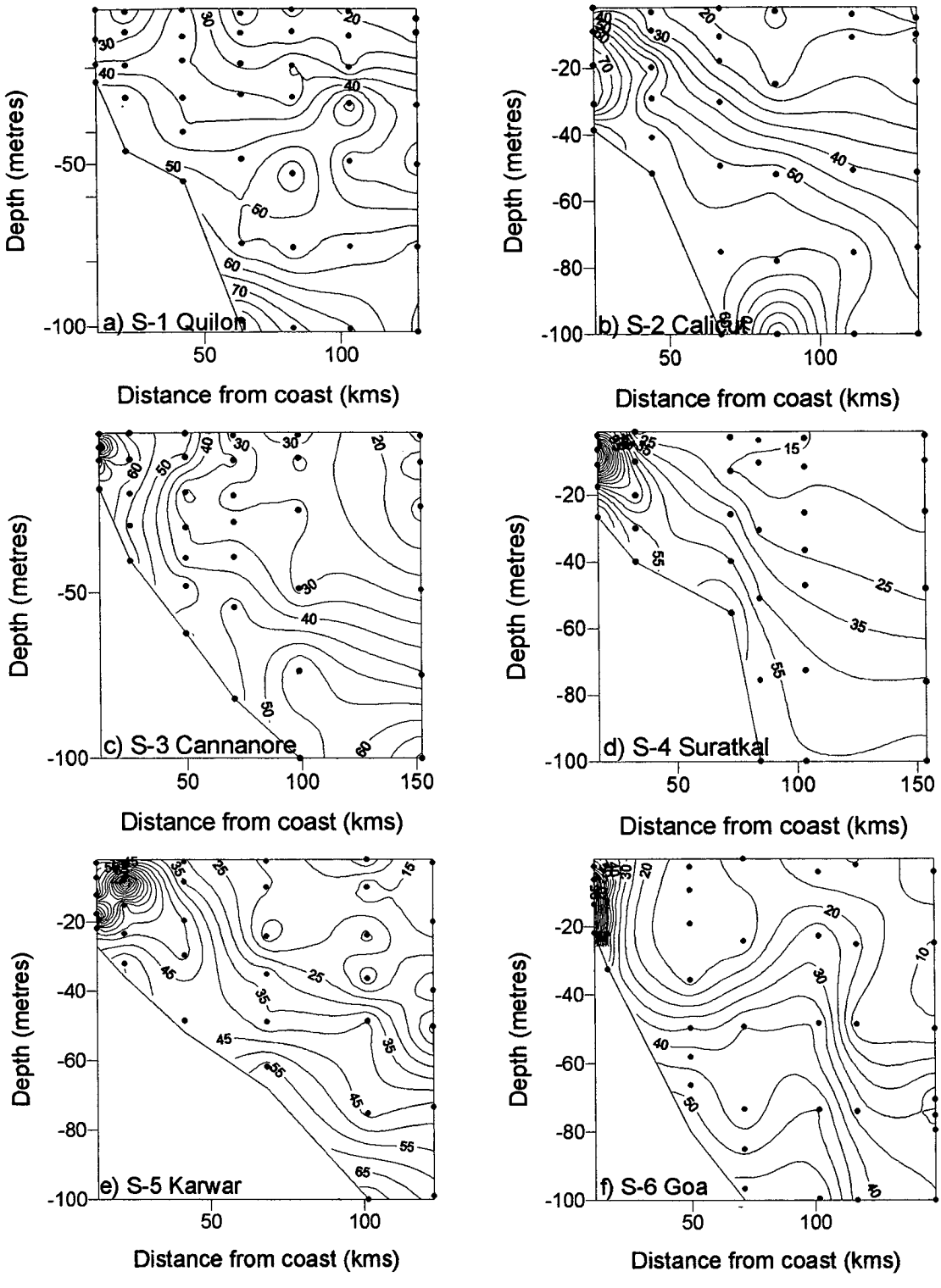

Fig.5.8. Distribution of N_2O (nM) along cross-shelf section during the SW monsoon (1997) along the SW coast of India.

concentration of nitrite (Fig. 5.12 a-f) indicating denitrifying conditions. As the productivity is very high and the oxygen content of the upwelled water is very low, NO_3^- is used as a terminal electron acceptor to oxidise the large quantity of organic matter. While in the subsurface waters affected by denitrification the N_2O concentration was low, it rose very steeply at the suboxic-oxic interface to extremely high levels (Fig.5.8). The water with the high concentration of N_2O was mostly capped with low salinity water (Fig. 5.10 a-f), thus inhibiting the escape of this gas to the atmosphere. However, at the shallow end of leg S-4, the surface concentration shot up to 106 nM, corresponding to a saturation of 1790%, which would sustain high fluxes of N_2O from the ocean to the atmosphere. Hence these upwelling regions not only act as a chimney of N_2O produced elsewhere in the ocean but also that produced *in situ* by the nitrifying-denitrifying activities, as the conditions are conducive with the O_2 values reaching close to zero in this region.

A previous survey made during the SW monsoon of 1995 (SK103) had also shown similar conditions along the SW coast of India. Temperature and nitrate distributions along three cross-shelf sections during the SW monsoon of 1995 are shown in figures 5.14.a-c and 5.15.a-c respectively. The upwelling process (Fig.5.14 a-c) was weaker along the section off Quilon (Fig.5.14 a) but it intensified towards north (Fig. 5.14 c). High concentrations of N_2O related to upwelling was also recorded during this cruise (Fig. 5.16 a-c). However, sampling was not done between 11 and 15°N during SK103, where the intense flux of N_2O was observed during the latter cruise. Along the 11°N section that was worked during both the cruises the surface values of N_2O were the same (i.e. ~55nM), and the maximum concentrations observed were also similar (115 and 128 nM), but the pattern of distribution was different.

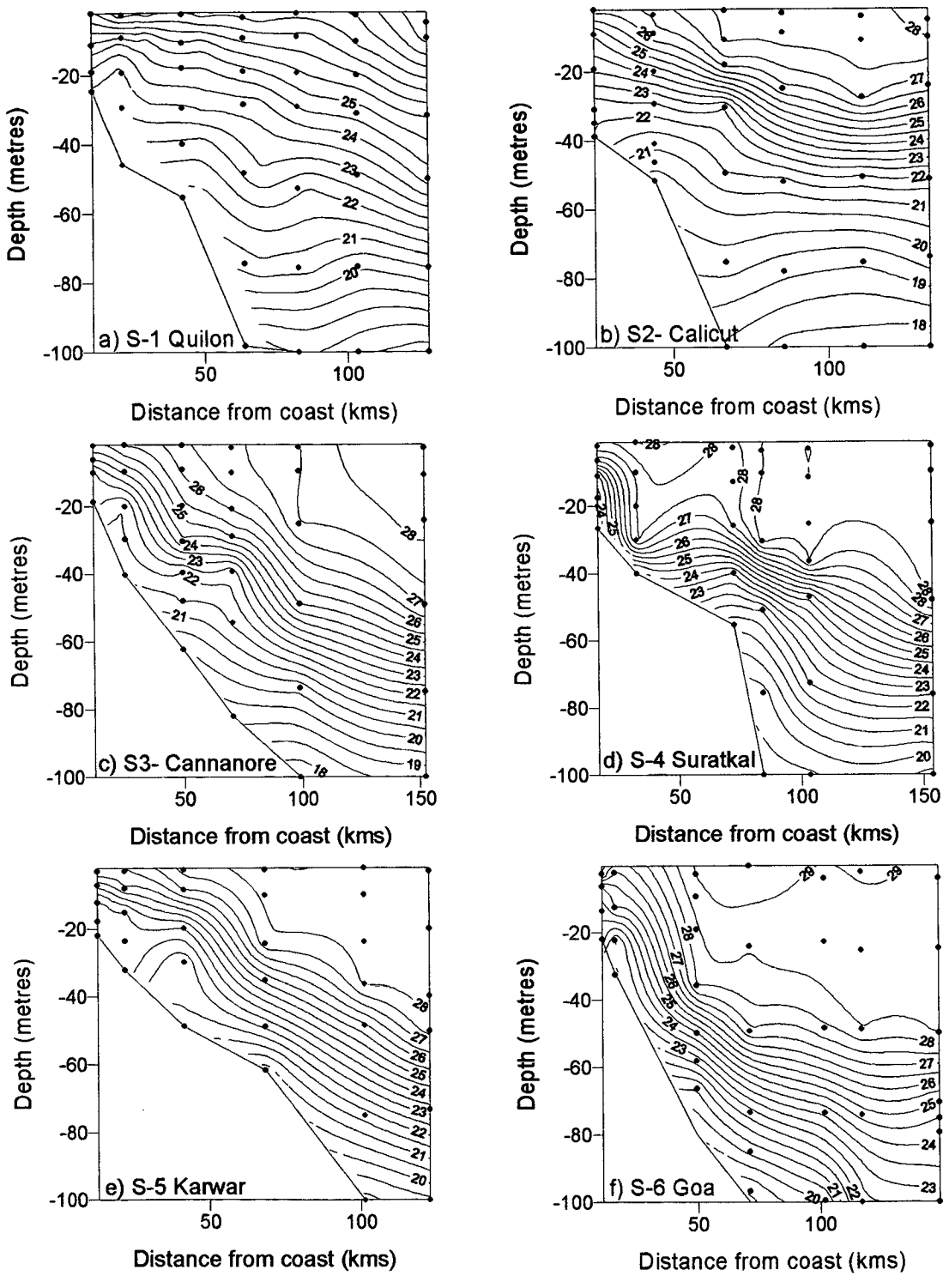

Fig.5.9. Potential temperature (°C) distribution along cross-shelf section during the SW monsoon (1997) along the SW coast of India.

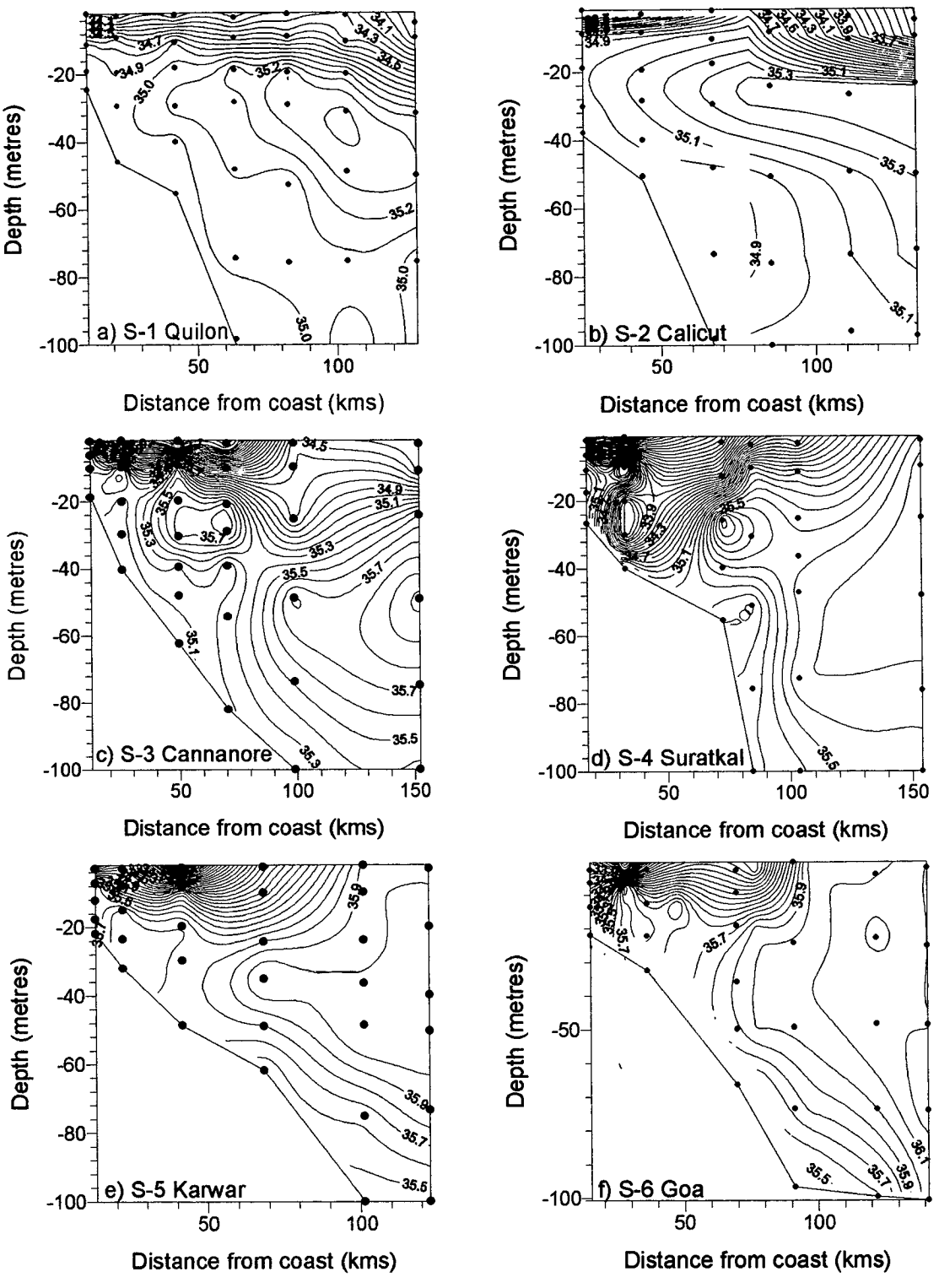

Fig.5.10. Salinity distribution along cross-shelf section during the SW monsoon (1997) along the SW coast of India.

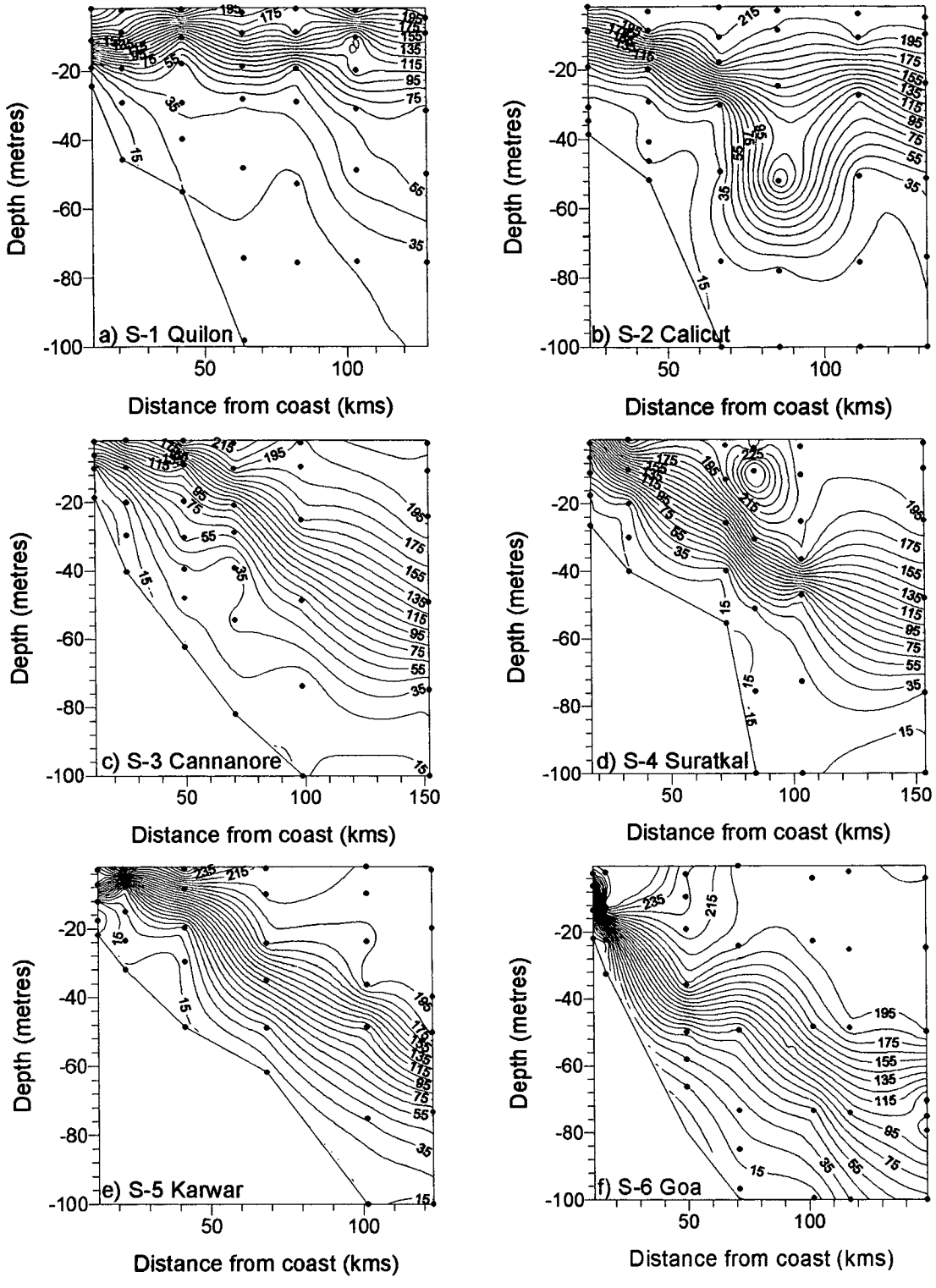

Fig.5.11. Dissolved oxygen (μM) distribution along cross-shelf section during the SW monsoon (1997) along the SW coast of India.

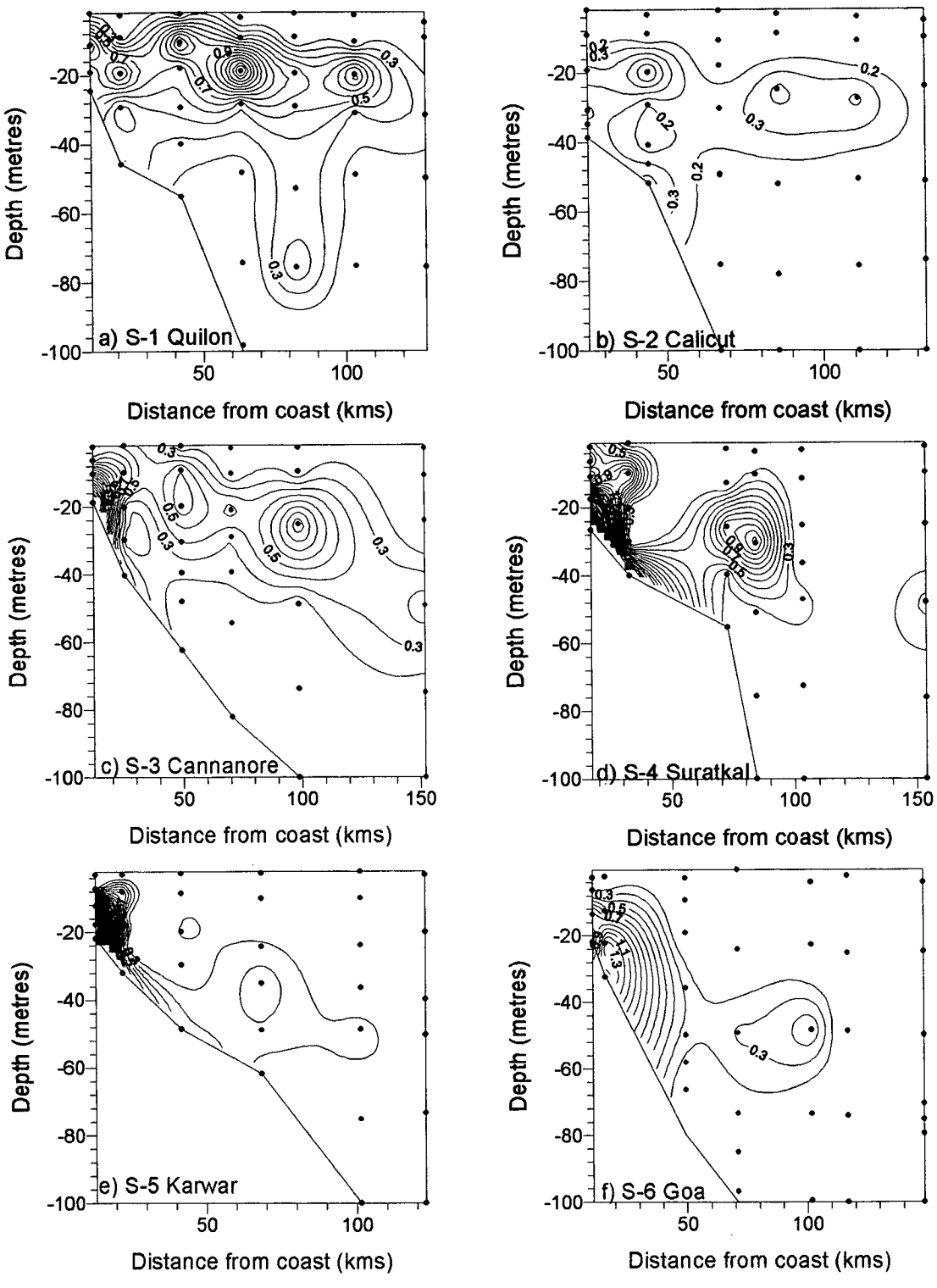

Fig.5.12. Nitrite (μM) distribution along cross-shelf section during the SW monsoon (1997) along the SW coast of India

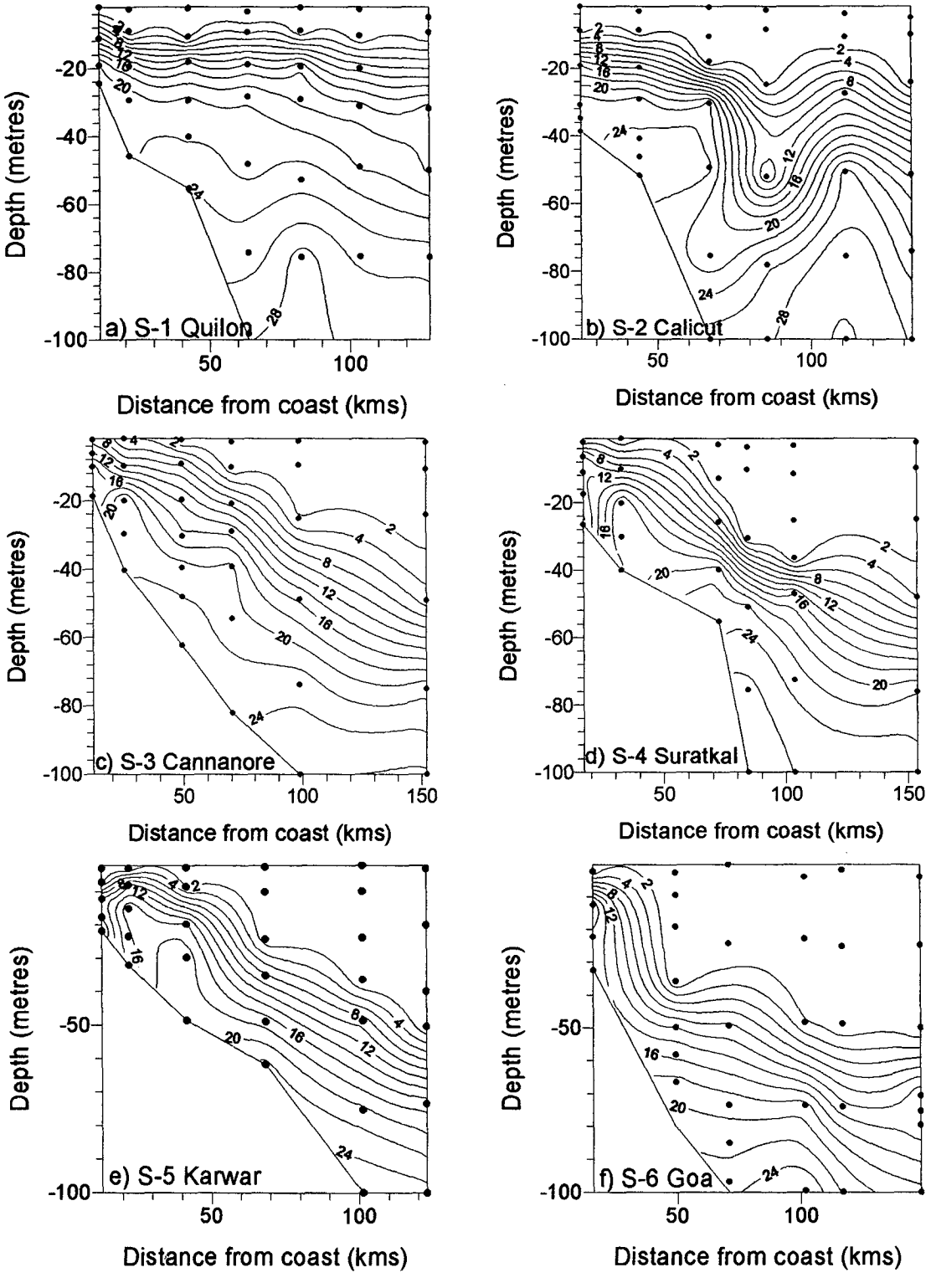

Fig.5.13. Nitrate(μM) distribution along cross-shelf section during the SW monsoon (1997) along the SW coast of India.

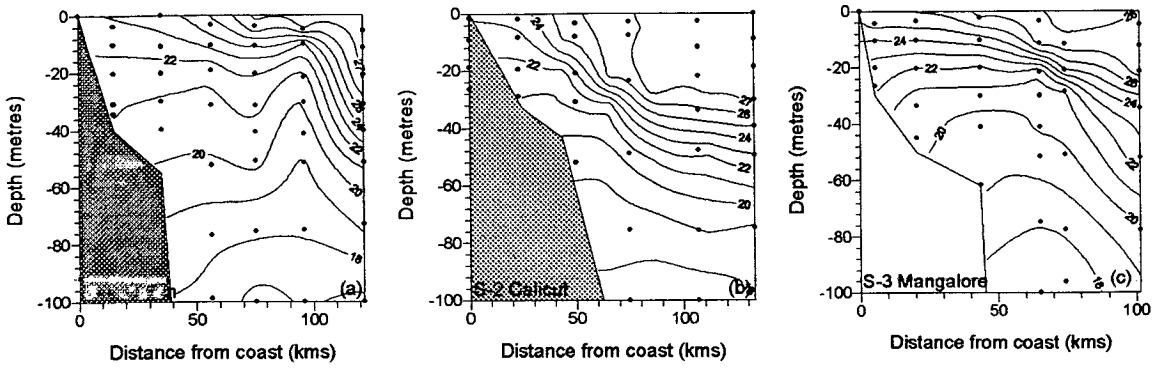

Fig.5.14. Temperature (°C) distribution along cross-shelf sections during the SW monsoon (1995) along the SW coast of India.

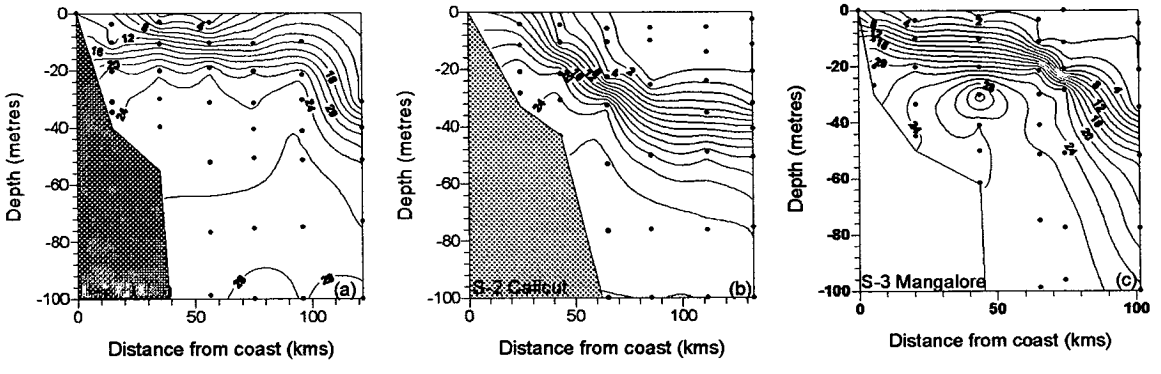

Fig.5.15. Nitrate (μM) distribution along cross-shelf sections during the SW monsoon (1995) along the SW coast of India.

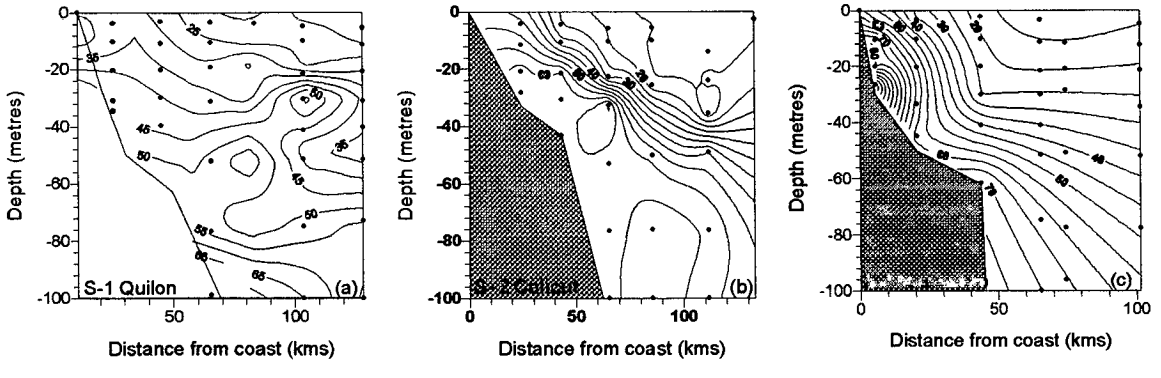

Fig.5.16. Nitrous oxide (μM) distribution along cross-shelf sections during the SW monsoon (1995) along the SW coast of India.

During the earlier cruise, there was a steady increase in N_2O concentration with depth, while during the latter cruise the maximum was located at mid depth. This was due to the occurrence of denitrification as a result of which N_2O in waters close to the bottom was consumed. The earlier cruise was undertaken during early July, while the latter cruise was in late August. It would appear that the high rate of primary production and consequently greater consumption of oxygen might have led to the development of reducing conditions during the latter cruise. Although the oxygen levels in the bottom waters were below 5μM during both the cruises the nitrite levels were higher during the latter observation, being 1.5 and 2.5 μM respectively. This also indicates that N_2O may get accumulated during the early part of denitrification and gets consumed as the process becomes more intense.

5.8. Distribution of Nitrous oxide in the Bay of Bengal:

Sampling in the Bay of Bengal was carried out during the pre-SW monsoon season. The surface waters were generally found to be supersaturated with N_2O, except for a few (five) stations where slight under-saturation was observed. The saturation values ranged between 89.3 and 213.9% with a mean $\pm$ 1 SD of 125.2 $\pm$ 25.4%. The highest supersaturations occurred at station C-2 (station locations in Table 2.1) followed by station C-3 (161.2%). This was associated with weak coastal upwelling as was evident from the physical and chemical oceanographic data. The surface waters at C-3 were cooler by 1.5 °C as compared to the offshore stations and the 26°C isotherm lay at ~20m at C-2 ~30m at C-3 and at depths > 50m at other stations. Significantly higher nutrient concentrations were observed within the euphotic zone at C-2 and C-3. These data suggest that slight changes in the hydrographical conditions can bring about potentially large changes in the fluxes of greenhouse gases across the air-sea interface in the northern Indian Ocean.

Unlike most parts of the northern Arabian Sea, where two maxima in N_2O are observed vertical profiles of dissolved N_2O in the Bay of Bengal generally exhibited a single pronounced maximum (Fig. 5.1) As the oxygen concentration in the Bay of Bengal do not reach suboxic levels (Rao et al., 1994), unlike in the Arabian Sea where it leads to denitrification, it is very unlikely that any loss of N_2O occurs within the water column in the Bay of Bengal. The maximal N_2O concentrations are among the highest observed in the open ocean. This is expected as the Bay of Bengal offers ideal conditions for N_2O accumulation in the water column. In order to estimate the total amount of ΔN_2O, the average profile of ΔN_2O (Fig. 5. 17) was determined and the area under the profile was integrated, yielding an inventory of 1.32g N_2O-N/m^2, which amounts to an overall inventory of ~5.4 Tg N for the Bay of Bengal.

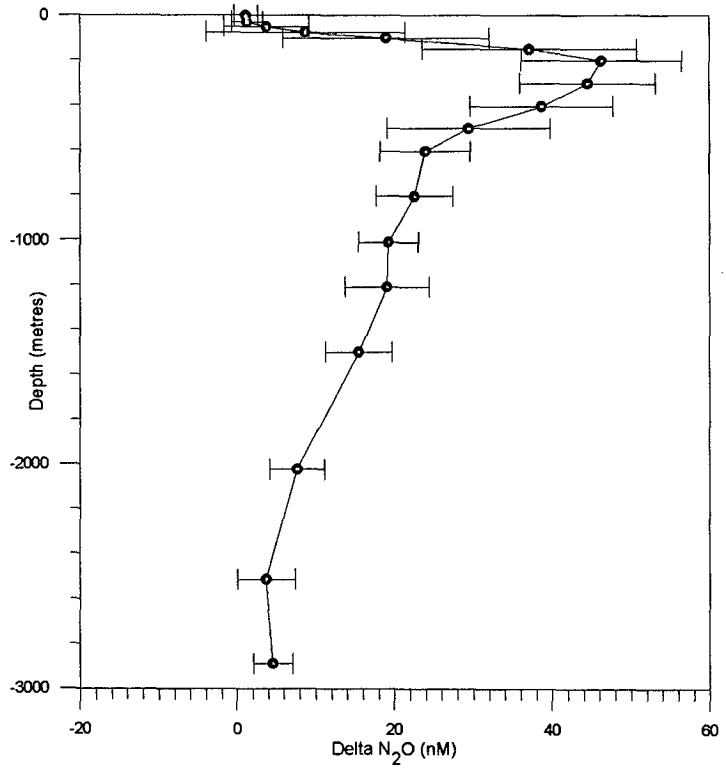

Fig.5.17. Average profile of excess N_2O (nM) in the Bay of Bengal. The error bars represent 1SD (n=27 stations)

Spatial variability of dissolved N_2O has been investigated through vertical sections along a transect oriented roughly in the N-S direction and three transects normal to the Indian coast (Fig. 5.18 a-d). Concentrations of N_2O within its maximum exhibit a steady increase towards the north. The highest concentration measured during the cruise (~80nM) was at 200m depth at sta. G-9 (Fig.5.18d), which was associated with very low oxygen(< 5μM) concentrations (Rao et al., 1994). Lower oxygen concentrations, often reaching the detection limit of the Winkler procedure (but still not low enough to trigger intense denitrification, with accumulation of NO_2^-) coupled with higher rates of biological productivity (Qasim, 1977) and higher particle fluxes as measured by the sediment traps (Ittekot et al., 1991) might result in the observed enhanced N_2O accumulation in the northern Bay of Bengal. The sections oriented normal to the coast reveal the occurrence of lower N_2O concentrations off the continental margin than in the offshore waters, particularly along Legs B and G (Fig.5.18 b,d). A more effective renewal of intermediate waters off the continental margin could account for the lower N_2O content of these waters.

5.9. N_2O-O_2 Relationship in the Bay of Bengal:

Vertical profiles of N_2O and O_2 in the Bay of Bengal showed a striking negative correlation as in other oceanic area (Yoshinari, 1976; Cohen and Gordon, 1978: Elkins et al., 1978: Rönner, 1983; Codispoti and Christensen, 1985: Cline et al., 1987; Butler et al., 1989; Oudot et al., 1990; Law and Owens, 1990; Naqvi and Noronha, 1991), However, a plot (Fig. 5.19) between the ΔN_2O and AOU shows that distinct linear relationships between the two may exist within three ranges: at AOU< 150 μM, from AOU ~ 150 μM to the N_2O maximum (depth ~ 300m), and at depths >~1000m. The correlation between Δ N_2O and AOU was statistically insignificant in the depth range ~300-1000m.

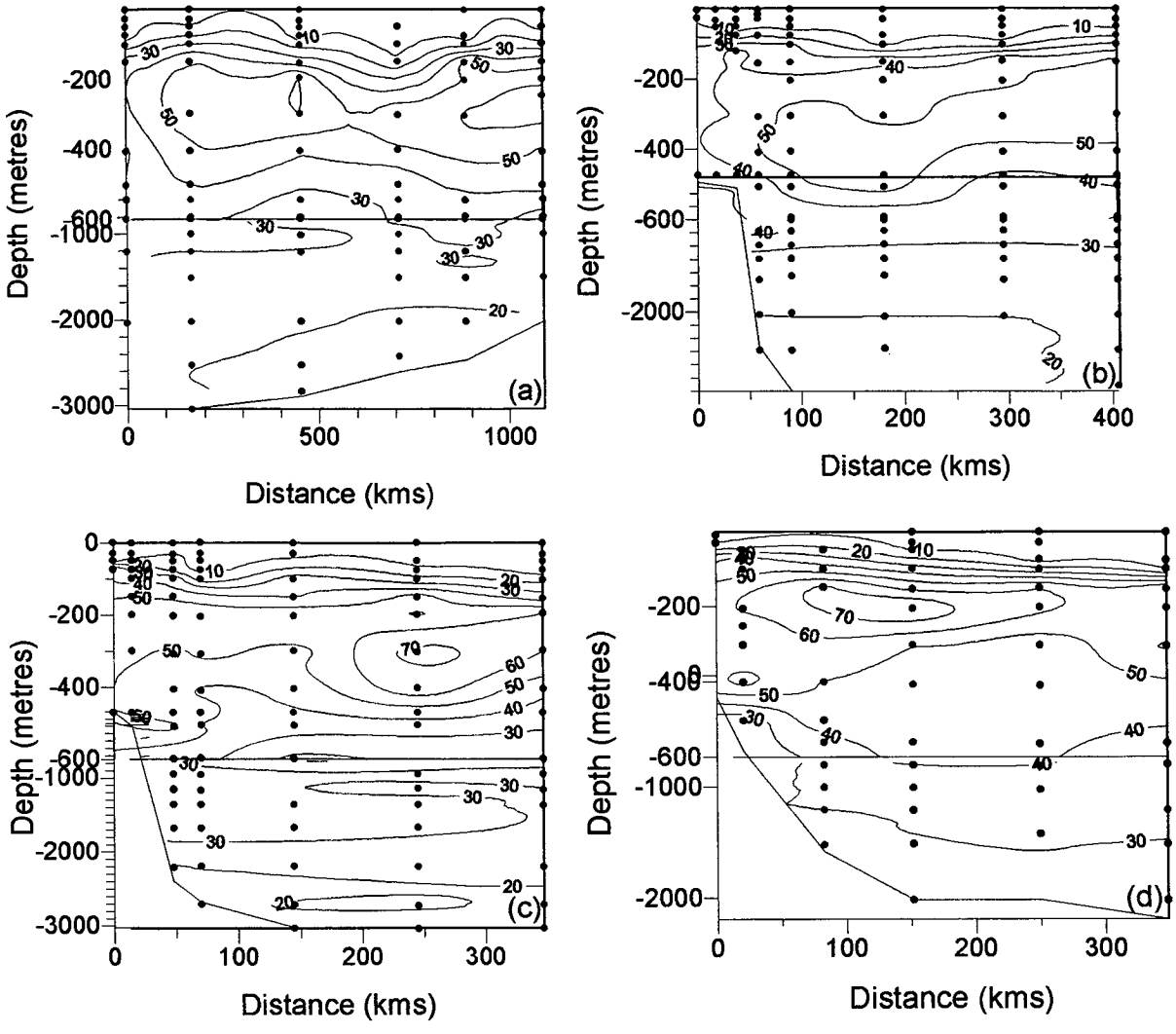

Fig.5.18. Distribution of nitrous oxide in the Bay of Bengal (a) along a transect oriented approximately N-S direction (b) along Leg B (c) along Leg E (d) along Leg G.

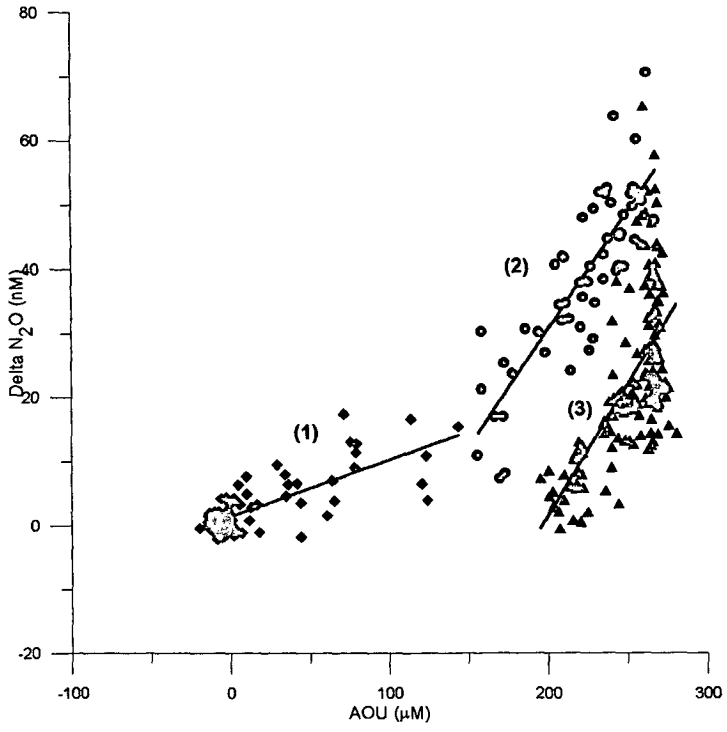

Fig.5.19. Relationship between the apparent N_2O production (ΔN_2O) and apparent oxygen utilization (AOU). The straight lines represent least square fits for three ranges (1) AOU < 150 μM (2) AOU ~150 μM to N_2O maximum (depth ~300m) (3) depths > ~1000m. The correlation was insignificant within the depth range ~300-1000m.

An anomalous aspect of the N_2O - O_2 relationship in the Bay of Bengal is that over a wide depth range (~300-1000m), ΔN_2O and AOU are apparently unrelated (Fig.5.19). This primarily results from the sensitivity of N_2O production to small changes in the ambient oxygen concentrations when the latter fall to near-zero levels. Thus, while the N_2O concentration varies greatly (with the peak values associated with the oxygen minimum at 200-300m), the AOU remains more or less constant within the above depth interval.

As stated above, a linear correlation between ΔN_2O and AOU also exists at depth > 1000 m. The deep waters in the Bay of Bengal could be formed through binary mixing involving the bottom water and North Indian high-salinity intermediate water (Rao et al., 1994). Hence their N_2O content may be

determined to a large extent by the mixing of high- N_2O intermediate water with the low-N_2O bottom water.

5.10. Conclusions:

The distribution of N_2O in the northern Indian Ocean was largely dependent on the distribution of dissolved O_2. In the northern Arabian Sea due to the mid- depth oxygen depletion the rates of both the production and consumption of N_2O are very high. Within the core of the denitrifying layer, low N_2O was associated with high nitrite and high ΔN indicating the consumption of N_2O during denitrification. On the other hand, while determining the relationship between AOU and ΔN_2O it was observed that the low O_2 levels also farm high rates of N_2O production. The threshold levels of dissolved O_2 where the change over from N_2O production to consumption takes place in the denitrification pathway could not be determined as the Winkler's method of dissolved O_2 estimation is not sensitive enough for this purpose. In the regions outside the active denitrification sites, no water column consumption of N_2O was observed. In the deep waters, the production of N_2O in the Arabian Sea seems to be higher than that observed in the rest of the world oceans indicating a high rate of N_2O turnover in this region.

Various physical processes play an important role in the distribution of N_2O in the northern Indian Ocean. In the northern regions of the Arabian Sea the Winter cooling results in the enhanced concentration of N_2O in the mixed layer. While in the SW and eastern coasts of India higher concentrations of N_2O in the shelf regions are resultant of upwelling. As the O_2 levels of the upwelled water is very low, and the nutrients levels are high, conditions are highly favourable for

enhanced production of N_2O in the shallow shelf regions. The annual reversal in the coastal circulation in the Arabian Sea determines the amount of O_2 being injected into the O_2 depleted waters of the northern Arabian Sea, which in turn determines the intensity of denitrification. As N_2O is both produced and consumed during denitrification the intensity of denitrification determines the distribution of N_2O. Also the outflow from the PGW determines the intensity of denitrification in the north-western Arabian Sea it is responsible for the distribution of N_2O at depths where this water mass flows. The immense river runoff results in strong stratification in the Bay of Bengal and this causes a lower surface saturation and consequently a smaller air -sea flux from the Bay. The distribution pattern of N_2O in the subsurface waters of the Bay of Bengal also seems to be influenced by the circulation pattern.

Another key factor in the distribution of N_2O is the distribution of organic carbon. High productivity during the SW and NE monsoon seasons leads to higher rates of sinking organic matter, which in turn consumes more oxygen from the already oxygen depleted waters at mid- depth. The higher rates of denitrification during these seasons accompanied by ΔN values in excess of 10 μM and high nitrite results in the extreme consumption of N_2O, leading to undersaturation of this gas.

6. Natural Abundance of Stable Isotopes in some Dissolved Nitrogen Species

6.1. Introduction:

Considerable amount of work on nitrogen cycling in suboxic waters of the Arabian Sea, carried out over the past two decades, has established it to be globally significant (Naqvi, 1994). However, these studies largely involved chemical and, to a lesser extent, biochemical measurements. Investigations on the natural abundance of stable isotopes in various dissolved nitrogen species is based on the fact that the biogeochemical processes involve characteristic mass-dependent discriminations between various isotopes. The isotopic data can provide useful insights into the pathways of nitrogen transformations (Wada and Hattori, 1991).

Abundance of ^{15}N in various components of the biosphere varies typically within 1 or 2% of the atmospheric N_2 (Junk and Svec, 1958). Although this difference arising from isotopic discrimination is small it can be measured precisely using suitable instrumentation. These differences in the isotopic composition has been used to identify different sources by estimating relative contribution from two immediate sources of N to a common sink and also to delineate the mechanism of a metabolic process by studying the isotopic discrimination associated with it. The results of the measurements of isotopic composition of N in N_2 and NO_3^-, and N and O in N_2O from the low oxygen environments of the Arabian Sea is presented below. The samples for these analyses were collected from the stations shown in Fig.6.1.

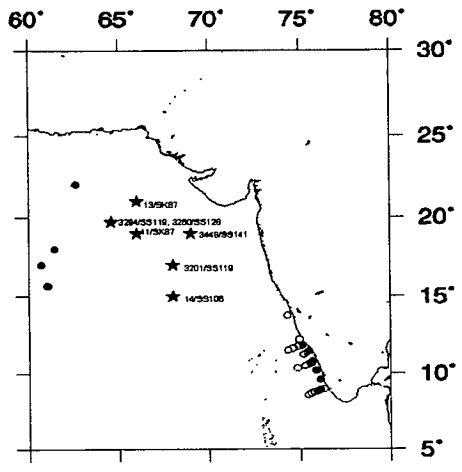

Fig. 6.1. Station locations for N-isotope studies (open circles - surface N_2O concentration only; filled circles - surface N_2O concentration and isotopes; stars - vertical profiles)

Results and Discussion

6.2. Nitrogen isotopic fractionation during denitrification:

The reduction of NO_3^- to N_2 by denitrifying bacteria is believed to occur through the pathway (Payne, 1973):

$$NO_3^- \rightarrow NO_2^- \rightarrow NO \rightarrow N_2O \rightarrow N_2 \qquad (6.1)$$

Nitrite (NO_2^-), the first intermediate of this reduction sequence, accumulates in the oceanic suboxic zones (Richards, 1965). In the Arabian Sea, as in the eastern tropical Pacific Ocean (Cline and Richards, 1972), the secondary nitrite maximum (SNM), located in the upper portion of the oxygen minimum zone (OMZ), is invariably associated with $O_2 < 0.1$ ml l^{-1}, in contrast to the primary NO_2^- maximum commonly found at the base of the euphotic zone. Precise O_2 measurements carried out during a U.S. JGOFS cruise in the Arabian Sea revealed that the threshold O_2 levels required for the NO_2^- build-up lie between 0.01 and 0.02 ml l^{-1} (S W A Naqvi and L A Codispoti, unpublished data). Dramatic changes in water chemistry are seen once this threshold is crossed. An

apparent spurt in denitrification activity causes a minimum in the vertical profile of NO_3^- (Fig.6.2). Interestingly, while NO_2^- accumulates under these conditions, N_2O, the other major intermediate, shows an opposite trend (e.g., Figs. 6.2 and 6.3), indicating that the reduction of NO_2^- may be the rate limiting step. These microbially-mediated

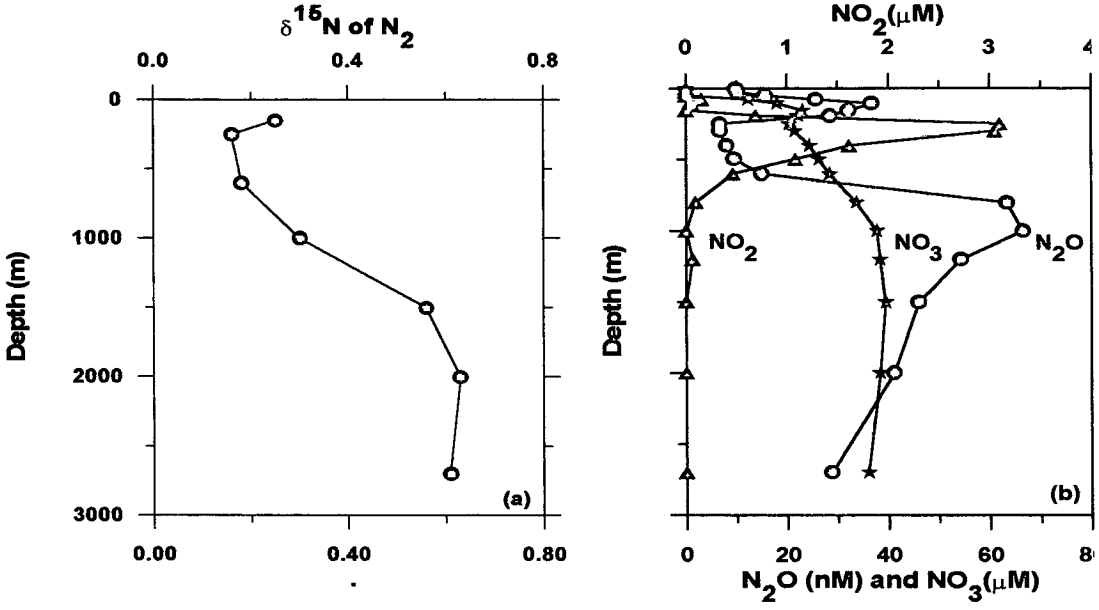

Fig.6.2. Vertical profiles of (a) $\delta^{15}N$ of N_2 (°/oo relative to air) and (b) concentrations of NO_3^- (μM), NO_2^- (μM) and N_2O (nM) at Sta. 3448/SS141.

transformations leave a strong imprint on the isotopic composition of dissolved nitrogen species. This is because, of the two nitrogen isotopes with mass numbers of 14 and 15 (^{14}N and ^{15}N), NO_3^- ions containing the more abundant ^{14}N are preferentially reduced during denitrification, leaving the residual NO_3^- enriched with ^{15}N. On the other hand N_2, the end product of denitrification, gets greatly enriched with ^{14}N. This is strikingly demonstrated by the present results. The vertical profile of $\delta^{15}N$ of N_2 at the strongly reducing Sta. 3448/SS141, located in the northeastern Arabian Sea, exhibits a pronounced minimum coinciding with the SNM with values dipping below 0.2 ‰ (Fig.6.2) (the $\delta^{15}N$ of

N_2 in surface waters in this region, not determined at this station, is generally greater than 0.5 ‰). Interestingly at 150 m depth, where the NO_3^- concentration was high (23 μM) and NO_2^- was not detectable, the $\delta^{15}N$ was still quite low (0.25 ‰) i.e., only marginally higher than the minimal value but less than half of the values observed in waters outside the O_2-deficient zone. Even at 1000 m depth the $\delta^{15}N$ was only 0.3 ‰.

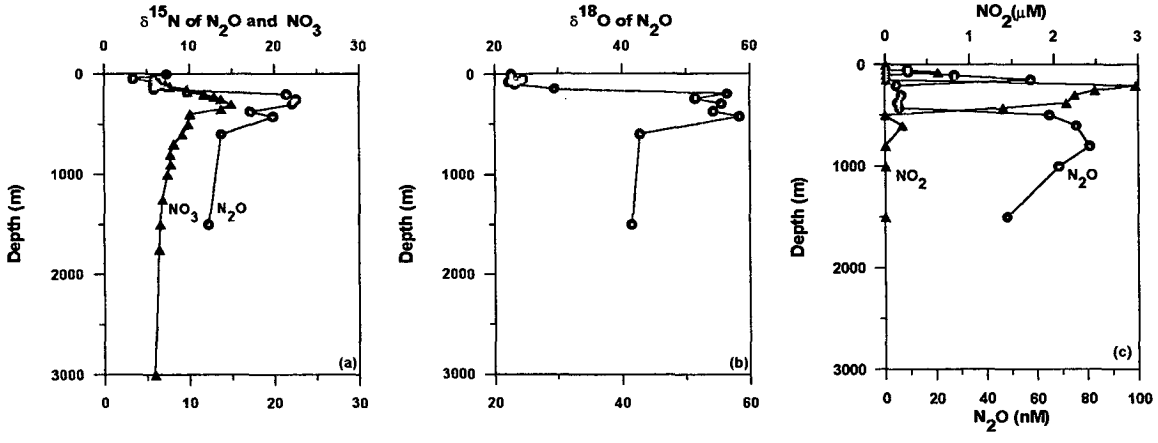

6.3. Vertical profiles of (a) $\delta^{15}N$ of NO_3^- and N_2O (°/oo relative to air), (b) $\delta^{18}O$ of N_2O (°/oo relative to air) and (c) concentrations of NO_2^- (μM, triangles) and N_2O (nM, circles) at Sta. 3201/SS119 (modified from Naqvi *et al*, 1998).

This indicates that the denitrification signature extends well outside the SNM. Similar pattern is also seen at Sta. 3204/SS119 (Fig. 6.4). This station had a thin, weakly-developed SNM associated with a minimum in $\delta^{15}N$ of N_2 (0.18 ‰) at 150-190 m. This was underlain by a layer with relatively high $\delta^{15}N$ of N_2 (maximum 0.39 ‰) which, going by its high salinity, evidently originated in the Persian Gulf. The O_2 concentrations, as determined by the Winkler method, were not appreciably different from those at Sta. 3201/SS119 (Fig.6.5). The association of a maximum in $\delta^{15}N$ of N_2 with the Persian Gulf salinity maximum layer shows that the former is a sensitive tracer of advection. Again the vertical extent of the $\delta^{15}N$-N_2 minimum is much larger than the SNM. This would mean

that substantial N_2 may be produced without the accumulation of NO_2^- or/and the rapid horizontal mixing results in the export of lighter N_2 out of the SNM.

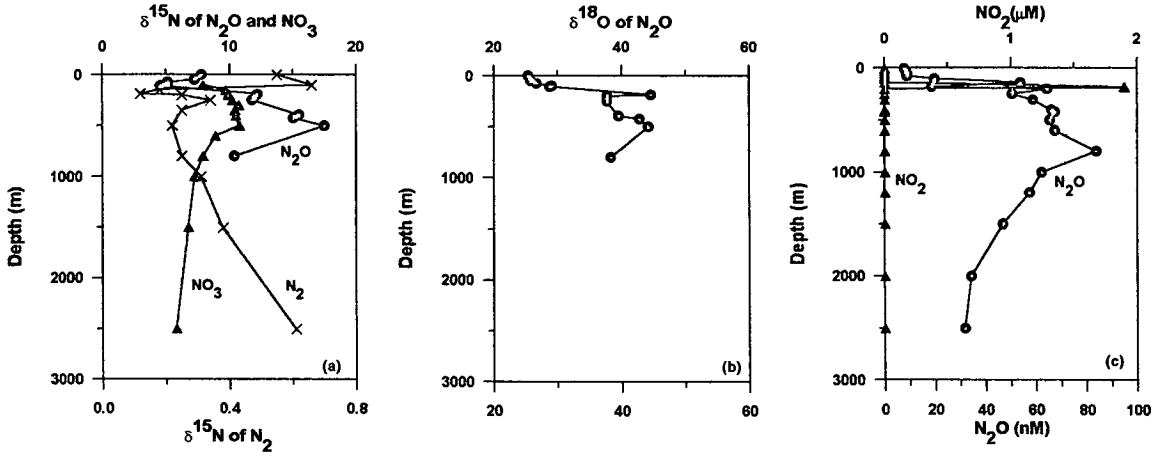

6.4. Vertical profiles of (a) $\delta^{15}N$ of N_2, NO_3^- and N_2O, (b) $\delta^{18}O$ of N_2O and (c) concentrations of NO_2^- (μM, triangles) and N_2O (nM, circles) at Sta. 3204/SS119 (the $\delta^{15}N$-NO_3^- profile at this site was obtained during SS128) (modified from Brandes *et al*, 1998; Naqvi *et al*, 1998).

The distribution of $\delta^{15}N$ of NO_3^- shows a good correspondence to that of secondary NO_2^- (Figs.6.3, 6.4 and 6.6). Sharp increases in $\delta^{15}N$ of NO_3^- (up to 15 ‰) were observed within the SNM at Stas. 3201/SS119 (Fig. 6.3) and 13/SK87 (Fig. 6.6) with both maxima being thicker at the latter site. In contrast, at Sta. 3204/SS119 where the SNM was weakly developed, the extent of ^{15}N enrichment in NO_3^- was considerably smaller (Fig. 6.4). At all the three stations, significant ^{15}N enrichment in NO_3^- [relative to the average value of 5.7 ‰ for the oceanic subsurface waters (Altabet *et al*, 1995)] persisted down to at least 1,500 m, consistent with the observed trends in $\delta^{15}N$ of N_2.

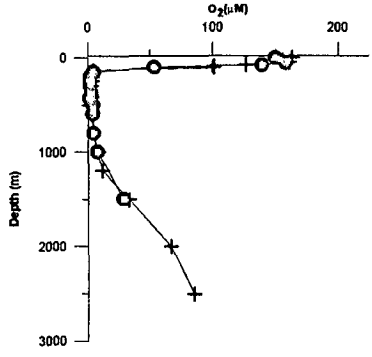

6.5. A comparison of vertical profiles of O_2 (µM) at Stas. 3201/SS119 (circles joined by dotted lines) and 3204/SS119 (triangles, joined by continuous lines) (modified from Naqvi *et al*, 1998).

These data on $\delta^{15}N$ of N_2 and NO_3^- can be used to compute the fractionation factor, ε_{denit} [$=10^3(1-\alpha)$, where α is the ratio between the rates of utilisation of $^{15}NO_3^-$ and $^{14}NO_3^-$], during denitrification using simple advection-reaction and diffusion-reaction models (Brandes *et al,* 1998). In the first case, diffusion is ignored and the water mass is assumed to advect into the OMZ without undergoing any mixing in the vertical and horizontal directions. The isotopic distribution can then be modelled with a simple Rayleigh equation (Bender, 1990):

$$\delta^{15}N\text{-}NO_3 = 10^3(\alpha-1)\ln f_{NO3} + (\delta^{15}N\text{-}NO_3)_{init} \qquad (6.2)$$

where f_{NO3} is the ratio between the observed and expected NO_3^- concentrations and $(\delta^{15}N\text{-}NO_3)_{init}$ gives the isotopic composition of the initial (unaltered) material. Values of f_{NO3} were computed using the relationships between a nitrate tracer (NO) and potential temperature and the observed NO_3^- and NO_2^- concentrations (Naqvi *et al*, 1990).

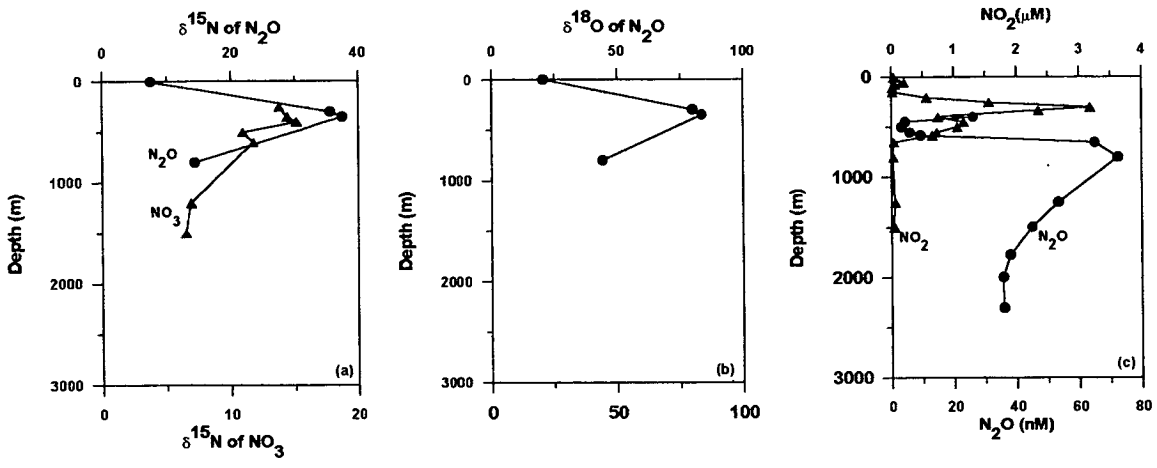

6.6. Vertical profiles of (a) $\delta^{15}N$ of NO_3^- and N_2O, (b) $\delta^{18}O$ of N_2O and (c) concentrations of NO_2^- (μM, triangles) and N_2O (nM, circles) at Sta. 13/SK87 (modified from Brandes *et al*, 1998; Yoshinari *et al*, 1997).

A plot of $\delta^{15}N$-NO_3 versus ln f_{NO3} for the depth range 200-600 m (Fig.6.7) shows a good linear relationship between the two (r^2=0.9). The slope of the regression line yields a value of 22‰ for $\varepsilon_{denit.}$, not too different from a similarly computed value (25‰) for the eastern tropical North Pacific (ETNP) (Brandes *et al*, 1998).

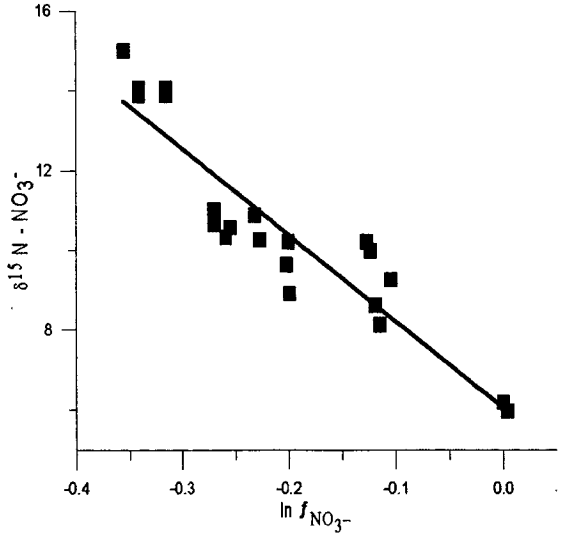

Fig.6.7.The $\delta^{15}N$-NO_3^- (‰ relative to air) vs. The natural log of *f*, the ratio of measured to expected nitrate concentrations (pooled data from three stations). The line gives the least squares fit to the data (modified from Brandes et al 1998).

The opposite extreme to the advection-reaction model is the reaction-diffusion model having no advective component. Such a model is expected to yield a larger fractionation factor than the advective model because the system being "open" allows the addition of new, unaltered material into the reaction region and the removal of old, altered material.
The reaction-diffusion equation is:

$$\partial[^{14}NO_3]/\partial t = J_{14NO3} + K_d\, \partial^2[^{14}NO_3]/\partial x^2 \qquad (6.3)$$

where J is the denitrification rate and K_d the horizontal eddy diffusivity along the 300 m isopycnal which was chosen because it lies close to the core of the denitrifying layer (Naqvi, 1987); x increases from the edge to the centre of the denitrifying zone. For $^{15}NO_3^-$ the equation is:

$$\partial[^{15}NO_3]/\partial t = \alpha([^{15}NO_3]/[^{14}NO_3])J_{14NO3} + K_d\, \partial^2[^{15}NO_3]/\partial x^2 \qquad (6.4)$$

Because there is no exact analytical solution for these equations, the values of both ^{14}N and ^{15}N were calculated numerically using a tridiagonal matrix solution method (Press *et al*, 1992). The boundary conditions were that the NO_3^- and $\delta^{15}N\text{-}NO_3$ compositions at x=0 were 28 μM (NO_3^- deficit=0) and 6 ‰, respectively, and that there was no NO_3^- or isotopic flux out of the centre of the OMZ. Alternative boundary conditions, such as an interior concentration boundary condition, would change ε by no more than 2 (Brandes *et al*, 1998).

The value of J was set at $1x10^{-7}$ μmoles N l^{-1} sec^{-1}. Although this value is only 1/2 of the rate estimated by Naqvi and Shailaja (1993) from the ETS data, it gives realistic nitrate deficit given a x_E of 500 km, which is the minimum distance between the southern boundary of the suboxic zone at 12°N and the southernmost station located at 17°N. The value of K_d was taken as 1800 m^2 sec^{-1} (Jenkins, 1990). Using these parameters, NO_3^- concentrations dropped to

~70% of the initial values in the interior of the denitrification zone, in agreement with the observations (Naqvi, 1987). With these values of J and K_d the best-fit to the data was obtained with a fractionation factor of 25 ‰ (Fig.6.8), only slightly lower than a similarly calculated value of 30 ‰ for the ETNP (Brandes *et al*, 1998). These values of ε are higher than those (15-20 ‰) derived from laboratory experiments of denitrification (Delwitche and Steyn, 1970; Mariotti *et al*, 1981), but lower than the estimate (30-60 ‰) of Cline and Kaplan (1975) derived from one-dimensional model fits to their ETNP data. However, the same data when fitted to the advection-reaction model described above yielded a value of ε (25‰) which compares very well with the present results.

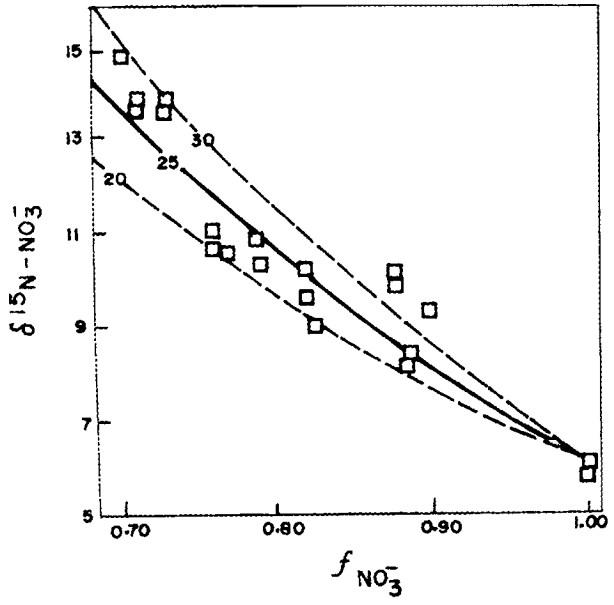

Fig.6.8. The $\delta^{15}N$ of NO_3^- (‰ relative to air) vs. *f*, the ratio of measured to expected nitrate concentrations. Also plotted are the diffusion-reaction model results with the numbers denoting fractionation factors (modified from Brandes et al, 1998).

Although, the above models ignore either diffusion or advection, and a more realistic approach should simultaneously consider both of these, the results of the two models are not too divergent. More significantly, as the estimates from the Arabian Sea and ETNP are not very different, it would appear that the fractionation factor is not strongly dependent on either the denitrification rate or the local hydrography of the region.

6.3. Nitrogen Fixation:

A very important aspect of the data is the strong decrease in $\delta^{15}N\text{-}NO_3$ in near-surface waters (Figs. 6.3 and 6.4). At 200 m, for example, the value is >10 ‰ but it declines to ~6 ‰ (close to the oceanic background) at 80 m. This trend is exactly opposite to that seen outside the OMZ (Sigman *et al,* 1997). The observed decrease can only result from an input of light nitrogen to the surface waters. The two possible sources are unaltered NO_3^- horizontally advected from outside the central Arabian Sea, and nitrogen fixation. The known pattern of water circulation in the Arabian Sea (Naqvi, 1987; Olson *et al,* 1993) makes the first mechanism less likely, and so the most plausible mode of input of isotopically light NO_3^- to the surface layer appears to be nitrogen fixation.

If NO_3^- from 200 m at 11 ‰ is being upwelled to the surface, and all nitrogen is removed by primary producers at 70-80 m, one can estimate the amount of nitrogen reaching the surface ocean that originally came from nitrogen fixation (Brandes *et al*, 1998). Assuming that the changes in isotopic composition below 80 m are due to dilution by remineralised nitrogen fixed at 0 ‰, about 40% of the NO_3^- present at 80 m should have been derived from nitrogen fixation. Using the data on primary productivity in this region this translates into a nitrogen fixation rate of up to 6 Tg N y^{-1} (1 Tg = 10^{12} g) or about 25% of the denitrification rate. Thus, in spite of a high rate of nitrogen fixation, the Arabian Sea still serves as a net sink of combined nitrogen. This is consistent with the data on N:P ratios in this region (Codispoti, 1997).

6.4. Dual isotopic composition of nitrous oxide:

As stated earlier, the eastern boundary upwelling environments that contain O_2-depleted waters are important for global N_2O cycling. This is because

of the extreme sensitivity of the processes involved in N_2O production and consumption to minor changes in ambient O_2 levels in the low range (<~0.5 ml l^{-1})(Codispoti and Christensen, 1985). An intense N_2O accumulation is found to occur as the O_2 concentrations approach, but do not reach, suboxia. However, under strongly reducing conditions, such as those found within the SNM, N_2O concentrations fall rapidly below saturation, evidently as a result of its reduction to N_2 (e.g., Figs. 6.2 and 6.3). Thus, the Arabian Sea contains sites, located in close proximity of each other, which act either as strong source or strong sink of N_2O (Naqvi and Noronha, 1991). Why a strong net accumulation of N_2O occurs in the low-O_2 zones is an issue that has not been fully resolved so far. This is because N_2O is an intermediate of both the oxidative and reductive sequences of the nitrogen cycle and can be produced both during nitrification and denitrification. The two pathways leave very different isotopic signatures: N_2O produced during denitrification is enriched with ^{15}N and ^{18}O while that formed during nitrification is depleted in these isotopes (e.g., Yoshida, 1988; Wada and Hattori, 1991; Yoshinari *et al,* 1997). Hence measurements of the $^{15}N/^{14}N$ and $^{18}O/^{16}O$ ratios in N_2O dissolved in seawater are expected to provide insights into the mechanisms of its transformations. However, while substantial data have now been generated on the dual isotopic composition of N_2O in seawater, their interpretation has not been straightforward, and indeed often contradictory (Yoshida *et al,* 1989; Kim and Craig, 1990). The Arabian Sea contains several diverse biogeochemical environments and offers the most extreme conditions for N_2O cycling (Burkill *et al,* 1993). The isotopic composition of N_2O in this region may therefore be helpful in improving the understanding of its transformations.

Data on the isotopic composition of N_2O at five stations (3201/SS119, 3204/SS119, 13/SK87, 11/SK87 and 14/SS106) are shown in Figs. 6.3, 6.4, 6.6, 6.9 and 6.10, respectively. The most prominent feature of the isotope profiles is the large enrichment of both ^{15}N and ^{18}O at all the stations although the degree of enrichment varies considerably. As stated earlier, Stas. 14/SS106 and

3204/SS119 experienced mildly reducing conditions (thin SNM) while the other three stations were strongly reducing. These differences in redox conditions are reflected in the isotope data.. The greatest enrichment is seen at Sta. 13/SK87; peak $\delta^{15}N$ and $\delta^{18}O$ values at this site (37.54 and 83.6 ‰, respectively) are the highest reported yet from a natural environment

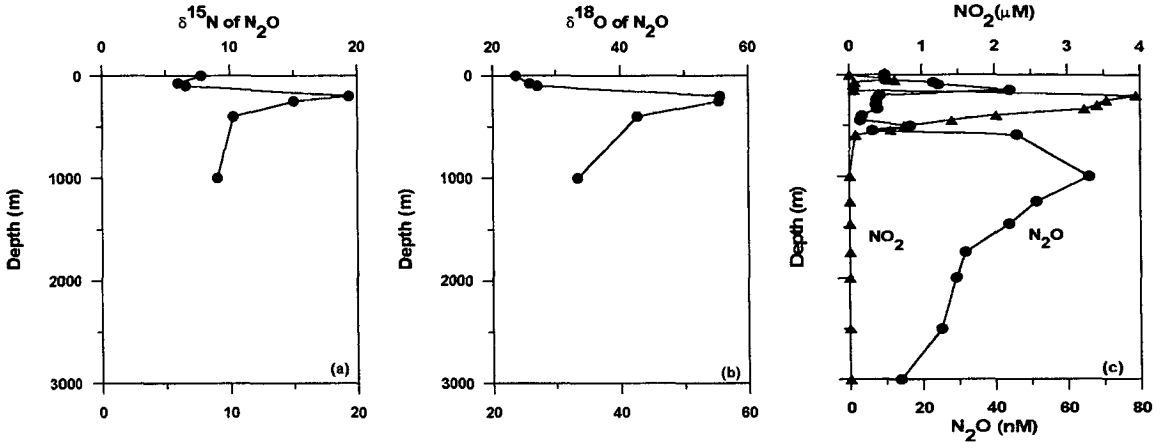

Fig.6.9. Vertical profiles of (a) $\delta^{15}N$ and (b) $\delta^{18}O$ of N_2O, and (c) concentrations of NO_2^- (μM, triangles) and N_2O (nM, circles) at Sta. 11/SK87 (modified from Yoshinari *et al*, 1997).

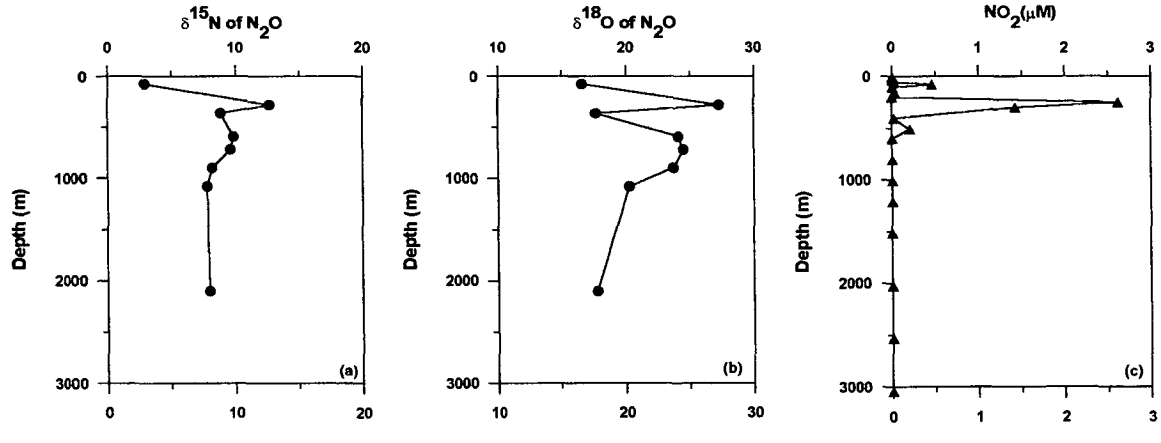

Fig.6.10. Vertical profiles of (a) $\delta^{15}N$ and (b) $\delta^{18}O$ of N_2O, and (c) concentration of NO_2^- (μM) at Sta. 14/SS106.

(Yoshinari *et al*, 1997). In contrast, the most southern Sta. 14/SS106 exhibited the least enrichment. However, it may be mentioned here that the samples from Sta. 14/SS106 were analysed following an older method [combustion of N_2O to N_2 and CO_2 (Yoshinari and Koike, 1994)]. It is possible that the oxygen isotope data at this station suffer from some contamination in CO_2 with traces of water leading to somewhat lower $\delta^{18}O$ values; this would, however, not affect the nitrogen isotope data.

Preferential loss of lighter N_2O to N_2 within the SNM evidently leads to the observed enrichments of ^{15}N and ^{18}O in residual N_2O. The N_2O concentration minimum is embedded between two maxima, but the isotopic compositions of these N_2O-rich layers are very different. Going upward from the OMZ, the $\delta^{15}N$ and $\delta^{18}O$ values fall sharply across the oxic-suboxic boundary with the former generally lower than the tropospheric value (7 ‰ - Kim and Craig, 1990) in the upper 150 metres. In contrast, although $\delta^{15}N$ and $\delta^{18}O$ also decrease below SNM, their levels remain much higher than the tropospheric values (20.7 ‰ for $\delta^{18}O$ - Kim and Craig, 1990) in the deep waters. Since the suboxic waters with huge enrichments of heavier isotopes are capped by a layer which has high concentrations of light N_2O, the N_2O escaping to the atmosphere in the region cannot be heavy. Thus the near-tropospheric isotopic values at the sea surface at the open ocean sites (mean$\pm$s.d = 7.65$\pm$0.47 ‰ for $\delta^{15}N$ and 23.45$\pm$1.35 ‰ for $\delta^{18}O$; n=11) probably reflect an active air-sea exchange. The fate of heavy N_2O is not known, but it is expected to be advected out of the region and contribute to the elevated $\delta^{15}N$ and $\delta^{18}O$ in N_2O observed outside the suboxic zones (Kim and Craig, 1990).

An important aspect of the data is that the $\delta^{15}N$ of NO_3^- is consistently lower than that of N_2O at depths exceeding ~200 m, and higher at shallower

depths (Figs. 6.3 and 6.4). This indicates that the intense N_2O accumulation in the upper and lower parts of the OMZ may be through different mechanisms. Greater enrichment of $\delta^{15}N$ in N_2O relative to NO_3^- appears to be characteristic of denitrification as revealed by recent culture experiments (M.A. Altabet, unpublished data). It may arise from a combination of much lower N_2O concentration than the amount of denitrified nitrogen and large kinetic isotope fractionation associated with the reduction of N_2O to N_2 (Yoshida *et al*, 1984). This pattern is the most pronounced within N_2O-depleted SNM at 3201/SS119. Its persistence even below SNM at 3201/SS119 and at depths exceeding ~200 m at 3204/SS119 suggests significant N_2O production through denitrification. This observation is consistent with the view that denitrification may lead to a net N_2O accumulation under certain conditions (Betlach and Tiedje, 1981; Capone, 1996). However, it has been noted that heavy isotope enrichment has also been observed, albeit to a lesser degree, in the more oxygenated deep waters of the Pacific Ocean by Kim and Craig (1990). It was attributed to partitioning of isotopes during nitrification by which the precursor species of N_2O [such as hydroxylamine(NH_2OH)] is enriched with ^{15}N and ^{18}O. But the problem with this mechanism is that it cannot explain the observed large increases in N_2O at O_2 levels approaching suboxia (Law and Owens, 1990; Naqvi and Noronha, 1991) over concentrations expected from linear relationships between N_2O production and O_2 utilisation commonly observed in the oceans (Yoshinari, 1976; Elkins *et al*, 1978). This obviously requires a reductive step in N_2O production. An alternative mechanism of the observed heavy isotope enrichment could be the consumption of N_2O within sediments (and in water in areas such as the Arabian Sea and eastern tropical Pacific) and subsequent transport of heavy N_2O to the ocean interior (Zafiriou, 1990). Lastly, coupling of nitrification and denitrification through common intermediates/by-products may also influence the isotopic composition of N_2O (Zafiriou, 1990; Naqvi and Noronha, 1991; Naqvi, 1991b).

Such a coupling should be especially important near the oxic-suboxic interface, and this could possibly account for the enigmatic isotopic trend seen in the upper layer of the Arabian Sea which defies conventional explanation. That is, while the lighter N_2O at depths less than ~200m is apparently not produced by denitrification, classical nitrification pathway ($NH_4^+ \rightarrow NO_2^- \rightarrow N_2O$) (Yoshida, 1988) also cannot fully explain the observed data for two reasons. First, as stated earlier, the $\delta^{15}N$ values are much higher than that reported (<-60 ‰) by Yoshida (1988) for or the production of N_2O from NH_4^+ via NO_2^- by *Nitrosomonas europaea.* [One may question the applicability of these experimental results, conducted with a high ammonium concentration, to the substrate-limited natural environments, but it may be noted that N_2O emitted from the soils is quite depleted in both ^{15}N and ^{18}O (see Fig. 6.12)]. Secondly, what is more significant is that the observed $\delta^{18}O$ is much higher than the value for nitrification expected from $\delta^{18}O$ of H_2O and O_2 [assuming that one oxygen atom in NO_2^- is derived from H_2O and the other from dissolved O_2 (Yoshinari *et al*, 1997) and using the data from GEOSECS station 416 (Ostlund *et al*, 1987), the $\delta^{18}O$ of nitrification-derived N_2O should have been <-3 ‰]. Given the very abrupt decrease in O_2 below the surface mixed layer and the expected abundance of large particles at this level, it seems very plausible (Naqvi and Noronha, 1991; Naqvi, 1991b) that an intermediate or by-product of nitrification such as NO enters the denitrification sequence and gets reduced to N_2O. As the oxygen atom of NH_2OH, the probable precursor of NO (Ward and Zafiriou, 1988), is derived from O_2 (Dua *et al*, 1979) which is characterised by high $\delta^{18}O$ (Ostlund *et al*, 1987), N_2O produced through this pathway is expected to be enriched in ^{18}O. Moreover, unlike N_2O, production of NO by nitrifying bacteria involves modest depletion of ^{15}N (Yoshida, 1988). Thus, N_2O produced through this pathway is expected to be moderately depleted in ^{15}N, but enriched in ^{18}O, as observed.

Therefore, it may be concluded that, in conformity with previous suggestions (Zafiriou, 1990; Naqvi, 1991b), there are probably several mechanisms of N_2O production in the ocean involving different isotopic fractionations. The relative contribution from various pathways is probably determined by the O_2 distribution and organic carbon availability, both of which vary in space and time. This not only brings about large spatial changes in N_2O production and consumption but, in response to temporal changes in the geographical extent and intensity of the O_2 minimum zones (Altabet *et al*, 1995; Geneshram *et al*, 1995) the oceanic N_2O source strength may also vary greatly with time contributing to fluctuations in the atmospheric N_2O content as recorded in ice cores (Leuenberger and Siegenthaler, 1992).

As stated earlier, the Arabian Sea is a region of high N_2O efflux to the atmosphere; the emission rate is particularly high in the three upwelling centres located off Somalia, Arabia and Southwest India (Bange *et al*, 1996; de Wilde and Helder, 1997; Naqvi *et al*, 1998). Observations made off the southwest coast of India during the summer monsoon of 1995 yielded some of the highest N_2O levels reported from the sea. At 23 stations sampled during SK103 (Fig. 1.2) the surface concentrations and saturations were 11.2-62.5 nM (mean $\pm$ s.d. = 28.5 $\pm$ 14.7 nM) and 193-953% (458 $\pm$ 223%), respectively. These values were associated with intense upwelling as manifested by low sea surface temperatures (minimum 22.8°C) and high NO_3^- (maximum 16 μM) which are comparable to those observed in the upwelling zones of the western Arabian Sea (Smith and Codispoti, 1980; Codispoti *et al*, 1996b). The $^{15}N/^{14}N$ and $^{18}O/^{16}O$ ratios in surface-water N_2O measured at eight of these stations together with those from eight open ocean stations are plotted versus percentage saturation in Fig. 6.11. The $\delta^{15}N$ and percentage saturation appear to be negatively correlated, with N_2O in upwelling waters of the southeastern Arabian Sea being

the most depleted in ^{15}N. A few measurements (not included in Fig. 6.11) were also made in subsurface waters. The lowest $\delta^{15}N$ (0.8 ‰) was recorded at 26 m at 11°51'N, 75°09'E; the corresponding N_2O concentration and saturation were 115.6 nM and 1709%, respectively. Since this is the lowest $\delta^{15}N$ ever recorded from the oceanic water column, and because at such high concentrations the signatures of background N_2O would be almost completely erased, it can be taken to represent the end-member composition of N_2O produced in seawater. It is substantially lower than the $\delta^{15}N$ of tropospheric N_2O, but much higher than the expected $\delta^{15}N$ of N_2O produced through nitrification (Yoshida, 1988). In contrast to $\delta^{15}N$, $\delta^{18}O$ did not exhibit a discernible relationship with percentage saturation, and with the exception of one sample, all $\delta^{18}O$ values were consistently higher than the $\delta^{18}O$ of tropospheric N_2O.

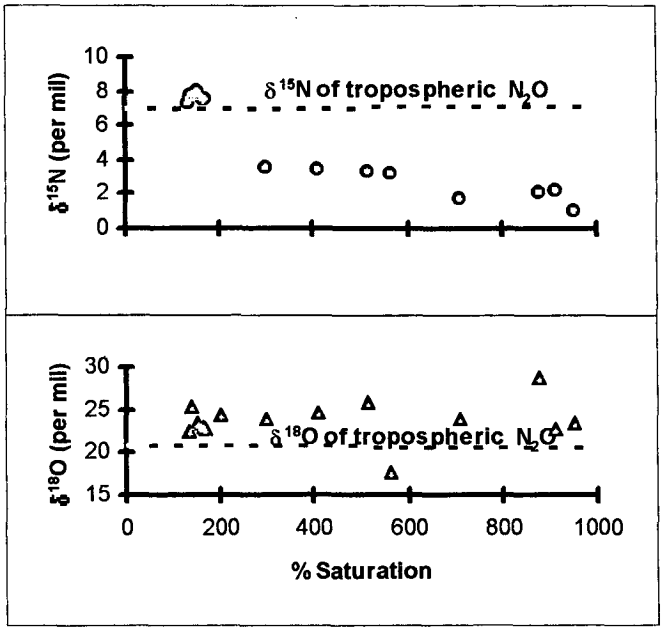

6.11: The $\delta^{15}N$ and $\delta^{18}O$ of N_2O as a function of N_2O saturation at sea surface (depth < 5m). Horizontal dashed lines indicate isotopic composition of N_2O in marine air (Kim and Craig, 1990). Values with moderate saturation and $\delta^{15}N$ close to the atmospheric value are from the northern Arabian Sea; all others are from the coastal upwelling zone off SW India (modified from Naqvi *et al*, 1998).

The above observations have an important implication for the atmospheric N_2O budget. Isotopic analysis of stratospheric N_2O at 68°N has shown large enrichments of $\delta^{15}N$ and $\delta^{18}O$ (~21 and 35 ‰, respectively) relative to the troposphere (Kim and Craig, 1993). This trend has been confirmed by more recent observations at 33-48°N, albeit with somewhat smaller enrichments in the lower stratosphere, but the causative mechanism is still not fully understood (Rahn and Wahlen, 1997; Cliff and Thiemens, 1997; Yung and Miller, 1997). However, the magnitude of ^{15}N and ^{18}O fluxes (~400 and 500 TgN ‰ y^{-1}, respectively, obtained from the older data and about half as much from recent results) are such that these cannot be balanced by air-sea exchange, as proposed (Kim and Craig, 1993; McElroy and Jones, 1996). Even if , as an extreme case, the lowest observed $\delta^{15}N$ value from the ocean (~1 ‰) is combined with the largest estimate of oceanic N_2O production (11 TgN y^{-1}) (Capone, 1996), the air-sea exchange can counter no more than 66 TgN ‰ y^{-1} of the stratospheric ^{15}N flux.

The reported ^{18}O fluxes are even more problematic since the observed opposite trends of ^{15}N and ^{18}O imply that the air-sea exchange will lead to an increase in the tropospheric ^{18}O inventory. The gravity of this issue is evident from the fact that on a $\delta^{15}N$ vs. $\delta^{18}O$ diagram constructed with the published data representing various planetary reservoirs of N_2O, the stratospheric composition conspicuously forms a "corner" (Fig. 6.12). Thus the tropospheric value, which does not fall on vectors joining the other end-members, cannot be explained by simple mixing between various reservoirs (Kim and Craig, 1993). In view of these observations, it is imperative that more measurements be made on N_2O in the stratosphere and that emitted from different terrestrial reservoirs. If the published data are representative, however, then there ought to exist some hitherto poorly known sources and/or sink of N_2O that may be vital for

tropospheric isotopic balance (Prasad, 1994; McElroy and Jones, 1996; Cliff and Thiemens, 1997).

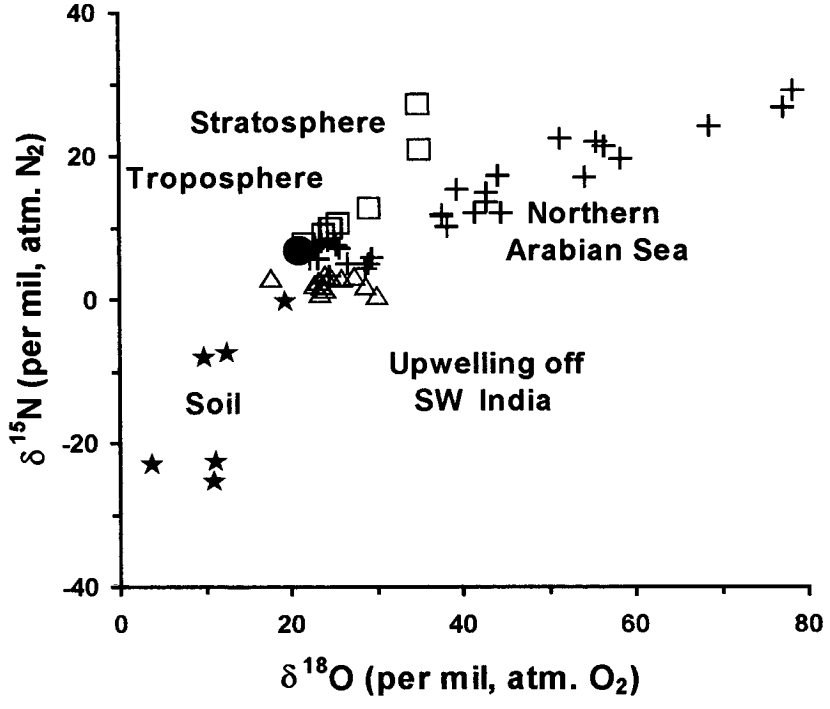

Fig. 6.12. Comparison of isotope data from the Arabian Sea with representative data from other environments (Kim and Craig, 1990; Rahn and Wahlen, 1997) (stars - soil gas; triangles - upwelling zone off SW India; crosses - northern Arabian Sea; squares - stratosphere; circle - troposphere). Note that the tropospheric value does not fall on vectors joining the other end members (modified from Yoshinari *et al*, 1997; Naqvi *et al*, 1998).

7. Flux of Nitrous Oxide and Methane

7.1. Introduction:

Nitrous oxide equilibrium solubility was computed according to the relationship reported by Weiss and Price (1980) using *in situ* temperature and salinity and an atmospheric mixing ratio of 311 ppb. A value of 311ppb was arrived at by scaling up the data reported by Weiss (1981) for an annual increase of 0.2 to 0.4% $(y)^{-1}$ (Khalil and Rasmussen, 1988). As very little variations are observed in the tropospheric N_2O levels (Butler et al., 1989; Naqvi and Noronha, 1991 and the references quoted therein), measurements of N_2O in the air samples were not made. Naqvi and Noronha, (1991) used a value of 310 ppb, whereas Oudot et al. (1990) reported a value of 311 $\pm$ 6 ppb from the tropical Atlantic. The degree of saturation (% saturation) of N_2O in surface waters was calculated from the observed N_2O values with reference to the equilibrium solubility. Fluxes (F) across the air- sea interface were computed using the equation:

$$F = V[(N_2O)_{obs} - (N_2O)_{eq}] \qquad (7.1)$$

Where V is the piston velocity, which is empirically related to the wind speed, the kinematic viscosity and the molecular diffusivity of the gas in question. Piston velocity was calculated using relationships given by Wanninkhof (1992) and the observed wind speed. However, as wind speed data were not available for cruises SS119, SS141 and SS150 climatic means of wind speed given in Hastenrath and Lamb (1979) were utilised.

Surface concentration, saturations and fluxes of N_2O from the coastal and open Arabian Sea are given in Table 7.1. During all the three seasons the flux of N_2O was directed from the sea to the atmosphere, since the surface waters were

invariably supersaturated with N_2O. The data from the coastal regions are mainly from 15°N, except for the SW monsoon season, where the data presented are the mean of the data collected between 9 and 15°N. The data collected within 100 km from the coast were pooled together to get the mean values for the coastal regions. For the open ocean, data from stations with water depth >1000 m were pooled together; these were generally located over 100 km from the coast.

7.2. Surface Distribution of Nitrous Oxide in the Arabian Sea:

In the open Arabian Sea the maximum flux of N_2O was observed during the SW monsoon, followed by the NE monsoon season. The lowest flux was during the pre-SW monsoon season. The winds are generally the strongest over the Arabian Sea during the SW monsoon season and this is one of the reasons for the high flux during the SW monsoon. The highest surface saturation was also observed during the SW monsoon season (178.13%). During the SW monsoon the mixed layer becomes shallow (Shetye et al., 1990) and the wind induced mixing is expected to lead to enhanced diffusion of N_2O across the thermocline and consequently, higher surface saturation during this season. Bange et al (1996) also observed a significant increase in the surface N_2O saturation in the central Arabian Sea during the SW monsoon, as compared to the pre-SW monsoon season. The surface saturation during NE monsoon was 160.23%, however at locations which experienced winter cooling the saturation was in excess of 300%. Naqvi and Noronha (1991) reported surface saturation ranging between 128 and 258% with an average of 186 ± 37% for the NE monsoon period.

In the northern Arabian Sea large spatial variability in the surface saturation was observed during the same season. For instance, during the NE

monsoon the average surface saturation along 15°N was 143% while at 21°N it was 174% during the same season. During this period the cooling of surface waters causes a deepening of the mixed layer through convective mixing which brings about large increases in surface saturation of N_2O, north of 17°N. The other process which plays a dominant role in determining the surface saturation of N_2O is the mid-depth O_2 depletion. The N_2O production is known to be greatly enhanced in waters experiencing O_2 depletion, but at O_2 levels approaching suboxia, N_2O is itself utilized by bacteria (Carlucci and McNally, 1969; Goreau et al., 1980; Cline et al., 1987; Naqvi and Noronha, 1991). Hence, the surface saturation of N_2O depends on the balance between the subsurface N_2O production and consumption and the supply of N_2O from the thermocline to the mixed layer. These processes may vary greatly in space and even during the same season.

Even within the northern Arabian sea there are slight differences in O_2 concentrations within the OMZ between two locations, which are not normally detected by the Winkler method (see Chapter.4) induced by the inflow of PGW and the organic substrate input into these depths, which bring about large changes in the N_2O cycling and surface saturation. Apart from the mid-depth O_2 levels, physical parameters such as advection and diffusivity play a key role in determining the surface saturation of N_2O. During the NE monsoon season the saturation anomaly in the surface waters is between 17.7 and 236.6%, during pre-SW monsoon it is between 5.5 and 111.7% and during the SW monsoon it is between 17.4 and 321.2%.

7.3. Surface Distribution of Nitrous Oxide in the coastal Arabian Sea:

In the coastal regions the surface N_2O saturation reached a maximum of 1364%, with a mean ±1 SD of 382.7 ± 222.2% during the SW monsoon season, due to the upwelling process. While the surface saturation of N_2O was 1364%,

just below the surface (~ 5-10 m) the saturation increased rapidly to a maximum of 2946%. These sharp gradients were caused by very strong vertical salinity barrier found close to the sea-surface formed as a result of land runoff and local precipitation.

During the non-upwelling seasons the mean saturations were much lower (NE monsoon season 144.6± 21.7%, pre-SW monsoon 173.3 ± 82.5%). During the SW monsoon season, there were large differences in surface saturation between the coastal and open ocean waters. While during the non-upwelling seasons the variability between the coastal and open Arabian Sea was not very large. During the NE monsoon season the open ocean saturation values were slightly higher than those from the coastal region, presumably due to the winter cooling process in the open northern Arabian Sea during this season (coastal mean 144.6 ± 21.7%, open ocean mean 160 ± 43.1%).

7.4. Emissions from the Arabian Sea:

The emission data for the three seasons from the open Arabian Sea and from the continental shelf regions are given in Table 7.2. The annual emission of N_2O from the open Arabian Sea was estimated to be 0.32 Tg N. The emission rate from the shelf regions of the SW coast of India was 0.013 Tg N.yr^{-1}, where 90% of the emission was during the SW monsoon season. The present study reveals that in the upwelling regions along the SW coast of India, the upwelling signatures were not very strong beyond a few tens of kilometres from the coast. Hence the mean flux was computed for a distance of ~100km from the coast. The computed emission of N_2O from the open Arabian Sea lies almost in the same range as reported earlier, although the present estimate is the mean of a large spatial and temporal coverage. Naqvi and Noronha (1991) reported an annual emission of 0.28 Tg N.yr^{-1}.

To estimate the emission from the upwelling regions of the western Arabian Sea the area covered by SST less than 25 °C was integrated using Wyrtki's (1971) Oceanographic Atlas. The estimated emissions from this region using the fluxes of Law and Owens (1990), Bange et al (1996) and de Wilde and Helder (1997) are presented in Table 7.3. The annual N_2O emission from the western Arabian Sea upwelling region ranges between 0.08 and 0.59 Tg-N.

The total annual emission of N_2O from the Arabian Sea, including both the upwelling regions and the open Arabian Sea thus varies between 0.41 and 0.92 Tg N. The present estimate agrees well with the estimate of Bange et al. (1996). Using data collected during two seasons they reported an emission between 0.51 and 0.95 Tg N. However, it may be noted that the area of upwelling used by Bange et al (1996) for their estimate is much larger than that used here, but their estimated flux from the open ocean is lower. de Wilde and Helder (1997) reported an emission of 0.02 - 0.03 Tg N from the western Arabian Sea upwelling region alone. The difference in emission between the present study and that reported by de Wilde and Helder (1997) is because the area and period of upwelling considered by the latter is much lower than that in the present study.

7.5. N_2O flux from the Bay of Bengal:

Surface waters in the Bay of Bengal were found to be generally supersaturated with N_2O except at 5 stations where slight undersaturation was observed. The degree of saturation varied from 89.3 to 213.9% with a mean ±1 SD of 125.2 ±25.4%. The highest supersaturations occurred at station C-2, followed by station C-3 (161.2%) (Refer Table 2.1, for station details). High saturation anomalies at these stations were associated with weak coastal upwelling as evident from the physical, chemical and biological data. For example, surface water at C-3 was approximately 1.5°C cooler as compared to

the offshore stations, and the 26°C isotherm lay at ~20m at C-2, ~30m at C-3, and at depths > 50 m at other stations. Similarly, significantly higher nutrient concentrations were observed within the euphotic zone at C-2 and C-3 leading to high chlorophyll concentrations (Dr.H.R.Gomes, unpublished data). Also, a pCO_2 exceeding 400 μatm was observed at the sea surface at C-3. These observations show how slight changes in the hydrographical conditions can bring about potentially large changes in the fluxes of greenhouse gases across the air-sea interface in the northern Indian Ocean.

The mean saturation anomaly observed in the Bay of Bengal (25%) is substantially higher than the global average (4%) obtained by Weiss (1978) from the analyses of 4200 samples collected from various oceanic areas. Butler et al.'s (1989) observations in the eastern equatorial Indian Ocean and the eastern Pacific during an El Niño year led to an even lower value (2.5%). However, their results from the eastern equatorial Indian Ocean (saturation anomaly ~37%) compare well with the present data. When compared to results from the Arabian Sea, where the N_2O supersaturations average around 68.4 % the saturation anomaly in the Bay of Bengal is much lower.

The flux of N_2O from the ocean to the atmosphere based on monthly means for March and April from the climatology of Hastenrath and Lamb (1979) ranged from -0.10 to 10.67 μmol $(N_2O)/m^2/d$, with an average of 0.65 ± 2.00 μmol $/m^2/d$. This is much smaller than the atmospheric fluxes computed for the Arabian Sea [4.46± 2.60 μmol $/m^2/d$ by Naqvi and Noronha (1991) and 8.64 ± 4.32 to 15.51 ± 7.66 μmol $/m^2/d$ by Law and Owens (1990)]. Reflecting the combined effect of a smaller super-saturation and weaker winds, this would correspond to an overall emission rate of N_2O from the Bay of Bengal (area 4.087 X 10^6 km^2) of 0.027 Tg N annually. However, this most likely is an underestimate since the mean winds during March-April are quite weak and not representative of the whole year. In order to fix an upper limit on the extent of

N_2O emission from the Bay, a mean annual wind speed of 5 m/s was used to arrive at the net N_2O flux of 0.077 Tg N/yr. Thus, it would appear that unlike the Arabian Sea (which occupies about 50% more area than the Bay of Bengal), where the overall N_2O flux has been estimated to range between 0.19 and 0.32 Tg $N.yr^{-1}$ (Law and Owens, 1990; Naqvi and Noronha, 1991; Naqvi et al., 1993; present study), the Bay of Bengal is a much weaker source of atmospheric N_2O.

Assuming that N_2O concentrations within the surface layers were regulated by turbulent fluxes from the thermocline, and that a steady-state existed whereby the N_2O input from the subsurface to surface waters was balanced by its escape to the atmosphere, the vertical exchange required to sustain the computed atmospheric N_2O flux has been estimated. Using data from all the stations the average N_2O concentrations at 7 depths between 30 and 250 m were determined and these were fitted to a polynomial to determine the N_2O gradient at the 100m level as 0.468 $\mu mol/m^4$. Combining this value with the computed N_2O flux, the vertical diffusivity was calculated as 0.16 cm^2/s. This value is less than 1/3 of the corresponding value (0.55 cm^2/s) for the Arabian Sea (Naqvi and Noronha, 1991). A slower rate of exchange between the surface and subsurface waters in the Bay of Bengal as implied by the N_2O data is perfectly compatible with a much stronger near-surface vertical stratification owing to the near estuarine character of the Bay. A more vigorous vertical mixing in the Arabian Sea probably sustains larger fluxes of nutrients to the euphotic zone, thereby contributing to column productivity rates that are on average a factor of three higher than those in the Bay of Bengal (Qasim, 1977).

7.6. Methane Flux from the Arabian Sea:

In the open Arabian Sea (depth > 1000 m) CH_4 saturation in the surface waters ranged from 110 to 256% with an average of 167±46% with respect to atmospheric concentration of 1720 ppbv during the two seasonal surveys. The

fluxes of CH_4 from the open Arabian Sea during the pre-SW monsoon were in the range 0.88-3.02 with an average of 1.64 ± 0.68 μmol m^{-2} day^{-1}. There are not enough observations to quantify the flux during the SW monsoon from the open Arabian Sea.

In the surface waters over the continental shelf, CH_4 saturations and computed fluxes were 193-195 (average 194±1%) and 1.35-1.39 (average 1.37±0.02 μmol m^{-2} day^{-1}) during pre-SW monsoon. The corresponding values during the SW monsoon were much higher: 140-2521 (average 710±582%) and 0.58-63.69 (average 11.25± 13.12 μmol m^{-2} day^{-1}), respectively. In comparison, Owens et al. (1991) reported fluxes in the range 4.6-13.9 μmol m^{-2} day^{-1} from the upwelling region off Oman during the monsoon period and, using the same model employed during the present study, Patra et al. (1998) computed average fluxes of 0.32, 5.02 and 10.37 μmol m^{-2} day^{-1} from the northern Arabian Sea during pre-SW monsoon, NE monsoon and SW monsoon seasons, respectively. Thus while the values obtained here for both the shelf and offshore waters are generally of the same order as those computed by other workers, the nearshore fluxes during the course of this study are higher by at least an order of magnitude. At the mouth of the Mandovi, for example, average fluxes were found to be 20.75± 15.81 μmol m^{-2} day^{-1} during pre-SW monsoon and 136.4± 31.70 μmol m^{-2} day^{-1} during the SW monsoon. However, even if these values are ignored and an average flux of 11.25 μmol m^{-2} day^{-1} is applied over an area of (1000x50=) 50,000 km^2, CH_4 flux from the coastal waters will be 0.0011 Tg for the four monsoon months. This is roughly 2.0-2.6% of the estimate for the northern Arabian Sea (Owens et al., 1991; Patra et al., 1998). Thus, while the coastal waters of the Arabian Sea may emit significant amounts of CH_4 to the atmosphere, these do not seem to dominate the total flux from the Arabian Sea into the atmosphere, at variance with previous suggestions (Karisiddaiah and Veerayya, 1994, 1996).

7.7. Conclusions:

The Arabian Sea was found to be a source of atmospheric N_2O in all the locations sampled and during all the three seasons. While the Bay of Bengal, was a source in almost all the locations sampled. The total emission from the Arabian Sea ranged between 0.41 and 0.92 Tg N y^{-1} which is about 12 to 15 times higher than that from the Bay of Bengal (0.027- 0.077 Tg N y^{-1}). Lower surface saturations and consequently smaller air-sea fluxes in the Bay of Bengal may result from strong stratification caused by the immense river runoff. The computed vertical exchange coefficient (0.16 cm^2/s) at the top of the thermocline is about 1/3 of the corresponding value (0.55 cm^2/s) in the Arabian Sea.

Due to upwelling along the SW coast of India, the flux rate of N_2O from this region was very high. The low salinity surface layer produced as a result of local precipitation and land runoff acts as a lid, thereby preventing higher emission to the atmosphere from this region. However, wind induced turbulence can break-up this lid and bring about larger fluxes from time to time.

The highest flux from the Arabian Sea occurs during the SW monsoon season, due to the high windspeed and high surface saturation during this season. High surface saturation may occur due to the shallow mixed layer and wind induced mixing during this season. During the NE monsoon high flux from the northern latitudes is due to winter cooling process. As a result of this process the open ocean flux was higher than the flux from the continental shelf, while an opposite trend is observed during the other seasons.

Various chemical and physical processes that take place in the water column determine the atmospheric flux of N_2O from the Arabian Sea. As these processes have a large temporal and spatial variability the flux also had a large variability temporally as well as spatially. The mid- depth oxygen depletion, upwelling and winter cooling are some of the dominant process that affect the emission from this region.

In conformity with previous reports the results obtained during the course of this study also show higher-than-average CH_4 emissions from the Arabian Sea with a pronounced seasonal variability. The waters over the continental shelf are significantly more enriched with CH_4 relative to the open ocean, particularly during the SW monsoon season when fairly intense upwelling takes place off the central and southwest coasts of India. Significant flux of methane to the atmosphere from the shallow continental shelf regions comes from land runoff and partly from *in situ* water column production.

Table 7.1. Flux densities of N_2O from the Arabian sea:

Season		Mean	Std. Dev	Max	Min
Coastal	N_2O (nM)	23.19	13.80	80.75	7.21
SW Monsoon	Saturation (%)	382.67	222.17	1364.12	129.95
	Flux (μ mole.m^{-2}.day^{-1})	33.50	35.56	143.97	0.77
Coastal	N_2O (nM)	8.15	1.26	10.32	6.67
NE monsoon	Saturation (%)	144.64	21.72	181.69	119.31
	Flux (μ mole.m^{-2}.day^{-1})	0.63	0.23	0.92	0.30
Coastal	N_2O (nM)	9.51	4.59	20.58	6.67
Pre-SW monsoon	Saturation (%)	173.30	82.52	372.85	122.62
	Flux (μ mole.m^{-2}.day^{-1})	3.29	3.70	12.24	1.01
Deep	N_2O (nM)	10.05	3.81	23.67	6.45
SW monsoon	Saturation (%)	178.13	65.90	421.16	117.39
	Flux (μ mole.m^{-2}.day^{-1})	9.03	6.94	30.54	0.63
Deep	N_2O (nM)	9.89	2.83	21.41	6.83
NE monsoon	Saturation (%)	160.23	43.08	336.61	117.72
	Flux (μ mole.m^{-2}.day^{-1})	4.38	3.04	12.48	0.19
Deep	N_2O (nM)	8.49	1.65	11.74	5.97
Pre-SW monsoon	Saturation (%)	153.77	29.63	211.67	105.47
	Flux (μ mole.m^{-2}.day^{-1})	2.08	1.31	5.01	0.17

Table 7.2: Nitrous oxide emission from the Open Arabian Sea and the SW Indian coastal regions:

Region	Season	Flux μ mole.m^{-2}.day^{-1}	Area m^2	Emission Tg N	Emission Tg N y^{-1}
Open Arabian Sea	SW monsoon	9.03	$6.225X10^{12}$	0.189	
Open Arabian Sea	NE Monsoon	4.38	$6.225X10^{12}$	0.092	
Open Arabian Sea	Pre SW monsoon	1.94	$6.225X10^{12}$	0.041	
Open Arabian Sea	Annual				0.322
SW Continental Shelf	SW monsoon	33.5	100000	0.0113	
SW Continental Shelf	NE Monsoon	0.63	100000	0.0002	
SW Continental Shelf	Pre SW monsoon	3.29	100000	0.0013	
SW Continental Shelf	Annual				0.013

Table 7.3. N_2O emissions from the Western Arabian Sea upwelling region between July and September:

Source	Flux Density $\mu mol.m^{-2}.day^{-1}$	Emission Range Tg.N
Law and Owens (1990)	61.08*	0.08
Bange et al (1996)	63.16 - 115.7	0.08 - 0.14
de Wilde and Helder (1997)	260 - 500	0.31 - 0.59
		0.08 - 0.59

* Calculated for a N_2O surface saturation of 246% [maximum surface saturation observed by Law and Owens (1990) in the upwelling region], wind speed of $10ms^{-1}$, salinity of 35 and a temperature of 25 °C.

Summary

As a result of human activity the atmospheric concentrations of radiatively active gases have been increasing over the last century. These trace gases possess strong absorption bands in the infrared region of the spectrum; hence the increased concentrations in turn increase the heat trapping ability of the atmosphere. Apart from being radiatively active, biogenic trace gases such as methane and nitrous oxide play an important role in the atmospheric chemistry.

Greenhouse gases are produced by anthropogenic as well as natural processes. But the extent of the contribution by various sources is uncertain. Hence attempts are being made to study the various source strength of greenhouse gases and their production mechanisms. More and more measurements of these gases are required to understand their natural cycling. Methane and nitrous oxide are two such greenhouse gases which are produced anthropogenically as well as naturally. Although we have a general understanding of their various sources, detailed measurements are required to understand and predict their changes in the global environment.

The current level of nitrous oxide in the atmosphere is around 312ppb which is rising steadily by 0.25% every year. The contribution from the oceans is about 4 Tg N yr^{-1}. Methane is a naturally occurring greenhouse gas whose concentration increased dramatically in the atmosphere over the last century. A decrease of ca. 30% was, however recorded during 1979-1985. The emission rate of methane from the oceans to the atmosphere is about 5-20 Tg per year. Thus the oceans play only a modest role in the global methane budget. Data on the magnitudes of sinks and individual sources of methane are still meagre and their quantification is necessary to predict further impacts on the world climate.

The Arabian Sea houses one of the world's largest oceanic oxygen deficient environments. It was postulated that the poor renewal of the intermediate waters in the Arabian Sea was responsible for the development of oxygen deficient conditions culminating in denitrification. However, the more recent work has shown that these waters are renewed at a faster rate than believed earlier. Thus the development of oxygen deficient conditions may be due to excessive oxygen consumption combined with the low oxygen content of waters responsible for renewal. However, the mechanisms bringing about the rapid changes remain largely unknown.

As a consequence of the low oxygen levels, the cycling of redox sensitive elements are expected to be different. Denitrification, a process by which nitrate is converted to molecular nitrogen, leads to both the production and consumption of nitrous oxide. The cycling of nitrous oxide is expected to be rapid in this environment. The role of oceans as a source of methane to the atmosphere is very poorly understood. There has been only two reports till date from the Arabian Sea. Earlier workers identified the potential of this region as a source of atmospheric methane. In view of this the present study was aimed at the following:

1. To study the temporal and spatial variability of the suboxic conditions and associated nitrogen cycling in the northern Indian Ocean.
2. To investigate the nitrous oxide (N_2O) cycling in the Arabian Sea.
3. To understand cycling of methane in the Arabian Sea.
4. To estimate the fluxes of N_2O and CH_4 from the northern Indian Ocean and the coastal environments to the atmosphere during various seasons.
5. To study the role of upwelling regions in the cycling of N_2O and CH_4

6. To apply stable isotopic tracers (natural abundance) as a tool to understand the mechanism of production and consumption of N_2O and to understand the implications of ocean-atmosphere exchange of N_2O in global cycling.

One way of studying the circulation of the intermediate waters of the Arabian Sea is by using chemical tracers such as nitrite and nitrate deficits. The nitrate deficit, a measure of the extent of gaseous nitrogen production through denitrification, is estimated using 'NO'. The results of computation of nitrate deficits combined with nitrite are used here to investigate the renewal of intermediate waters in the northern Arabian Sea and the role of circulation in supplying oxygen to the suboxic environment. Data collected along mostly zonal sections at 15°N during three seasons, namely SW monsoon, NE monsoon and pre-SW monsoon and repeated observations made at three locations - 19° N, 67°E (Location A), 19.75°N, 64.62°E (Location B), and 17°N, 68°E (Location C) are presented here.

Overall the deficits were found to be the lowest during the Pre-SW monsoon and the highest during the NE monsoon seasons. Along 15°N, maximum deficit was observed during November, followed by July. Repeated observations at the same locations also showed that the lowest deficit occurred between April and July after which the deficits increased. The deficits at location A was higher than those at the other two locations, and during the NE monsoon period the deficits reached very high levels. Nitrate deficits and nitrite along 15 °N seem to follow the circulation pattern described by earlier workers. During the SW monsoon the advection of the water mass from the south with its core centred around 400 m some 200 km from the coast results in lower deficits in this region. The undercurrent bringing in O_2 - rich waters from outside the denitrification zone obviously accounts for the low ΔN and NO_2^- values off the continental margin below the upper 150m. The upper water coming from the north has relatively high ΔN and high NO_2^-. During November, beginning of NE

monsoon, flow of water from the south above 400 m depth extending off the continental margin to a distance of about 400 km results in the low nitrate deficits with no nitrite. As the NE monsoon progresses these waters seem to be more influenced by the adjacent watermass, where denitrification is quite intense. Although the dissolved oxygen content of the upper mid-water responsible for renewal is only marginally higher than that of the water existing in this region it plays an important regulating role in the intensity of denitrification in this region. A narrow band of deficit along the bottom waters of the shelf as a result of denitrification associated with the upwelling process was also observed. Deficit distribution during the pre-SW monsoon season suggests that the circulation during this season is a transition between the SW and NE monsoons.

Studies on the temporal variations at the same site suggest that within the core of the denitrifying regime, at location A, the denitrification process is intense throughout the year. The extent of denitrification was maximal during the NE monsoon season with the deficits exceeding 10μM NO_3. Location B, lies at the periphery of the denitrification zone and so the denitrification signal shows a much larger temporal variability. The deficit starts increasing at the end of the SW monsoon season and high values persist till the end of the NE monsoon. It falls thereafter to the lowest values during the pre- and early SW monsoon periods. The annual deficit cycle seems to follow the primary productivity pattern suggesting a link between deficit and productivity. The advection of the Persian Gulf Water (PGW) influences the intensity of denitrification to a large extent, eventhough the O_2 content of this water mass is only marginally higher. This water mass originally has a fairly high oxygen content but as it mixes with the Arabian Sea low-oxygen water, the oxygen content falls rapidly, thereby reducing the intensity of denitrification till the O_2 of this water mass falls down to the ambient level. Location B lying more towards the west is expected to be more influenced by this water mass as compared to location A and hence has lower deficits during all the seasons. Although Location C experiences

denitrifying conditions throughout the year the deficits are lesser than those at location A. As this location lies more south it receives more O_2 supply relative to location A.

Measurements of methane (CH_4) made during the two surveys in the eastern and central Arabian Sea in April-May, 1996 (pre-SW monsoon) and August-September, 1997 (SW monsoon) reveal high spatial and temporal variability in surface saturations (110-2521%) and sea-to-air fluxes (0.58-63.69 $\mu mol\ m^{-2}\ day^{-1}$). The highest values are observed in waters over the continental shelf where intense coastal upwelling occurs during the SW monsoon. These appear to result in part from high CH_4 inputs from coastal wetlands through large seasonal runoff (which contributes to the maintenance of a 5-10 m thick fresher water lens that caps the upwelled water) as extremely high saturations (up to ~13,000%) are recorded in the estuarine surface water. *In situ* production of CH_4, favoured by very high biological production in conjunction with prevalence of suboxic conditions in the upwelled water, may be other major CH_4 source. In comparison, sedimentary inputs of CH_4 seem to be of lesser importance in spite of the previously reported occurrence of gas-charged sediments in this region. The contribution of continental margins in sustaining high rates of CH_4 emissions from the Arabian Sea as a whole is not very large.

Two maxima in CH_4 concentrations are observed in vertical profiles in the open central Arabian Sea. The more pronounced deeper maximum, occurring at 150-200 m depth, is similar to the feature seen elsewhere in the oceans, but is probably intensified here due to an acute oxygen deficiency. It shows some correlation with the subsurface particle maximum characteristic of the denitrifying layer. The dominant mechanism of its formation may be *in situ* CH_4 production within particles rather than advection from the continental shelf as concluded by previous workers. The less pronounced and previously unreported shallower maximum, occurring in the well-oxygenated upper 50 m of the water column, is

more dynamic probably as a result of variability of the balance between CH_4 production due to biological activity and its losses through microbial oxidation and air-sea exchange.

In the oxygen minimum zone of the northern and central Arabian Sea N_2O profiles are characterised by two maxima separated by a minimum. However, outside this region in the Arabian Sea and in the Bay of Bengal, only one broad maximum is observed. Overall the distribution of N_2O was closely correlated with that of dissolved oxygen. The N_2O minimum coincided with the O_2 minimum; above and below this the N_2O concentrations increased. At the core of the denitrifying layer, the concentrations of N_2O fell below saturation. The N_2O minimum also coincided with the maxima in ΔN and nitrite. The N_2O concentrations at the mid-depth minimum generally decreased offshore. The above pattern in the distribution of N_2O arises from the mid-depth O_2 depletion in these waters. Under normal conditions, when O_2 levels have not reached low enough to trigger denitrification, N_2O and O_2 concentrations are negatively correlated. However, when the environment becomes suboxic and reducing, N_2O becomes an electron acceptor and gets reduced to N_2.

Nitrous oxide distribution along 15°N section showed that overall the seasonal variation of N_2O followed that of denitrification as represented by nitrate deficit. However during the SW Monsoon season due to upwelling process N_2O concentrations showed high values (60 nM) at the primary maximum (depth ~ 100m) in the shelf regions. N_2O distribution along 15 °N was influenced to a large extent by the circulation. The N_2O frequently fall below saturation at mid- depths accompanied by high ΔN and high nitrite depending on the oxygen content of the water mass. This suggests that N_2O gets consumed during intense denitrification, which leads to extreme undersaturations. The minimum in N_2O at the mid-depth with low saturation would probably reflect the stage of denitrification.

Above and below the denitrifying layer the concentration of N_2O was high. Generally, the concentration of N_2O in the upper or primary maximum was not as high as that at deeper maximum. The primary N_2O maxima could be a resultant of both nitrification and denitrification processes. As this primary N_2O maximum is below the thermocline, active upward diffusion of N_2O across the barrier is reduced leading to the accumulation of N_2O in this layer. However, in the regions influenced by winter cooling, as the thermocline deepens due to this process, N_2O which normally accumulates below the thermocline gets injected into the mixed layer and results in the high supersaturations in the mixed layer.

With a few exceptions, the high nitrite concentrations were associated with low N_2O, and high N_2O was mostly associated with low nitrite concentration. Within the oxygen minimum zone there was no correlation between NO_2^- and N_2O. High NO_2^- with low N_2O would indicate intense denitrification. Intense denitrification in the northern Arabian Sea seems to be always accompanied by extreme N_2O under-saturation and high nitrite. AOU exhibited a linear relationship with ΔN_2O in two ranges. However this relationship did not extend into the OMZ where ΔN_2O exhibited very high and low values within a narrow range of AOU. This indicates that the rate of production and consumption of N_2O is very high within this layer as the N_2O production efficiencies increase to a large extent at low concentrations of O_2.

Observations along the SW coast of India during the upwelling season showed that the upwelling regions not only act as a chimney of N_2O produced elsewhere in the ocean but also that produced *in situ* by the nitrifying-denitrifying activities, as the conditions are conducive with the O_2 values reaching close to zero in this region. Stations located closest to the shore had the highest N_2O concentration. The concentrations recorded was 233nM, corresponding to a saturation of 3866%. This is the highest N_2O concentration

reported from the water column in the world oceans. The concentrations were especially high off Mangalore, and decreased both to the north and south of this region.

In the Bay of Bengal, marked accumulation of N_2O occurs in subsurface layers with the total inventory of excess of nitrous oxide (ΔN_2O) estimated as ~ 5.4 Tg N. Since the Bay of Bengal is not an active water-column denitrification site, there appears to be no loss of N_2O through bacterial reduction. Vertical profiles of N_2O are characterized by a pronounced maximum at ~200-300 m which intensifies northward. The N_2O distribution seems to be influenced by the subsurface circulation. The relationship between Δ N_2O and AOU is linear in three ranges. Within the depth range 300-1000m, however Δ N_2O and AOU are not significantly correlated due to large changes in N_2O concentrations associated with small variations in the ambient oxygen levels.

Measurements of $^{15}N/^{14}N$ in dissolved molecular nitrogen (N_2), nitrate (NO_3^-) and nitrous oxide (N_2O) and $^{18}O/^{16}O$ in N_2O [expressed as $\delta^{15}N$ and $\delta^{18}O$, relative to atmospheric N_2 and oxygen (O_2), respectively] have been made in water column at several locations in the Arabian Sea. Denitrification appears to greatly affect the natural isotopic abundances. The $\delta^{15}N$ of NO_3^- increases from 6 ‰ in deep waters (2500 m) to 15 ‰ within the core of the denitrifying layer (250-350 m); the $\delta^{15}N$ of N_2 concurrently decreases from 0.6 ‰ to 0.25 ‰. Values of the isotopic fractionation factor (ε) during denitrification estimated using simple advection-reaction and diffusion-reaction models are 22 ‰ and 25 ‰, respectively. A strong decrease in $\delta^{15}N$ of NO_3^- is observed from ~200 m (>11 ‰) to 80 m (~6 ‰); this is attributed to the input of isotopically light nitrogen through nitrogen fixation. Isotopic analysis of N_2O reveals extremely large enrichments of both ^{15}N and ^{18}O within the OMZ, presumably due to the preferential reduction of lighter N_2O to N_2. However, isotopically light N_2O is observed to accumulate in high concentrations above the OMZ indicating that

the N_2O emitted to the atmosphere from this region cannot be very heavy. The isotope data from the intense upwelling zone off the southwest coast of India, where some of the highest concentrations of N_2O ever found at the sea surface are observed, show moderate depletion of ^{15}N, but slight enrichment of ^{18}O relative to air. These results suggest that the ocean-atmosphere exchange cannot counter inputs of heavier isotopes (particularly ^{18}O) associated with the stratospheric back flux, as proposed by previous workers. This calls for additional sources and/or sinks of N_2O in the atmosphere. Also, the N_2O isotope data cannot be explained by production through either nitrification or denitrification, suggesting a possible coupling between the two processes as an important mechanism of N_2O production.

The Arabian Sea was found to be a source of atmospheric N_2O in all the locations sampled and during all the three seasons. While the Bay of Bengal was also a source in almost all the locations sampled, except a few, the total emission from the Arabian Sea (0.41 - 92 Tg N y^{-1}) was about 12 to 15 times higher than that of the Bay of Bengal (0.027- 0.077 Tg N y^{-1}). The severe depletion of O_2 at mid-depths leading to denitrification is the major reason for the higher emission from the Arabian Sea. Lower surface saturations and consequently smaller air-sea fluxes in the Bay of Bengal may result from strong stratification caused by the immense river runoff. The computed vertical exchange coefficient (0.16 cm^2/s) at the top of the thermocline is about 1/3 of the corresponding value (0.55 cm^2/s) in the Arabian Sea.

Due to upwelling along the SW coast of India, the flux of N_2O from this region was very high. But as the area of upwelling is very small the contribution to the total emission is not too large. Land-runoff produced a low-salinity surface water which acts as a lid, preventing emission of N_2O to the atmosphere from this region. However, turbulence produced by wind can break-up this lid and can bring about larger fluxes from time to time.

The highest flux from the Arabian Sea was during the SW monsoon season, due to the strong wind and high surface saturation during this season. High surface saturation may occur due to the shallow mixed layer and wind induced mixing during this season. During the NE monsoon high flux from the northern latitudes were due to winter cooling process. As a result of this process the open ocean flux was higher than the flux from the continental shelf, while during the other seasons the flux from the continental shelf was higher.

Various chemical and physical processes that take place in the water column determine the atmospheric flux of N_2O from the Arabian Sea. As these processes have a large temporal and spatial variability the flux also had a large variability temporally as well as spatially. The mid- depth oxygen depletion, upwelling and winter cooling are some of the dominant processes that affect the emission from this region.

In conformity with previous reports the results obtained during the course of this study also show higher-than-average CH_4 emissions from the Arabian Sea with a pronounced seasonal variability. The waters over the continental shelf are significantly more enriched with CH_4 relative to the open ocean, particularly during the SW monsoon season when fairly intense upwelling takes place off the central-and southwest coasts of India. Significant flux of methane to the atmosphere from the shallow continental shelf regions arises from land runoff and *in situ* water column production as conditions are conducive.

References

Alldredge A.A. and Y. Cohen (1987). Can microscale chemical patches persist in the sea? Microelectrode study of marine snow, faecal pellets. *Science*, 235, 689-691.

Alperin M.J., and W.S. Reeburgh (1984). Geochemical evidence supporting anaerobic methane oxidation, In: R. Crawford, and R. Hanson (Editors), *Microbial Growth on C_1 compounds*, American Society for Microbiology, Washington, D.C., 282-289p.

Altabet M.A., Francois R., Murray D.W. and Prell W.L. (1995). Climate-related variations in denitrification in the Arabian Sea from sediment $^{15}N/^{14}N$ ratios. *Nature,* 373, 506-509.

Bange H.W., U.H. Bartell, S. Rapsomanikis, and M.O. Andreae (1994). Methane in the Baltic Sea and North Seas and a reassessment of the marine emissions of methane. *Global Biogeochem. Cycles*, 8, 465-480.

Bange H.W., Rapsomanikis S. and Andreae M.O. (1996). Nitrous oxide in coastal waters. *Global Biogeochem. Cycles,* 10, 197-207.

Bange H.W., Rapsomanikis S. and Andreae M.O. (1996). Nitrous oxide emissions from the Arabian Sea. *J.Geophys. Res. Lett.,* 23, 3175-3178.

Banse K. (1959). On upwelling and bottom trawling off the southwest coast of India. *J. Mar. Biol. Ass. India*, 1, 33-49.

Banse K. (1968). Hydrography of the Arabian Sea Shelf of India and Pakistan and effects on demersal fishes. *Deep-Sea Res.*, 15, 45-79.

Bates T.S., K.C. Kelly, J.E. Johnson and R.H. Gammon(1996). A reevaluation of the open ocean source of methane to the atmosphere. *J. Geophys. Res.*, 101, 6953-6961.

Bender M.L. (1990). $\delta^{18}O$ of dissolved O_2 in seawater: A unique tracer of circulation and respiration in the deep sea. *J. Geophys. Res.,* 95, 22243-22252.

Bendschneider K. and R.J. Robinson, (1952). A new spectrophotometric method for the determination of nitrite in seawater. *J. Mar. Res.,* 11, 87-96.

Bethoux J.P. (1988). Red Sea geochemical budgets and exchanges with the Indian Ocean. *Mar. Chem.*, 24, 83-92.

Betlach M.R. and Tiedje J.M. (1981). Kinetic explanation for accumulation of nitrite, nitric oxide and nitrous oxide during bacterial denitrification. *Appl. Environ. Microbiol.* 42, 1074-1084.

Bhattathiri P.M.A., Pant A., Sawant S., Gauns M., Matondkar S.G.P. and Mohanraju R. (1996). Phytoplankton production and chlorophyll distribution in the eastern and central Arabian Sea in 1994-1995. *Curr. Sci.*, 71, 857-862.

Blake D.R. and F.S. Rowland (1988). Continuing world-wide increase in tropospheric methane 1978 to 1987. *Science*, 239, 1129-1131.

Bolle H. J., W. Seiler and B. Bolin (1986). Other green house gases and aerosols In: B. Bolin, B.R. Doos, J. Jager and R.A. Warrick (Editors), *The Greenhouse Effect, Climate Change, and Ecosystems*, John Wiley & Sons, New York, 157-205p.

Brandes J. A. and A.H. Devol (1997). Isotopic fractionation of oxygen and nitrogen in coastal marine sediments. *Geochim. Cosmochim. Acta,* 61, 1793-1802.

Brandes J. A., A. H. Devol, D.A. Jayakumar, T. Yoshinari and S.W.A. Naqvi (1998). Isotopic composition of nitrate in the central Arabian Sea and eastern tropical North Pacific: a tracer for mixing and nitrogen cycles. *Limnol. Oceanogr.*, (in press).

Broecker W.S. (1974). 'NO', a conservative water mass tracer. *Earth Planet. Sci. Lett.*, 23, 100-107.

Brooks J.M., and W.M. Sackett (1973). Sources, sinks, and concentrations of light hydrocarbons in the Gulf of Mexico. *J. Geophys. Res.*, 78, 5248-5258.

Brooks J.M., D.F. Reid, and B.B. Bernard (1981). Methane in the upper water column of northwestern Gulf of Mexico. *J. Geophys. Res.*, 86, 11,029-11,040.

Bryden H.L. (1973). New polynomials for thermal expansion, adiabatic temperature gradient and potential temperature of sea water. *Deep-Sea Res.*, 25, 315-322.

Burke R.A.Jr., D.F. Reid, J.M. Brooks, and D.M. Lavoie (1983). Upper water column methane geochemistry in the eastern tropical North Pacific. *Limnol. Oceanogr.*, 28, 19-32.

Burkill P.H., R.F.C. Mantoura and N.J.P. Owens (1993). Biogeochemical cycling in the northwestern Indian Ocean: a brief overview. *Deep-Sea Res. II,* 40, 643-649.

Butler J., J.W. Elkins, T.M. Thompson and K.B. Egan (1989). Tropospheric and dissolved N_2O of the West Pacific and East Indian Oceans during the El Niño Southern Oscillation Event of 1987. *J. Geophys. Res.,* 94, 14865-14877.

Capone D.G. (1995). A biologically constrained estimate of oceanic N_2O flux . In : D.P. Adams, S.P. Seitzinger and P.M. Crill (Editors). *Cycling of reduced gases in the hydrosphere,* E. Schweizerbart'sche Verlagsbuchhandlungen, Stuttgart.

Capone D. G. (1996). A biologically constrained estimate of oceanic N_2O flux. *Mitt. Internat. Verein. Limnol.* 25, 105-114.

Carlucci A.F. and P.M. Mcnally (1969). Nitrification by marine bacteria in low concentrations of substrate and oxygen. *Limnol. Oceanogr.*, 14, 736-739.

Carpenter J. H. (1965). The Chesapeake Bay Institute technique for the Winkler dissolved oxygen method. *Limnol. Oceanogr.*, 10, 141-143.

Cicerone R.J. and R.S. Oremland (1988). Biogeochemical aspects of atmospheric methane. *Global Biogeochem. Cycles*, 2, 299-327.

Cliff S.S. and M.H. Thiemens (1997). The $^{18}O/^{16}O$ and $^{17}O/^{16}O$ ratios in atmospheric nitrous oxide: a mass-dependent anomaly. *Science,* 278, 1774-1776.

Cline J.D. and F.A. Richards (1972). Oxygen deficient conditions and nitrate reduction in the eastern tropical North Pacific Ocean. *Limnol. Oceanogr.*, 17, 885-900.

Cline J.D. and I.R. Kaplan (1975). Isotopic fractionation of dissolved nitrate during denitrification in the eastern tropical North Pacific. *Mar. Chem.*, 3, 271-299.

Cline J.D., D.P. Wisegarver and K. Kelly-Hansen (1987). Nitrous oxide and vertical mixing in the equatorial Pacific during the 1982-1983 El Niño. *Deep-Sea Res.*, 34, 857-873.

Codispoti L.A. and Christensen J.P. (1985). Nitrification, denitrification and nitrous oxide cycling in the eastern tropical South Pacific Ocean. *Mar. Chem.,* 16, 277-300.

Codispoti L.A. (1989). Phosphorus vs. nitrogen limitation of new (export) production. In: W. Berger, V. Smetacek and G. Wefer (Editors), *Productivity of the ocean: present and past,* John Wiley and Sons, 377-394p.

Codispoti A and J. M Morrison 1995. The U.S. JGOFS Arabian Sea Hydrographic Program: Progress and Prospects. U.S. JGOFS Newsletter, vol. 7, No.1, pg.4.

Codispoti L.A., A. Devol, A. Minas, H. Paerl, S.W.A. Naqvi, J. Christensen, P. Becker and T. Yoshinari (1996a). A revised oceanic combined nitrogen budget and its implications for exchange of carbon dioxide between the atmosphere and ocean. *Carib. J. Sci.*, 32, 284-285.

Codispoti L.A., J. Morrison and B. Jones (1996b). The chemical hydrographic milieu of the U.S. JGOFS Arabian Sea Process Study. *EOS - Trans. Amer. Geophys. Union* OS23.

Codispoti L.A. (1997). The limits to growth. *Nature,* 387, 237-238.

Cohen Y. and L. Gordon (1978). Nitrous oxide in the oxygen minimum of the eastern tropical North Pacific: evidence for its consumption during denitrification and possible mechanisms for its production. *Deep- Sea Res.*, 25, 509-524.

Cohen Y. and L. Gordon (1979). Nitrous oxide production in the ocean. *J. Geophys. Res.*, 84, 347-353.

Craig H. and L. I. Gordon (1963). Nitrous oxide in the ocean and marine atmosphere. *Geochim. Cosmochim. Acta*, 27, 949-955.

Crutzen P.J.(1991). Methane's sinks and sources. *Nature*, 350, 380-381.

Cutler A.N., and J.C. Swallow (1984). Surface currents of the Indian Ocean (To 25°S, 100°E): compiled from historical data archived by the Meteorological office, (Bracknell, UK, : *Institute of Oceanographic Sciences*, Wormley, Report No. 187, 36 Charts), 8pp.

Cynar F.J. and A.A. Yayanos (1991). Enrichment and characterization of methanogenic bacterium from the oxic upper layer of the ocean. *Curr. Microbiol.*, 23, 89-96.

Delwitche C.C. and P.L. Steyn (1970). Nitrogen isotope fractionation in soils and microbial reactions. *Environ. Sci. Tech.*, 4, 929-935.

Deuser W.G. (1975). Reducing environments. In: J P Riley and G Skirrow (Editors), *Chemical Oceanography* Vol. 3, Academic Press, 1-37p.

Deuser W.G., E.H. Ross, and Z.J. Mlodzinska (1978). Evidence for and rate of denitrification in the Arabian Sea. *Deep-Sea Res.*, 25, 47-146.

de Wilde H.P.J. and W. Helder (1997). Nitrous oxide in the Somali Basin: the role of upwelling. *Deep-Sea Res. II,* 44, 1319-1340.

Dietrich G. (1973). The unique situation in the environment of the Indian Ocean. In: B. Zeitzschel (Editor), *The Biology of the Indian Ocean,* Springer Verlag, 1-6p.

Dlugokencky E.J., L.P. Steele, P.M. Lang and K.A. Masarie (1994). The growth and distribution of atmospheric methane. *J. Geophys. Res.*, 99, 17021-17043.

Dua R. D., B. Bhandari and D.J.D. Nicholas (1979). Stable isotope studies in the oxidation of ammonia to hydroxylamine by *Nitrosomonas europaea. FEBS Lett.* 106, 401-404.

Ducklow H.W. (1993). Bacterioplankton distributions and production in the northwestern Indian Ocean and Gulf of Oman, September 1986. *Deep-Sea Res.II*, 40, 753-771.

Elkins J.W., S.C. Wofsy, M.B. McElroy, C.E. Colb and W. Kaplan (1978). Aquatic sources and sinks for nitrous oxide. *Nature,* 275, 602-606.

Floodgate G.D. and A.G. Judd (1992). The origins of shallow gas. *Cont. Shelf Res.*, 12, 1145-1156.

Fofonoff N.P. (1977). Computations of potential temperature of seawater for an arbitrary reference pressure. *Deep-Sea Res.*, 24, 489-491.

Galloway J.N., W.H. Schlesinger, H. Levy, A. Michaels and J.L. Schnoor (1995). Nitrogen fixation: anthropogenic enhancement - environmental response. *Global Biogeochem. Cycles,* 9, 235-252.

Ganeshram R.S., T.F. Pederson, S.E. Calvert and W.L. Prell (1995). Large changes in oceanic nutrient inventories from glacial to interglacial periods. *Nature,* 376, 755-758.

Garfield P.C., T.T. Packard, G.E. Friederich and L.A. Codispoti (1983). A subsurface particle maximum layer and enhanced microbial activity in the

secondary nitrite maximum of the northeastern tropical Pacific Ocean. *J. Mar. Res.*, 41, 747-768.

Goreau T.J., W.A. Kaplan, S.C. Wofsy, M.B. McElroy, F.W. Valois, and S.W. Watson (1980). Production of NO_2^- and N_2O by nitrifying bacteria at reduced concentrations of oxygen. *Appl. Environ. Microbiol.*, 40, 526-532.

Grasshoff K. (1964). Zur Bestimmung von Nitrat in Meeres-und Trinkwasser. *Kieler Meeresforschungen*, 20, 5-11.

Grasshoff K. (1969). Zur Chemie des Roten Meeres und des inneren Golf von Aden nach Beobachtungen von F S 'Meteor' wahrender Indischen ozean Expedition 1964/65. *Meteor Foprschungsergeb*, Reihe A, A6, 76pp.

Grasshoff K. (1975). The hydrochemistry of landlocked basins and fjords. In: J. P. Riley and G. Skirrow (Editors), *Chemical Oceanography*, Vol. 2, Academic Press, New York, 455-597pp.

Grasshoff K., M. Ehrhardt and K. Kremling (1983). *Methods of Seawater Analysis*, Verlag Chemie, New York, NY, 419pp.

Hahn J. (1974). The North Atlantic Ocean as a source of atmospheric N_2O. *Tellus,* 26, 160-168.

Harrits S.M., and R.S. Hanson (1980). Stratification of aerobic methane-oxidizing organisms in Lake Mendota, Madison, Wisconsin. *Limnol. Oceanogr.*, 25, 412-421.

Hartmann M., H. Lange, E. Seibold and E. Walger (1971). Oberflaschensedimente im Persischen Golf und Golf von Oman. I. Geologisch-hydrologischer Rahmen und erste sedimentologish Ergebnisse. *Meteor Forschungsergebnisse*, Reihe C, 4, 1-76.

Hastenrath S., and P.J. Lamb (1979). *Climate Atlas of the Indian Ocean, Part 1* (Madison: University of Wisconsin Press) 97 charts.

Hein R., P.J. Crutzen, and M. Heimann (1997). An inverse modelling approach to investigate the global atmospheric methane cycle. *Global Biogeochem. Cycles*, 11, 43-76.

Houghton J.T., B.A. Callander and S.K. Varney (Editors), (1992). *Climate Change 1992. The Supplementary Report to the IPCC Scientific Assessment.* Cambridge University Press, New York, 200pp.

Houghton J.T., L.G.M. Filho, J. Bruce, H.S. Lee, B.A. Callander, E. Haites, N. Harris, and K. Maskell (Editors), (1995). *Climate Change 1994. Radiative Forcing of Climate Change and an Evaluation of the IPCC IS 92 Emission Scenarios. Published for the Intergovernmental Panel on Climate Change,* Cambridge University Press, Cambridge 339pp.

Houghton J.T., L.G.M. Filho, A.A. Callander, N. Harris, A. Kattenberg, and K. Maskell (Editors) (1996). *Climate Change 1995 - The Science of Climate Change*, Cambridge University Press, Cambridge, 572 pp.

Ittekkot V., R.R. Nair, S. Honjo, V. Ramaswamy, M. Bartsch, S. Manginini, and B.N. Desai (1991). Enhanced particle fluxes in Bay of Bengal induced by injection of fresh water. *Nature*, 351, 385-387.

Ivanenkov V.N and F.A. Gubin (1960). Watermasses and hydrochemistry of western and southern parts of the Indian Ocean. *Acad. Nauk. USSR*, 22, 27-99.

Jenkins W.J. (1990). Determination of isopycnal diffusivity in the Sargasso Sea. *J. Phys. Oceanogr.*, 21, 1058-1061.

Jorgensen K., H.B. Jensen, and J. Sorensen. (1984). Nitrous oxide production from nitrification and denitrification in various sediments at low oxygen concentrations. *Can. J. Microbiol.*, 30, 1073-1078.

Junge C. and J. Hahn (1971). N_2O measurements in the North Atlantic. *J. Geophys. Res.*, 76, 8143-8146.

Junk G. and H.V. Svec (1958). The absolute abundance of the nitrogen isotopes in the atmosphere and compressed gas from various sources. *Geochim. Cosmochim. Acta,* 14, 234-243.

Karisiddaiah S.M. and M. Veerayya (1994). Methane-bearing shallow gas-charged sediments in the eastern Arabian Sea: A probable source for greenhouse gas. *Cont. Shelf Res.*, 14, 1361-1370.

Karisiddaiah S.M. and M. Veerayya (1996). Potential distribution of subsurface methane in the sediments of the eastern Arabian Sea and its possible implications. *J.Geophys.Res.*, 101, 25, 887-25,895.

Karl D.M. and B.D. Tilbrook (1994). Production and transport of methane in oceanic particulate organic mater. *Nature*, 368, 732-734.

Keeling R.F, R.G. Najjar, M.L. Bender and P.P. Tans (1993). What atmospheric oxygen measurements can tell us about the global carbon cycle. *Global Biogeochem. Cycles*, 7, 37-67.

Khalil M.A.K. and R.A. Rasmussen (1988). Trace gases over the western Atlantic Ocean: fluxes from the eastern United States and distributions in and above the planetary boundary later. *Global Biogeochem. cycles*, 2, 63-71.

Kiene R.P. (1991). Production and consumption of methane in aquatic systems, In: J.E. Rogers and W.B. Whitman (Editors), *Microbial Production and Consumption of Greenhouse Gases: Methane, Nitrogen Oxides, and Halomethanes*, American Society for Microbiology, Washington, DC, 111-146pp.

Kim K.R. and H. Craig (1990). Two isotope characterisation of N_2O in the Pacific Ocean and constraints on its origin in deep water. *Nature,* 347, 58-61.

Kim K.R. and H. Craig (1993). Nitrogen-15 and oxygen-18 characteristics of nitrous oxide: a global perspective. *Science,* 262, 1855-1857.

Kumar S.P. and T.G. Prasad (1996). Winter cooling in the northern Arabian Sea. *Curr. Sci.* 71, 834-841.

Lashof D.A. and D. Ahuja (1990). Relative contributions of greenhouse gas emissions to the global warming. *Nature*, 344, 529-531.

Law C.S. and N.J.P. Owens (1990). Significant flux of atmospheric nitrous oxide from the northwestern Indian Ocean. *Nature,* 346, 826-828.

Leuenberger M. and U. Siegenthaler (1992). Ice-age atmospheric concentration of nitrous oxide from an Antarctic ice core. *Nature,* 360, 449-451.

Logan J.A., M.J. Prather, S.C. Wofsy and M.B. McElroy (1981). Tropospheric chemistry: a global perspective. *J. Geophys. Res.*, 86, 7210-7254.

Mantoura R.F.C., C.S. Law, N.J.P. Owens, P.H. Burkill, E.M.S. Woodward, R.J.M. Howland, and C.A Llewellyn (1993). Nitrogen biogeochemical cycling in the north western Indian Ocean. *Deep-Sea Res.II,* 40, 651-671.

Mariotti A., J.C. Germon and H. Petal (1981). Experimental determination of nitrogen kinetic isotope fractionations: some principles; illustration for denitrification and nitrification processes. *Plant and Soil,* 62, 413-430.

Marty D., P. Nival and W.D. Yoon (1997). Methanoarchaea associated with sinking particles and zooplankton collected in the Northeastern tropical Atlantic. *Oceanologica Acta*, 20, 863-869.

McAullife C. (1971). GC determination of solutes by multiple phase equilibration. *Chem. Tech.*, 1, 46-50.

McCreary J.P. (1981). A linear stratified ocean model of the coastal undercurrent. *Phil. Trans. Royal Soc. Lond.*, 302, 385-413.

McCreary J.P. Jr., P.K. Kundu and R.L. Molinari (1993). A numerical investigation of dynamics, thermodynamics and mixed-layer processes in the Indian Ocean. *Progress in Oceanography*, 31, 181-244.

McElroy M.B. (1983). Marine biological controls of atmospheric CO_2 and climate. *Nature,* 302, 328-329.

McElroy M.B. and D.B. Jones (1996). Evidence for an additional source of atmospheric N_2O. *Global Biogeochem. Cycles,* 10, 651-659.

Millero F.J., C.T. Chen, A.L. Bradsha, and K. Schleiche (1980). A new high pressure equation of State for Sea water. *Deep-Sea Res.*, 27, 255-264.

Morcos S.A. (1970). Physical and Chemical Oceanography of the Red Sea. *Oceanogr. Mar. Biol. Ann. Rev.*, 8, 73-202.

Morris A.W. and J.P. Riley (1963). The determination of nitrate in sea water. *Anal. Chim. Acta,* 29, 272-279.

Murphy J. and J.P. Riley (1962). A modified single solution method for the determination of phosphate in natural waters. *Anal. Chim Acta*, 27, 31-36.

Naqvi S.W.A., R.J. Noronha and C.V.G. Reddy, (1982). Denitrification in the Arabian Sea. *Deep-Sea Res.*, 29, 459-469.

Naqvi S.W.A. and R. Sen Gupta (1985). 'NO' a useful tool for the estimation of nitrate deficits in the Arabian Sea. *Deep-Sea Res.*, 35, 665-674.

Naqvi S.W.A. (1986). *Relationships between nutrients and dissolved oxygen and nitrate reduction in the Arabian Sea,* Ph. D. Dissertation, University of Poona, Pune, 123 pp.

Naqvi S.W.A. (1987). Some aspects of the oxygen-deficient conditions and denitrification in the Arabian Sea. *J. Mar. Res.*, 49, 1049-1072.

Naqvi S.W.A., R.J. Noronha, K. Somasundar and R. Sen Gupta (1990). Seasonal changes in the denitrification regime of the Arabian Sea. *Deep-Sea Res.,* 37, 693-711.

Naqvi S.W.A . (1991a). Geographical extent of denitrification in the Arabian Sea in relation to some physical processes. *Oceanologica Acta*, 14, 281-290.

Naqvi S.W.A. (1991b). N_2O production in the ocean. *Nature,* 349, 373-374.

Naqvi S.W.A. and R.J. Noronha (1991). Nitrous oxide in the Arabian Sea. *Deep-Sea Res.,* 38, 871-890.

Naqvi S.W.A., M.D. Kumar, P.V. Narvekar, S.N. De Sousa, M.D. George, and C. D'Silva (1993). An intermediate Nepheloid layer associated with high microbial metabolic rates and denitrification in the Northwest Indian ocean. *J. Geophys. Res.*, 98, 16,469-16,479.

Naqvi S.W.A., R. Sen Gupta and M.D. Kumar (1993). Carbon dioxide and nitrous oxide cycling in the Arabian Sea. In: G.A. McBean and M. Hantel (Editors), Interactions between global climate subsystems, the legacy of Hann, *Geophys. Monograph*, 75, 85-92.

Naqvi S.W.A. and M.S. Shailaja (1993). Activity of the respiratory electron transport system and respiration rates within the oxygen minimum layer of the Arabian Sea. *Deep-Sea Res. II,* 40, 687-695.

Naqvi S.W.A. (1994). Denitrification processes in the Arabian Sea. *Proc. Indian Acad. Sci. (Earth & Planet Sci.),* 103, 279-300.

Naqvi S.W.A., T. Yoshinari , D.A. Jayakumar, M.A. Altabet, P.V. Narvekar, A.H. Devol, J.A. Brandes and L.A. Codispoti (1998). Budgetary and biogeochemical implications of N_2O isotope signatures in the Arabian Sea. *Nature,* 394, 462-464.

Nevison C.D., R.F. Weiss and D.J. Erickson III (1995). Global oceanic emissions of nitrous oxide. *J. Geophys. Res.*, 100 (C8), 15,809-15,820.

Olson D.B., G.L. Hitchcock, R.A. Fine and B.A. Warren (1987). Anoxic layers in the Arabian Sea and their relationship to mixed-layer processes. *EOS*, 68, 1693.

Olson D.B., G.L. Hitchcock, R.A. Fine and B.A. Warren (1993). Maintenance of the low- oxygen layer in the Arabian Sea. *Deep-Sea Res. II,* 40, 673-685.

Ostlund H.G., H. Craig, W.S. Broecker and D. Spencer (1987). *GEOSECS Atlantic, Pacific, and Indian Ocean Expeditions Vol 7, Shorebased Data and Graphics*, National Science Foundation, 200 pp.

Oudot C., C. Andrie and Y. Montel (1990). Nitrous oxide production in the tropical Atlantic Ocean. *Deep-Sea Res.*, 37, 183-202.

Owens N.J.P., C.S. Law, R.F.C. Mantoura, P.H. Burkill, and C.A. Lewellyn (1991). Methane flux to the atmosphere from the Arabian Sea, *Nature,* 354, 293-295.

Paerl H.W. and L.E. Prufert (1987). Oxygen-poor microzones as potential sites of microbial N_2 fixation in nitrogen-depleted aerobic marine waters. *Appl. Environ. Microbiol*, 53, 1078-1087.

Paropkari A.L., Ch.M. Rao and P.S.N. Murthy (1987). Environmental controls on the distribution of organic matter in recent sediments of the western continental margin of India. In: R.K. Kumar, P. Dwivedi, V. Banerjie, and V.Gupta (Editors), *Petroleum Geochemistry and Exploration in Afro Asian Region*, Balkema, Rotterdam, pp347-361.

Patra P.K., S. Lal, and S. Venkataramani (1998). Seasonal variability in distribution and fluxes of methane in the Arabian Sea. *J. Geophys. Res.*, 103, 1167-1176.

Payne W.J. (1973). Reduction of nitrogenous oxide by microorganisms. *Bacteriol. Rev.*, 37, 409-452.

Payne W.J. (1981). The status of nitric oxide and nitrous oxide as intermediates in denitrification. In C.C. Delwiche (Editor), *Denitrification, Nitrification and Atmospheric Nitrous Oxide.* John Wiley & Sons, Inc., New York, 85-104p.

Pierotti D. and R.A. Rasmussen (1980). Nitrous oxide measurements in the eastern tropical Pacific Ocean. *Tellus*, 32, 56-72.

Prasad S.S. (1994). Natural atmospheric sources and sinks of nitrous oxide I An evaluation based on ten laboratory data. *J. Geophys. Res.,* 99, 5285-5294.

Press W.H., B.P. Flannery, S.A. Teukolsky and W.T. Vetterling (1992). *Numerical Recipes in C, The Art of Scientific Computing*, Cambridge University Press, 996 pp.

Prinn R., D. Cunnold, R. Rasmussen, P. Simmonds, F. Alyea, A. Crawford, P. Fraser and R. Rosen (1990). Atmospheric emissions and trends of nitrous

oxide deduced from 10 years of ALE-GAGE data. *J. Geophys. Res-Atmos.*, 95, 18369-18385.

Qasim S.Z. (1977). Biological productivity of the Indian Ocean. *Indian J. Mar. Sci.*, 6, 122-137.

Qasim S.Z. (1982). Oceanography of the northern Arabian Sea. *Deep-Sea Res.*, 29, 1041-1068.

Rahn T., and M. Wahlen (1997). Stable isotope enrichment in stratospheric nitrous oxide. *Science,* 278, 1776-1778.

Ramesh Babu V., M.J. Varkey, V. Kesava Das and A.D. Gouveia (1980). Water masses and general hydrography along the west coast of India during early March. *Indian J. Mar. Sci.,* 9, 82-89.

Rao C.K., S.W.A. Naqvi, M.D. Kumar, S.D.J. Varaprasad, D.A. Jayakumar, M.D. George and S.Y.S. Singbal, (1994). Hydrochemistry of Bay of Bengal: possible reasons for a different water-column cycling of carbon and nitrogen from the Arabian Sea. *Mar.Chem.*, 47, 279-290.

Rasmussen R.A., and M.A.K. Khalil (1981). Atmospheric methane (CH_4): Trends and season cycles. *J. Geophys. Res.,* 86, 9826-9832.

Redfield A.C., B.H. Ketchum, and F.A. Richards, (1963). The influence of organisms on the composition of seawater. In: M.N. Hill, (Editor) *The Sea*, Vol. 2, Interscience, New York, 26-77 pp.

Richards F.A. (1965). Anoxic basins and fjords; In: J.P. Riley and G. Skirrow (Editors), *Chemical Oceanography,* Vol. 1, Academic Press, 611-645.

Ritchie G.A.F. and D.J.D. Nicholas (1972). Identification of the sources of nitrous oxide produced by oxidative and reductive processes in *Nitrosomonas europaea. Biochem. J.,* 126, 1181-1191.

Robinson M.K. (1966). Arabian Sea, In: R. Fairbridge, (Editor), *The Encyclopaedia of Oceanography*, Reinhold Publ. Corp., New York, 40-43pp.

Rochford D.J. (1964). Salinity maxima in the upper 1000 meters of the Northern Indian Ocean. *Aust. J. Mar. Freshw. Res.*, 15, 1-24.

Rodhe H. (1990). A comparison of the contribution of various gases to the greenhouse effect. *Science,* 248, 1217-1219.

Rönner U. (1983). Distribution, production and consumption of nitrous oxide in the Baltic Sea. *Geochim. Comochim. Acta,* 47, 2179-2188.

Rudd J.W.M., A. Furutani, R.J. Flett and R.D. Hamilton (1976). Factors controlling methane oxidation in shield lakes: the roles of nitrogen fixation and oxygen concentration. *Limnol. Oceanogr.*, 21, 357-364.

Rudd J.W.M., and C.D. Taylor (1980). Methane cycling in aquatic environments. *Adv. Aquat. Microbiol.*, 2, 77-150.

Sastry J.S. and R.S. D'Souza (1972). Upwelling and upward mixing in the Arabian Sea. *Indian J. Mar. Sci.*, 1, 17-27.

Schafer P. and V. Ittekkot (1995). Isotope biogeochemistry of nitrogen in the northern Indian Ocean. *Mitt. Geol.-Palaont. Inst. Univ. Hamburg,* 78, 67-93.

Schott G. (1935). *Geographie des Indischen und Stillen Ozeans, Verlag Boysen,* Hamburg.

Scranton M.I. and P.G. Brewer (1977). Occurrence of methane in the near-surface waters of the western subtropical North Atlantic. *Deep-Sea Res.*, 24,127-138.

Scranton M.I. and J.W. Farrington (1977). Methane production in the waters off Walvis Bay. *J. Geophys. Res.*, 83, 4947-4953.

Sen Gupta R., M.D. Rajagopal, and S.Z. Qasim, (1976). Relationship between dissolved oxygen and nutrients in the northwestern Indian ocean. *Indian J. Mar. Sci.*, 5, 201-211.

Sen Gupta R. and S.W.A.Naqvi (1984). Chemical oceanography of the Indian Ocean, north of the equator. *Deep-Sea Res.*, 31, 671-706.

Sen Gupta R., S.P. Fondekar and R. Alagarsamy (1993). State of oil pollution in the northern Arabian Sea after the Gulf oil spill. *Mar. Pollut. Bull.*, 27, 85-91.

Shetye S.R., A. Gouveia, S.S.C. Shenoi, D. Sundar, G.S. Michael, A.M. Almeida, and K. Santanam (1990). Hydrography and circulation off west coast of India during the Southwest Monsoon. *J. Mar. Res.*, 48, 359-378.

Shetye S.R., A. Gouveia, S.S.C. Shenoi, G.S. Michael, D. Sundar, A.M. Almeida, and K. Santanam (1991a). The coastal current off western India during northeast monsoon. *Deep-Sea Res.,* 38, 1517-1529.

Shetye S.R., S.S.C. Shenoi, A. Gouveia, G.S. Michael, D. Sundar,and Nampoothiri G. (1991b). Wind driven coastal upwelling along the western boundary of the Bay of Bengal during the southwest monsoon. *Cont. Shelf Res.*, 11, 1397-408.

Shetye S.R., A. Gouveia, S.S.C. Shenoi, D. Sundar, G.S. Michael and Nampoothiri G. (1993). The western boundary current of the seasonal subtropical gyre in the Bay of Bengal. *J. Geophys. Res.*, 98, 945-954.

Siddiquie H.N., D. G. Rao, K.H. Vora, and R.S. Topgi (1981). Acoustic masking in sediments due to gases on the western continental shelf of India, *Mar. Geol.*, 39, M27-M37.

Sieburth J.McN. (1987). Contrary habitats for redox specific processes: Methanogenesis in oxic waters and oxidation in anoxic waters. In: M.A. Sleigh (Editor), *Microbes in the sea*, John Wiley and sons N. York, 11-38.

Sigman D.M., M.A. Altabet, R. Michener, D.C. McCorkle, B. Fry and R.M. Holmes (1997). Natural abundance-level measurement of the nitrogen isotopic composition of oceanic nitrate: an adaptation of the ammonia diffusion method. *Mar. Chem.*, 57, 227-242.

Smith R.L. and J.S. Bottero (1977). On upwelling in the Arabian Sea. In: M. Angel, (Editor), *A Voyage of Discovery,* Pergamon Press, Oxford, 291-304p.

Smith S.L. and L.A. Codispoti (1980). Southwest monsoon of 1979: chemical and biological response of Somali coastal waters, *Science,* 209, 597-600.

Somasundar K. and S.W.A. Naqvi (1988). On the renewal of the denitrifying layer in the Arabian Sea. *Oceanologica Acta*, 11, 167-172.

Steele L.P., E.J. Dlugokencky., P.M. Lang, P.P. Tans, R.C. Martin and K.A. Masarie (1992). Slowing down of the global accumulation of atmospheric methane during the 1980's. *Nature*, 358, 313-316.

Swallow J.C. (1984). Some aspects of the physical oceanography of the Indian Ocean. *Deep-Sea Res.,* 31, 639-650.

Tchernia P., H. Lacombe and P. Guibout (1958). Sur quelques nouvelles observations hydrologiques relative a la region equatoriale de l'Ocean Indien. *Bull Inf. Com. Cent. Oceanogr. Etude Côtes*, 10, 115-143.

Tilbrook B.D. and D.M. Karl (1995). Methane sources, distributions and sinks from California coastal waters to the oligotrophic North Pacific gyre. *Mar. Chem.*, 49, 51-64.

Van Campo E. (1986). Monsoon fluctuations in two 20,000 yr B.P. oxygen-isotope/pollen records of southwest India. *Quat. Res.*, 26, 376-388.

Venkateswaran S. V. (1956). On evaporation from the Indian Ocean. *Indian J. Met. Geophys.*, 7, 265-284.

Wada E. and A. Hattori (Editors.) (1991). In: *Nitrogen in the Sea: Forms, Abundances and Rate Processes*, CRC Press, 208 p.

Wanninkhof R. (1992). Relationship between wind speed and gas exchange over the ocean. *J. Geophys. Res.*, 97, 7373-7382.

Ward B.B. and O.C. Zafiriou (1988). Nitrification and nitric oxide in the oxygen minimum of the eastern tropical North Pacific. *Deep-Sea Res.*, 35, 1127-1142.

Ward B. B., M.E. Hogan, A. Jayakumar, and W.A. Naqvi (1998). Denitrification Parameters in the Arabian Sea. *EOS, Trans. AGU*, 79(1):OS83, January 1998.

Weiss R.F. (1978). Nitrous oxide in the surface water and marine atmosphere of the North Atlantic and Indian Oceans. *EOS Trans. Am. Geophys. Union*, 59: 1101.

Weiss R.F. and B.A. Price (1980). Nitrous oxide solubility in waters and seawater. *Mar. Chem.*, 8, 347-359.

Weiss R.F. (1981). The temporal and spatial distribution of tropospheric nitrous oxide. *J. Geophys. Res.*, 86, 7185-7195.

Whittenbury R. and N.R. Kreig (1984). *Methanococcaceae*,. In: N R. Kreig (Editor) *Bergy's Manual of systematic Bacteriology*, vol. 1. The Williams and Wilkins Co., Baltimore, 256-261.

Wiesenburg D.A. and N.L. Guinasso, Jr. (1979). Equilibrium solubilities of methane, carbon monoxide, and hydrogen in water and sea water. *J.Chem. Eng. Data*, 24, 356-360.

Wolfe R.S. (1971). Microbial formation of methane. *Adv. Microbiol. Physiol.*, 6, 107-146.

Wooster W.S. and J.L. Reid (1963). Eastern boundary currents. In: M.N. Hill (Editor), *The Sea*, Vol. 2, Interscience, New York, 253-280p.

Wyrtki K. (1971). *Oceanographic Atlas of the International Indian Ocean Expedition*, National Science Foundation, Washington D.C., 531p.

Wyrtki K. (1973). Physical oceanography of the Indian Ocean. In: B. Zeitzschel, (Editor), *The biology of the Indian Ocean,* Springer-Verlag, Berlin, pp 18-36p.

Yoshida T. and M. Alexander (1970). Nitrous oxide formation by *Nitrosomonas europaea* and heterotrophic microorganisms. *Soil Sci. Soc Amer. Proc.*, 34, 880-882.

Yoshida N., A. Hattori, T. Saino , S. Matsuo and E. Wada (1984). $^{15}N/^{14}N$ ratio of dissolved N_2O in the eastern tropical Pacific Ocean. *Nature,* 307, 442-444.

Yoshida N. (1988). ^{15}N-depleted N_2O as a product of nitrification. *Nature,* 335, 528-529.

Yoshida N., H. Morimoto, M. Hirano, I. Koike, S. Matsuo, E. Wada, T. Saino and A. Hattori (1989). Nitrification rates and ^{15}N abundances of N_2O and NO_3 in the western North Pacific. *Nature,* 342, 895-897.

Yoshinari T. (1976). Nitrous oxide in the sea. *Mar. Chem.,* 4, 189-202.

Yoshinari T. (1980). N_2O Reduction by *Vibrio succinogenes. Appl. Environ. Microbiol.,* 39, 81-84.

Yoshinari T. and I. Koike (1994). The use of stable isotopes for the studies of gaseous nitrogen species in the marine environment. In: K. Lajtha and R. Michener (Editors), *Stable Isotopes in Ecology and Environmental Science,* Blackwell Scientific, 114-137p.

Yoshinari T., M.A. Altabet, S.W.A. Naqvi, L.A. Codispoti, A. Jayakumar, M. Kuhland and A. Devol (1997). Nitrogen and oxygen isotopic composition of N_2O from suboxic waters of the eastern tropical North Pacific and the Arabian Sea - measurement by continuous-flow isotope ratio monitoring. *Mar. Chem.,* 56, 253-264.

Yung Y.L. and C.E. Miller (1997). Isotopic fractionation of stratospheric nitrous oxide: is there a chemical source? *Science,* 278, 1778-1780.

Zafiriou O.C. (1990). Laughing gas from leaky pipes. *Nature,* 347, 15-16.

Zehnder A.J.B. (1978). Ecology of methane formation. In: R. Mitchell (Editor), *Water Pollution Microbiology*, Wiley Interscience, New York, 349-376p .

Zeikus J.G. (1977). The biology of methanogenic bacteria. *Bacteril. Rev.*, 41, 514-541.